CENTER FOR ENERGY AND ENVIRONMENT RESEARCH
UNIVERSITY OF PUERTO RICO

FINAL REPORT

Oceanic Corrosion Test of Bare and Zinc-Protected Aluminum Alloys for Seawater Heat Exchangeers

prepared by

Donald S. Sasscer, Thomas O. Morgan, Carlos Rivera
Center for Energy and Environment Research
University of Puerto Rico
College Station
Mayaguez, Puerto Rico 00708

Mr. Richard Ernst
The Trane Company

and

Mr. Arthur C. Scott and
T. J. Summerson
Kaiser Aluminum Chemical Corporation

November, 1982

Prepared for National Aeronautics
and
Space Administration
under
Grant No. NAGW-198

ABSTRACT

In a cooperative research effort between The Puerto Rico Center for Energy and Environment Research, Kaiser Aluminum and Chemical Corporation and The Trane Company, a six month study was made of the seawater corrosion performance of various aluminum materials to test their suitability for use in seawater heat exchangers. The materials tested included bare 3004 tubes, 7072 Alclad 3004 tubes and bare and zinc diffusion treated 3003 extrusions from a brazed aluminum, plate-fin heat exchanger developed by The Trane Company. The test materials were exposed to 1.8 m/sec flowing seawater aboard an open ocean test facility moored 3.4 km off the southeast coast of Puerto Rico. After six months exposure, the average corrosion rates for most varieties of aluminum materials converged to a low value of 0.015 mm/yr (0.6 mils/yr). Pitting did not occur in bare 3003 and 3004 samples during the six month test. Pitting did occur to varying degrees in the Alclad and zinc diffusion treated material, but did not penetrate to the base metal. Biofouling countermeasures (intermittent chlorination and brushing) did not affect the corrosion rates to any significant extent. Intermittent chlorination at a level of 0.5 ppm for 28 minutes daily controlled microbiofouling of the samples but did not prevent the development of a macrobiofouling community in areas of the plumbing with low flow.

TABLE OF CONTENTS

LIST OF TABLES

LIST OF FIGURES

1. INTRODUCTION

Historically, aluminum has not been widely used for seawater heat exchangers because of its susceptibility to localized corrosion attack, mainly in the form of pitting and crevice corrosion. The life of aluminum in seawater can be greatly extended by the application of a sacrificial cladding layer such as 7072 alloy, which contains 1% zinc, to a conventional aluminum alloy such as 3003 or 3004. The purpose of the sacrificial cladding layer is to prevent pitting from extending into the core material. Past experience with 7072 Alclad 3004 products for purposes such as roofing, irrigation pipes and culverts, etc. has been encouraging. In his review of candidate materials for OTEC heat exchangers, LaQue has concluded that Alclad tubing could last for as long as ten years (1).

Alclad tubes are well suited for use in shell-and-tube-type heat exchangers, but the use of cladding layers in plate-fin-type heat exchangers is not generally practical. Conventional brazed heat exchangers face the additional problem of severe crevice corrosion when exposed to seawater. The Trane Company has developed a brazed aluminum, plate-fin heat exchanger specifically for use in seawater environments (2,3). By using one-piece hollow extrusions for the seawater passages, crevice corrosion sites are entirely eliminated. Pitting corrosion is controlled by a patented zinc-diffusion process applied after the heat exchanger has been brazed. The resulting integral layer of zinc-aluminum alloy was expected to provide 7072

Alclad-type protection to reduce pitting attack on the base alloy (4).

As a rule, the rate of corrosive attack on aluminum surfaces exposed to seawater decreases as a function of time. Two factors appear to contribute to this progressive reduction in corrosion rate with time. The most obvious is the build-up of a hard layer of aluminum oxide on the exposed surface. In addition, LaQue has suggested that the accumulation of biogrowth on aluminum surfaces exposed to seawater may help protect these surfaces from corrosive attack (1). In order to maintain heat transfer efficiency in seawater heat exchangers at an acceptable level, it is necessary to periodically employ some form of biofouling countermeasures. These can be either mechanical (e.g. brushes, sponge balls, abrasive slurries, etc.) or chemical (e.g. chlorination). However, periodic mechanical cleaning may remove the protective inorganic and organic films covering the metal surfaces and expose fresh surfaces thereby greatly increasing the corrosion rate of the metal and, in addition, may erode the surface. The effect of chlorination on corrosion rates of aluminum surfaces exposed to seawater has not been evaluated extensively.

The object of the present investigation was to test the corrosion resistance of roll formed and welded (RFW) 7072 Alclad 3004 and of zinc-diffusion protected 3003 aluminum extrusions under conditions which simulated the open ocean heat exchanger environment which would be experienced, for example, by an Ocean Thermal Energy Conversion power plant evaporator. The materials

were exposed to a flow of open ocean water at 1.8 m/s the consequent biofouling resulting from this exposure and to biofouling countermeasures (brush cleaning and chlorination). Uninterrupted flow was maintained through the system from the time flow was intitiated, on 28 May 1981, until the end of the experiment on 28 November 1981.

This project was a joint undertaking of the Center for Energy and Environment Research (CEER) of the University of Puerto Rico, The Trane Corporation, Kaiser Aluminum and Chemical Corporation, and Solar America Inc. Argonne National Laboratory of the U.S. Department of Energy provided the test facility along with technical aid.

2. TEST SITE

The experiment was conducted at a potential OTEC site off Punta Tuna on the southeast coast of Puerto Rico (Figure 1). The site (17^{o} 57.6' N, 65^{o} 51.9' W) lay approximately 3.4 km off the Puerto Rico coast where the water depth was 1100 m deep. Several site characterization studies have been conducted at this location (5,6,7,8). Figure 2 shows a plot of temperature vs. depth at the site.

A tension moored buoy system designed by Mr. Daniel C. Probert of the Naval Air Development Center in Key West, Florida was placed at the site. The system consisted of a 1360 kg Danforth anchor, a 1000 m section of 2.54 cm stud link chain, a 1000 m section of 4.6 cm Kevlar line, and a four meter diameter light buoy. The research platform was attached to the mooring

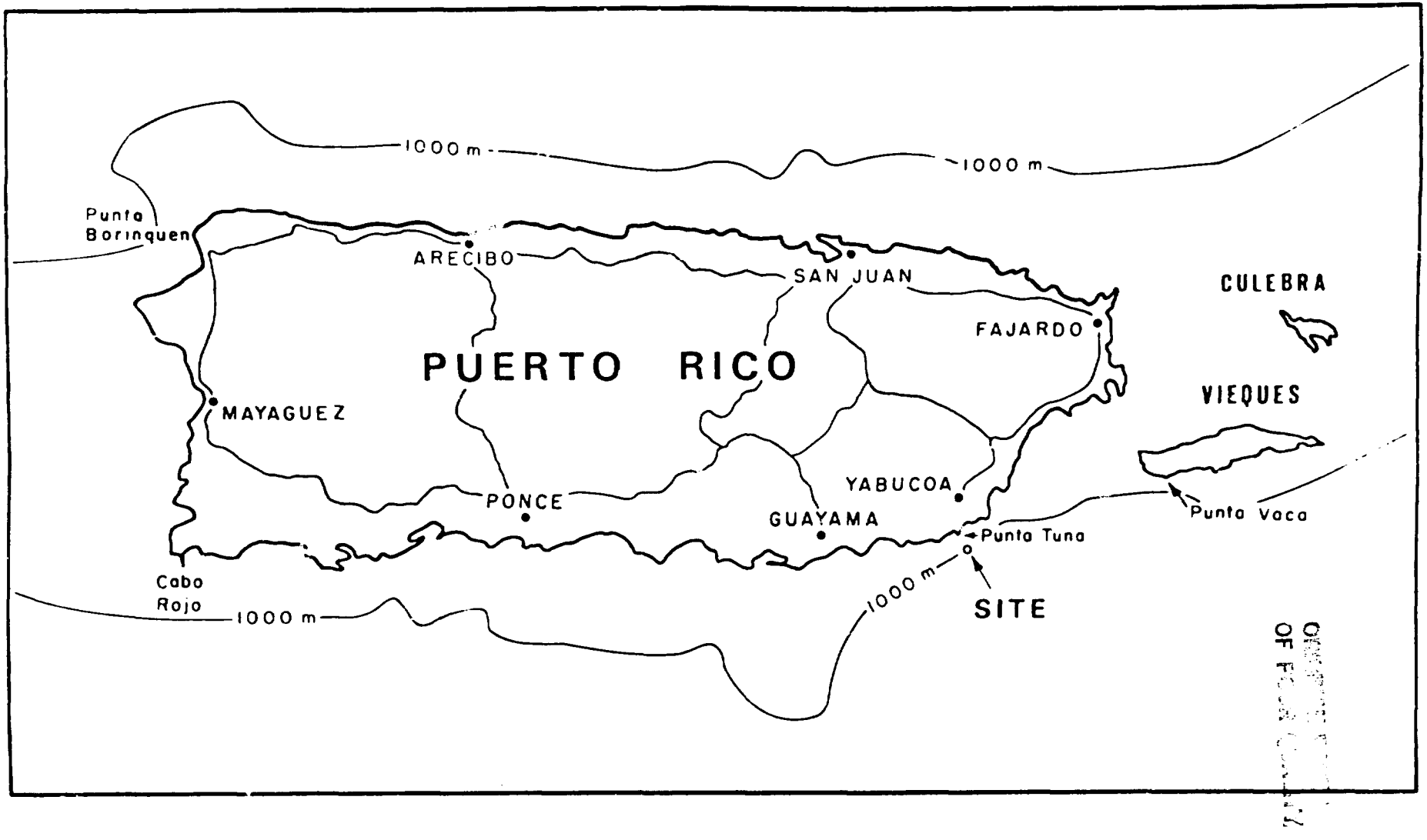

FIGURE 1. Map of Puerto Rico showing location of test site.

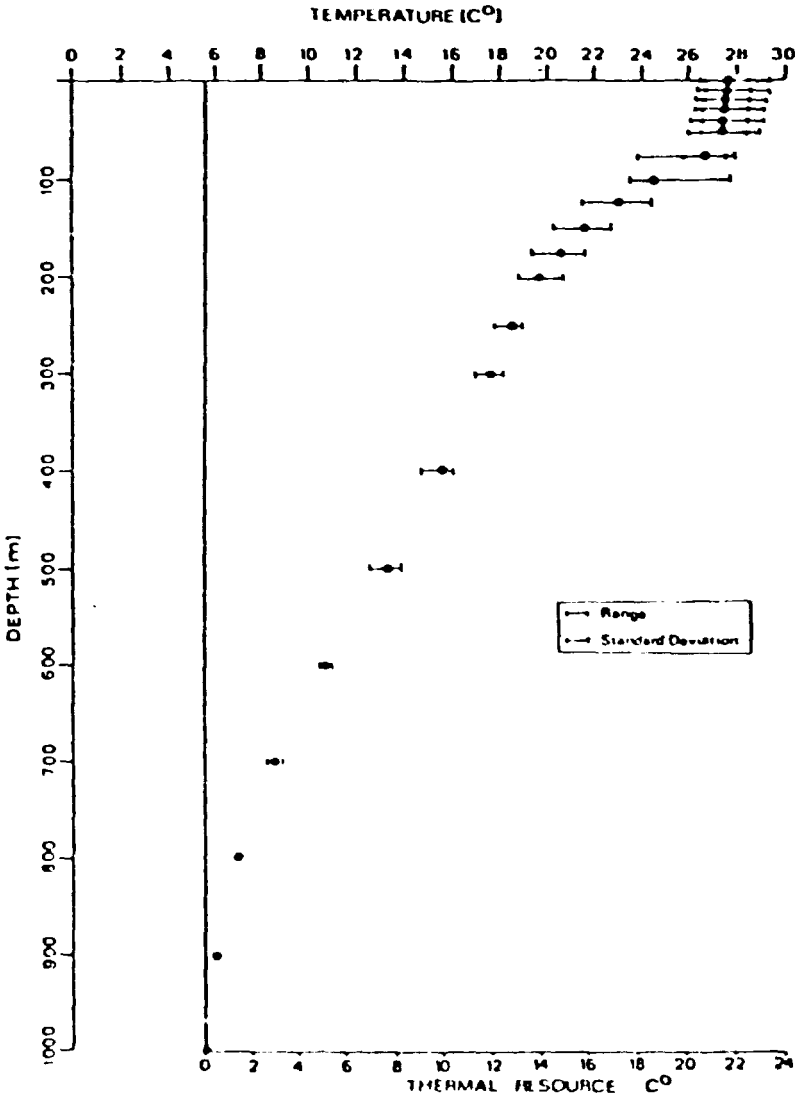

FIGURE 2. Temperature profile of the averaged temperature data taken at Punta Tuna, from August 1978 to June 1979.

by a 120 m section of 4.6 cm nylon line.

3. TEST FACILITIES

3.1 RESEARCH PLATFORM. The vessel used as a research platform was a Landing Craft, Utility (LCU) which had been an active vessel of the U.S. Army Heavy Boat Company of Moorehead City, North Carolina until the summer of 1978 when it was transferred to the DOE for OTEC experimental use (Figures 3 and 4). The LCU was a 320 ton vessel, 35 m long with a 10.4 m beam and was powered by three 165 hp diesel engines. Electrical power for housekeeping purposes was provided by two 20 kW DC diesel-electric generators. The LCU proved to be ideal for use as a research platform because it had approximately 150 m^2 of open, usable deck area, boat motion was minimal during normal weather due to its wide, flat bottom, and because it could accomodate up to 14 people. A detailed description of the research platform can be found in earlier publications (9,10).

3.2 MODIFICATIONS TO VESSEL. The following modifications were made to the LCU for use as an open ocean, heat exchanger corrosion and biofouling test facility.

a) A 0.46 m diameter well was made through the deck near the center of the vessel. The seawater intake and exhaust hoses passed through this well.

b) An "A" frame was placed over the well (Figure 5) to support a weighted cable to which the intake and exhaust hoses were attached.

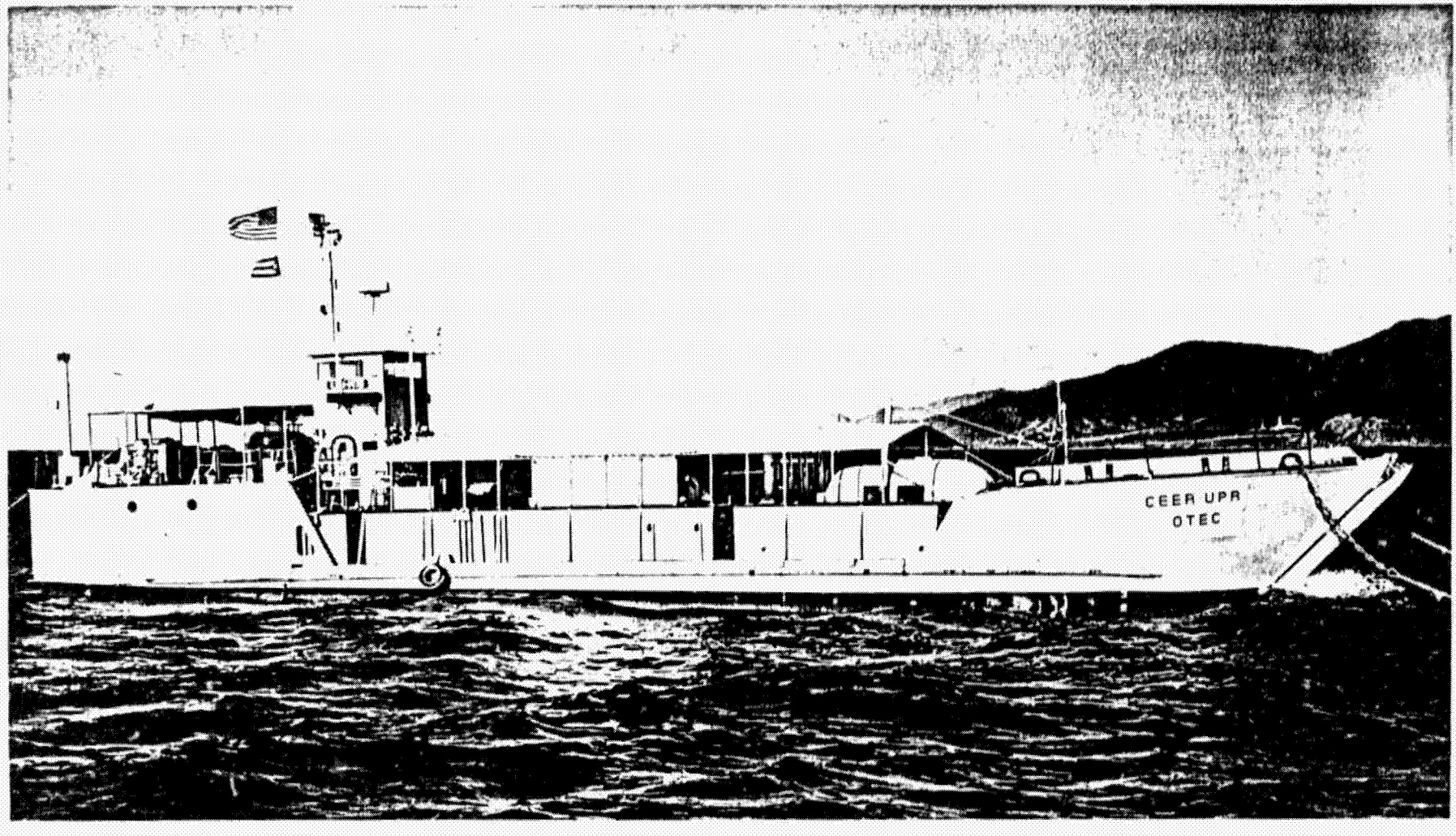

FIGURE 3. The Landing Craft, Utility (LCU) research platform moored on site at Punta Tuna, Puerto Rico.

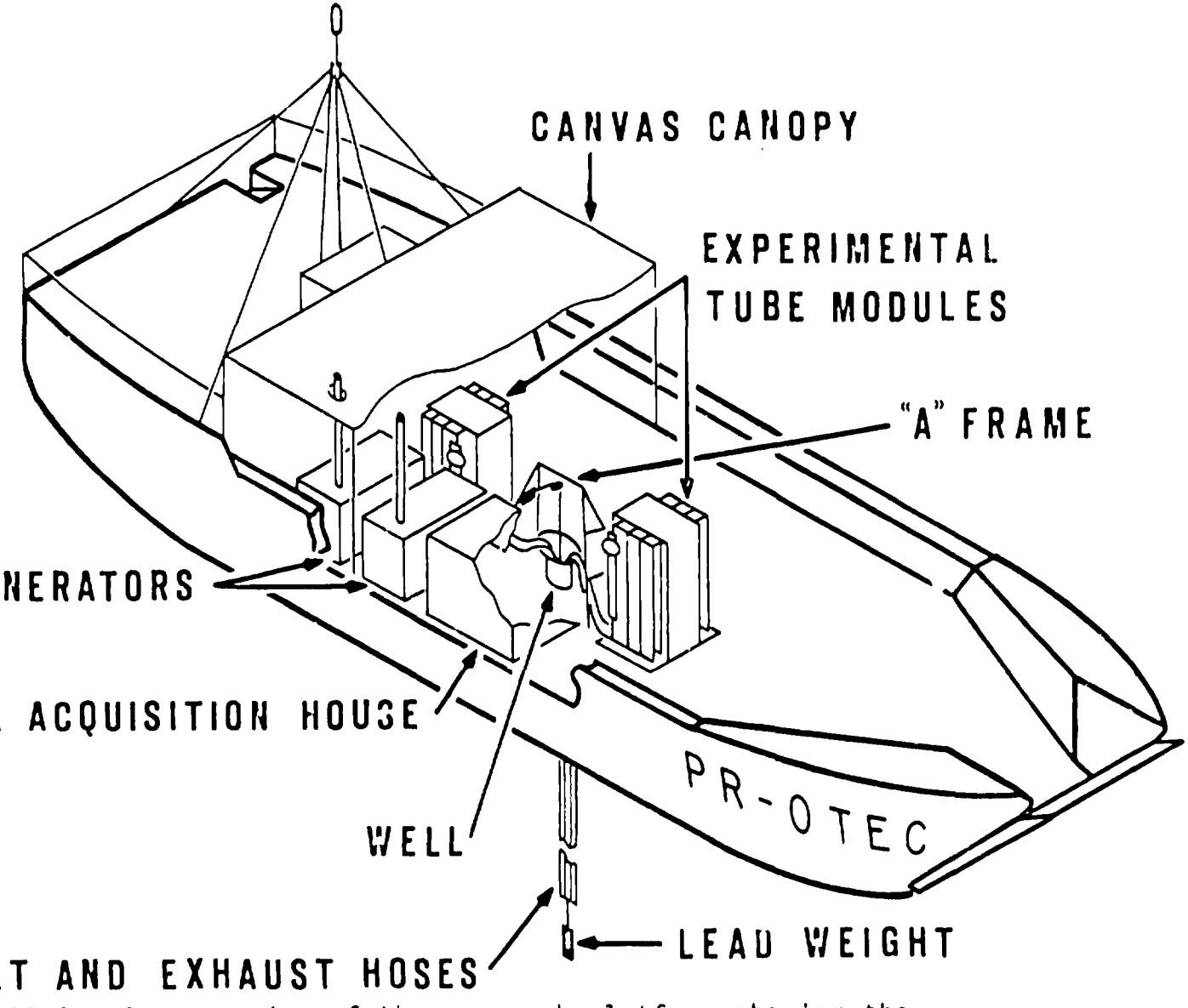

FIGURE 4. Cutaway view of th research platform showing the arrangement of the experimental equipment.

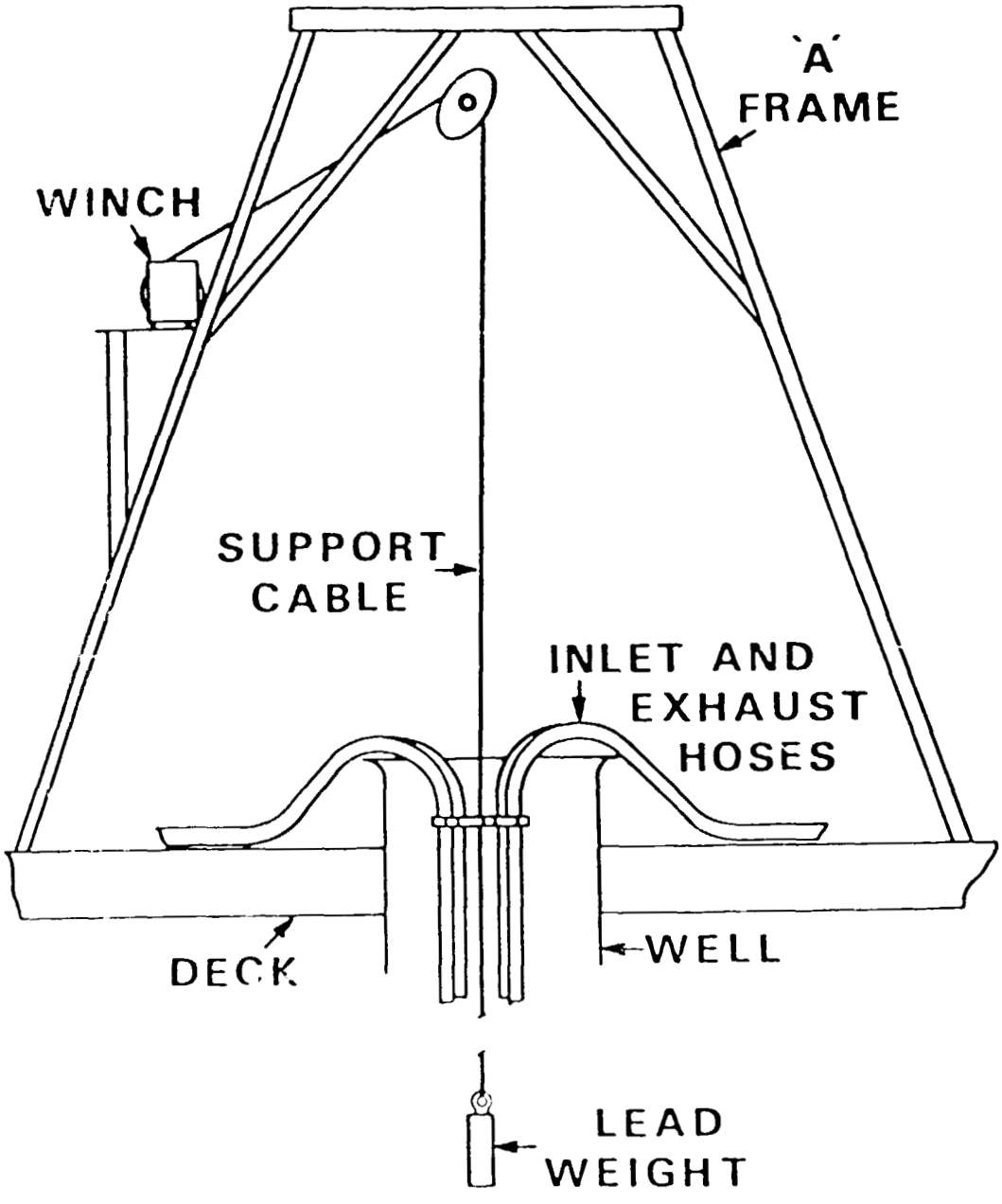

Figure 5. Through deck well and "A" frame for deployment of intake and exhaust hoses.

c) Two support frames (Figure 6) were situated fore and aft of the well. Each frame held three pumps and two experimental modules.

d) An air-conditioned, fiberglass house was placed beside the well to house the data acquisition system and other electronics.

e) Two 50 KVA, diesel-electric AC generators were added on deck to supply power for the experiment. The generators were rotated daily.

f) Two of the ballast tanks were converted to fuel tanks to increase the fuel capacity.

g) The deck was covered by a canopy to provide partial protection from the sun and the rain.

3.3 FLOW SYSTEM. The flow system (Figure 7) was designed by Southwest Research Laboratory of San Antonio, Texas according to specifications provided by the Center. To minimize fluctuations in flow rate due to boat motion, the intake and exhaust hoses passed through a well near the center of mass of the platform. The intake hoses drew water from a depth of 17 m, and the exhaust hoses discharged water 1 m below the vessel. To avoid chafing of these hoses against the well wall, they were suspended from the "A" frame, and a toroidal bumper system was attached to the suspending cable just above the bottom of the well. To prevent the intake hoses from flexing sharply below the vessel and thereby causing them to fatigue, they were reinforced with 1.2 m sections of 7.6 cm, T22 discharge hose;

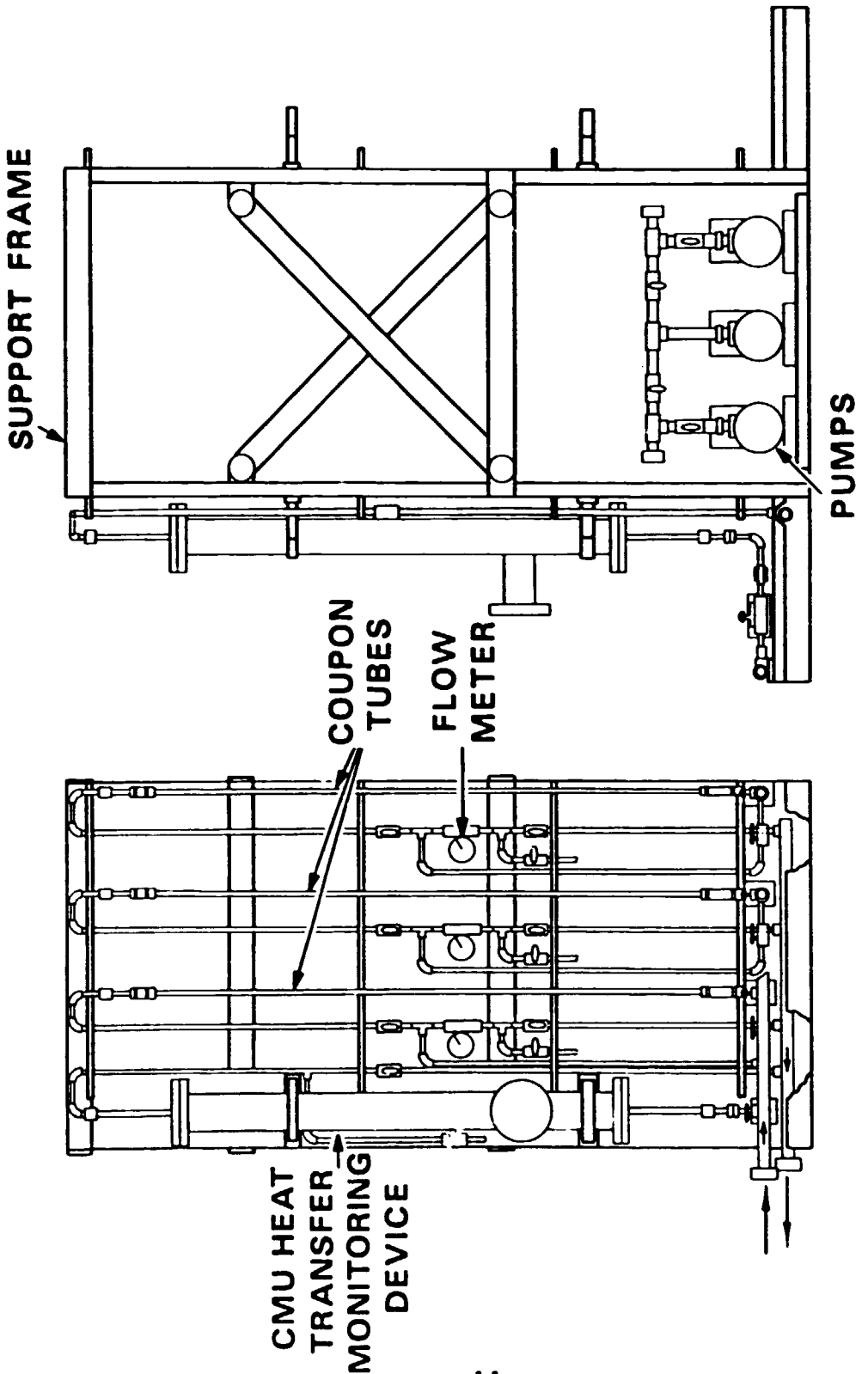

FIGURE 6. Support frame with one of the two experimental modules mounted.

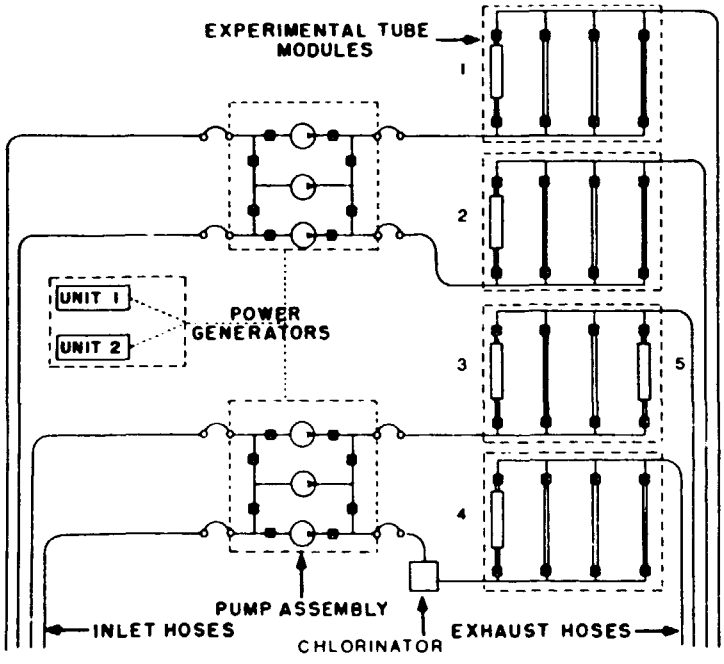

FIGURE 7. Schematic of flow system.

and to prevent them from swinging excessively beneath the platform, the cable to which they were attached was weighted with 227 kg of lead. The lead was hung 4.6 m below the intake hoses by a 1.2 cm nylon line which had been substituted for the last 9 m of cable so that there was no metal near the water intake which might affect the results of the experiment.

The intake hoses were fitted with PVC strainers 0.9 m long with a slit width of 0.47 cm. Biogrowth was removed from the strainers by cleaning them underwater with a brush at least once a month.

Each experimental module (Figures 6 and 7) had an independent flow system consisting of an intake hose, a pump, the module and an exhaust hose. The modules consisted of four parallel flow loops which insured that each flow path had the same potential for biofouling. One loop contained a modified Carnegie Mellon University heat transfer monitoring (HTM) device mounted on a 2.54 cm i.d. pipe. Units one and three were mounted on 5052 aluminum pipes, while units two and four were mounted on ASTM grade 2 pipes. Modules one, two, and four had corrosion samples in the remaining three flow paths. A Special Heat Transfer Monitor (STM) was installed in one of the flow paths in module three, so this module had corrosion samples in only two of its flow loops. The STM is essentially the same as an HTM but measures heat transfer in a single, rectangular flow path from the Trane brazed aluminum heat exchanger (11). A pair of modules was vertically mounted back-to-back on a frame, and each pair had a third, auxiliary pump to guarantee continuous

operation. Seawater velocity through the modules was controlled manually by two ball valves in series and was maintained at approximately 1.8 m/s. An electrolytic chlorinator was installed between the pumps and module four so that all flow loops in this module could be chlorinated.

In order to prevent metallic contamination of the circulated water, intake hoses were made of nylon reinforced, flexible polyvinyl chloride (PVC) hose, all tube fittings and fixtures were of PVC, and Marlowe chemical service pumps with NORYL pump housings were used.

This was the second deployment of the LCU for seawater heat exchanger investigations. Prior to this deployment, the intake strainers and hoses were replaced and portions of the modules which were not replaced were washed thoroughly with a brush and detergent and then soaked in household bleach (NaClO). The HTM pipes were scrubbed with detergent, soaked in bleach, and then swabbed with trichloroethylene.

3.4 SHIPBOARD PROCEDURES. On board at all times were four crewmen (one engineer, two seamen, and one cook) who maintained a 24 hour watch and at least one member of the scientific staff. In addition to normal shipboard responsibilities, the crewman on watch was expected to check the experiment hourly to assure that everything was functioning properly.

4. EXPERIMENTAL MATERIALS

A description of all materials tested is given in Table 1.

4.1 RFW TUBING. The roll formed and welded (RFW) tubes were prepared by Gifford-Hill Corporation from sheet provided by Kaiser Aluminum and Chemical Corporation. Dimensions of the tubing were 2.54 cm (1 in) O.D. with 1.52 mm (0.06 in) wall thickness. Alclad samples with nominal cladding thicknesses of 5% (actual measured cladding thickness of 0.076 mm or 0.003 in) and of 10% (actual measured cladding thickness of 0.178 mm or 0.007 in) were tested (Figure 8). The longitudinal seam weld in the RFW tubes was made by a fusion welding process and was approximately 3.2 mm (0.125 in) wide. The weld seam was not covered by 7072 cladding (Figure 9).

4.2 ZINC DIFFUSION PROTECTED EXTRUSIONS. The remaining samples were prepared by The Trane Company. They were sections of single water passages cut from 3003 aluminum extrusions used in the fabrication of the Trane brazed aluminum heat exchanger. The extrusions had rectangular cross sections with outside dimensions of 2.576 cm (1.014 in) by 3.442 cm (1.355 in) with 0.305 cm (0.120 in) wall thickness. Chemical analysis of the 3003 extrusions is given in Table 2.

Since both flux brazing and vacuum brazing processes are commonly used in the manufacture of plate-fin heat exchangers, samples were exposed to either one or the other of these environments. The extrusion samples were first subjected to the time and temperature cycles used in the flux braze or vacuum

Code	Type	Processing
Bare 3004	Bare 3004 alloy	Roll formed and welded tube
7072-5% Alclad	7072 Alclad 3004 5% cladding	Roll formed and welded tube
7072-10% Alclad	7072 Alclad 3004 10% cladding	Roll formed and welded tube
FB-Bare	3003 flux brazed	Processed through flux braze cycle not plated
FB-ZN	3003 flux brazed plus diffused zinc	Processed through flux braze cycle, zinc plated
VB-ZN	3003 vacuum brazed plus diffused zinc	Processed through vacuum braze cycle (exposed to magnesium vapor), zinc plated
FB ETCH 1 ZN	3003 flux brazed plus diffused zinc and etched to remoe zinc rich surface	Processed through flux braze cycle, zinc plated, etched to level of 1-1.5% zinc concentration
FB ETCH 1/2 ZN	3003 flux brazed plus diffused zinc with approx. 0.5% zinc at surface	Processed through flux braze cycle, zinc plated, etched to level of approx. 0.5% zinc conc.
FB-ZN-FE	3003 flux brazed plus diffused zinc, containing residual iron	Processed through flux braze cycle, treated with zinc plating process that also deposits low concentration of iron, etched

TABLE 1. Description of materials tested in corrosion study.

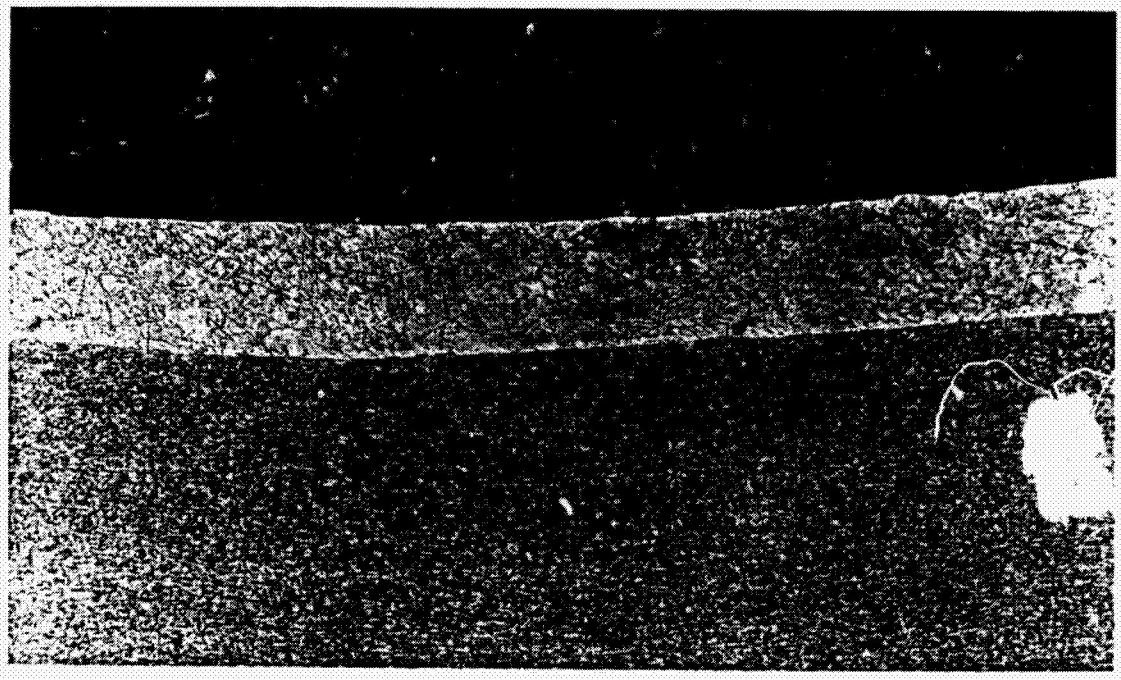

7072 layer is 0.007 in. thick on the 10% Alclad tube. Etch - Kellers, magnification 100X.

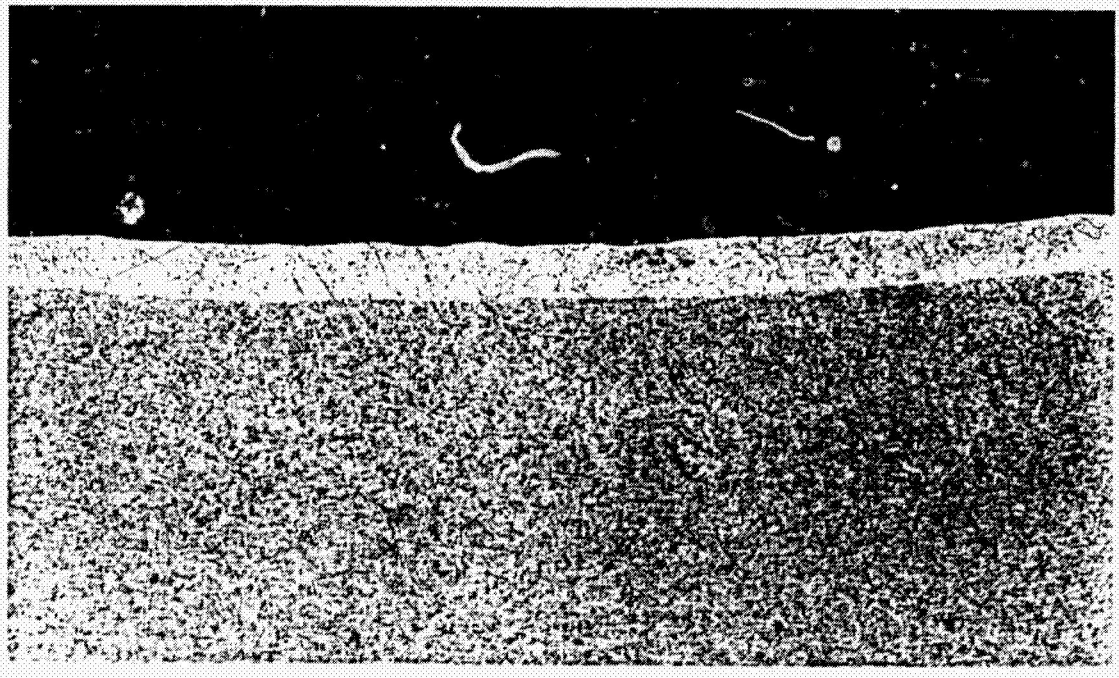

7072 layer is 0.003 in. thick on the 5% Alclad tube. Etch - Kellers, magnification 100X.

FIGURE 8. 7072 Alclad layers on 3004 RFW tube samples.

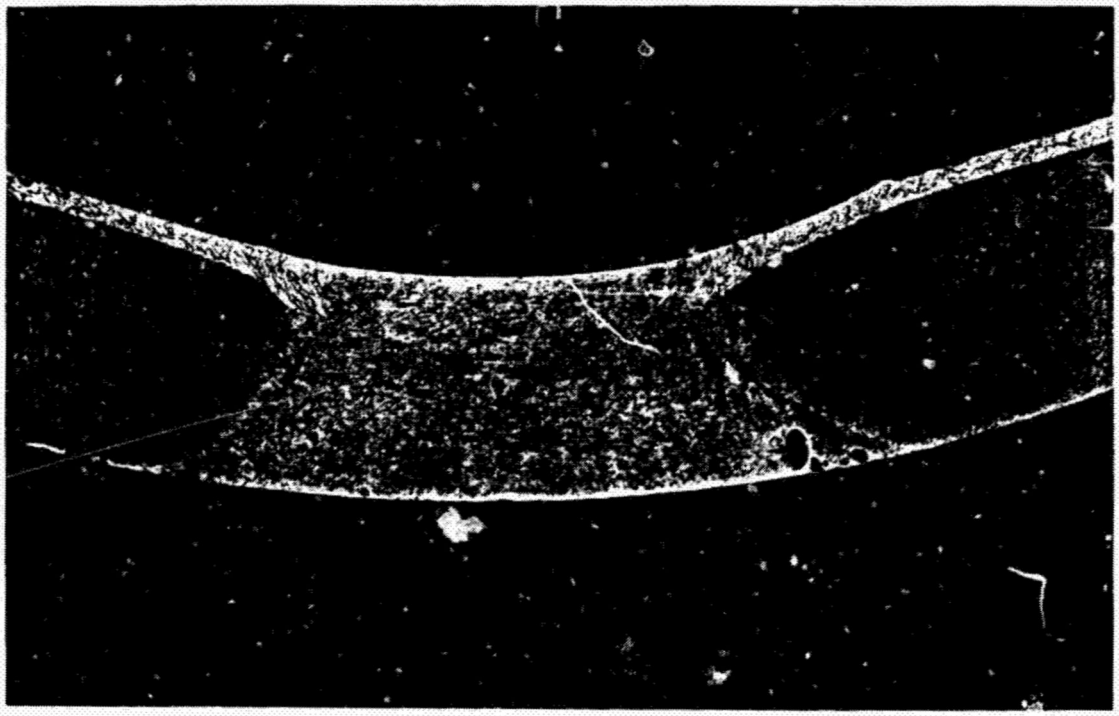

FIGURE 9. Weld seam on the RFW tubes. The seam was approximately 3.2 mm wide and was not covered by Alclad. Etch - Kellers, magnification 20X.

TABLE 2.

COMPOSITION OF 3003 EXTRUSIONS
USED TO PREPARE CORROSION SAMPLES

Element	Content, Wt %	Composition Specified for 3003 Alloy
Manganese	1.20	1.0-1.5
Copper	0.07	0.05-0.20
Silicon	0.21	0.60 Max.
Iron	0.63	0.70 Max.
Zinc	<0.10	0.10 Max.
Aluminum	Balance	Balance

braze processes before being treated to produce three levels of diffused zinc concentrations (Figure 10). Samples emerged from the zinc diffusion process with a surface layer of about 45% zinc, and a zinc concentration of approximately 2% at 0.013 mm (0.0005 in) below the surface. The FB-ZN and VB-ZN samples were tested in this condition. The FB-ETCH-1 ZN and FB-ETCH-1/2 ZN samples were chemically etched with Poulton's Etchant to remove the high-zinc surface layer. These samples contained zinc concentrations near 1% and 0.5%, respectively, at 0.013 mm (0.0005 in) below the surface. The depth of zinc diffusion expected to provide cathodic protection to the 3003 ranged from about 0.25 mm (0.010 in) to 0.38 mm (0.015 in). Appearance of the zinc diffused layer on etched cross sections is shown in Figure 11.

The 2% zinc level in the FB-ZN and VB-ZN samples was expected to accelerate the corrosion attack of the diffused layer and increase the understanding of the corrosion behavior within the six-month test period. The lower zinc levels of the FB-ETCH-1 ZN and FB-ETCH-1/2 ZN materials were expected to produce lower corrosion rates.

The FB-ZN-FE samples (see Table 1) had similar zinc levels to those of the FB-ETCH-1ZN samples but were treated with a zinc plating process which also deposited a low concentration of iron. This was not considered a candidate material, but was included in the test at the suggestion of Mr. Frank LaQue. Since residual iron is known to lower corrosion rates of zinc anodes, it was thought that this process might lower the

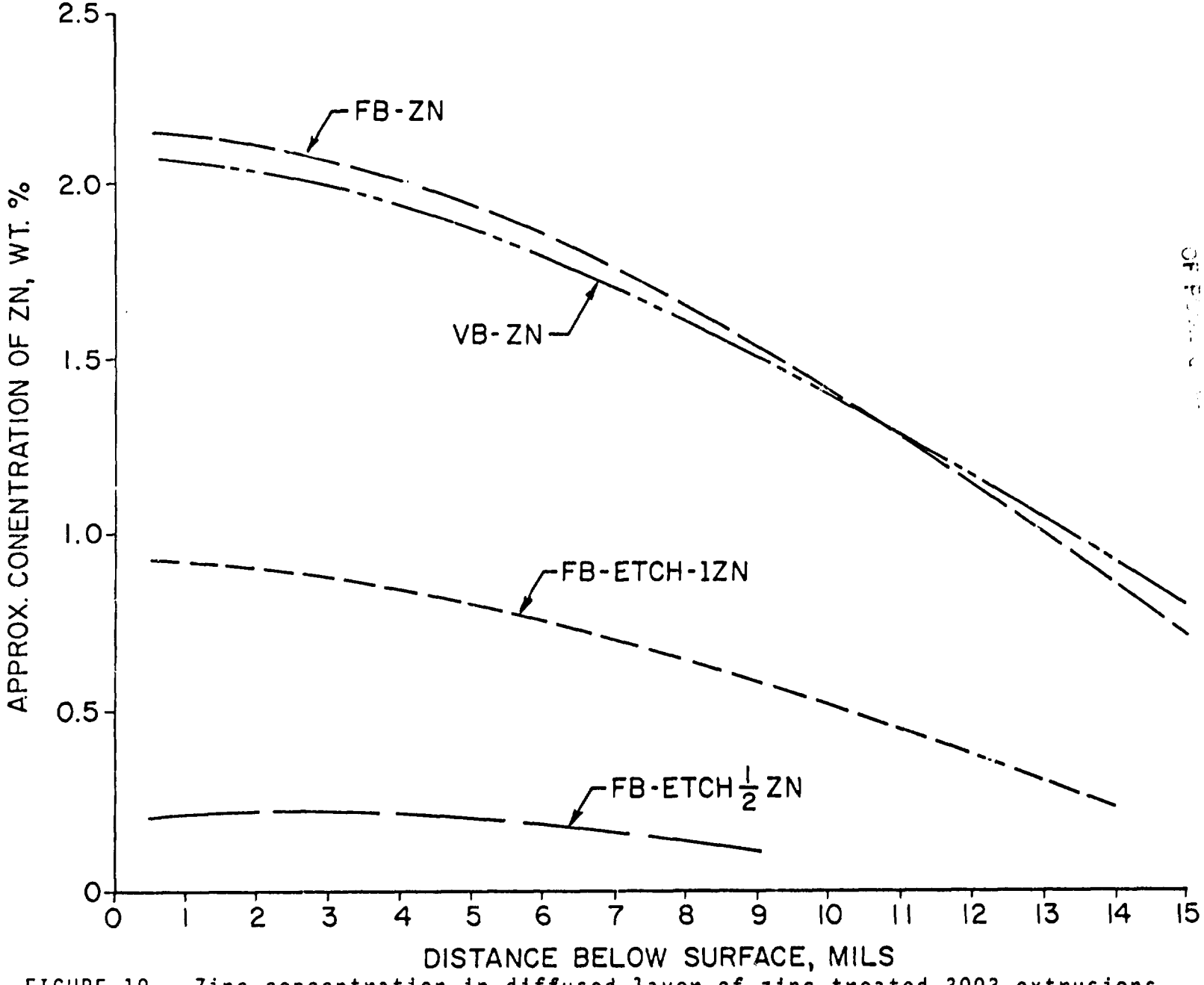

FIGURE 10. Zinc concentration in diffused layer of zinc treated 3003 extrusions.

FB-ZN

VB-ZN

FIGURE 11. Appearance of the zinc diffused layer on 3003 extrusion samples after etching (Poulton's Etchant). (The Etch does not reveal the full depth of zinc diffusion indicated by X-ray analysis). Magnification 100X for all photographs.

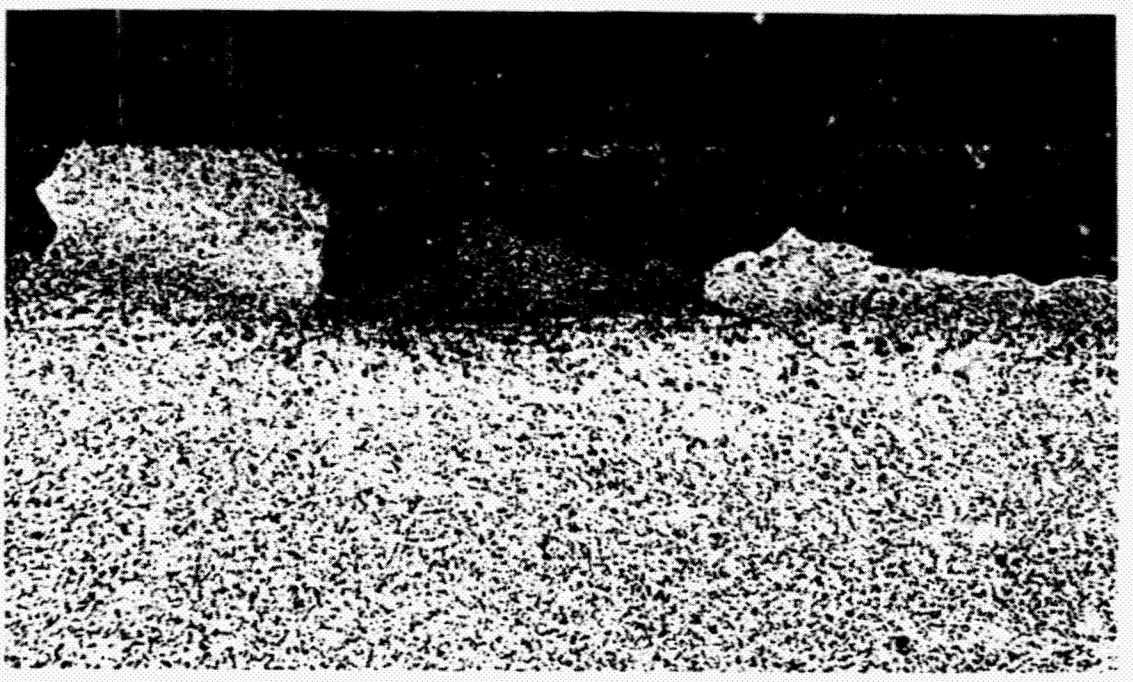

FB-ETCH-1ZN

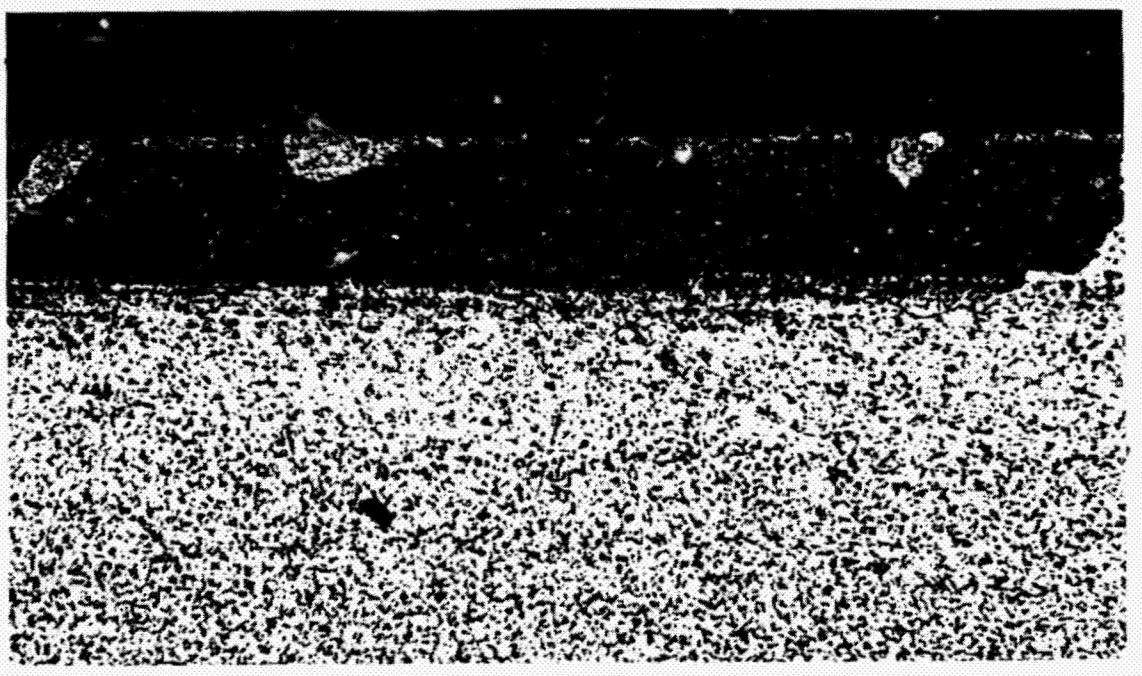

FB-ETCH-1/2 ZN

FIGURE 11. (continued from previous page)

corrosion rate of the diffused layer.

Bare RFW 3004 tubes and bare 3003 extrusions were included in the test as a baseline for evaluating the effectiveness of 7072 Alclad and of the zinc diffusion process. The 7072 Alclad also provided a baseline for evaluating the diffusion-zinc-treated material.

Measurements of the corrosion potential of the zinc diffused layer verses the 3003 alloy have confirmed that the diffused layer is anodic to 3003 and should provide galvanic protection to reduce pitting attack on the 3003 alloy. The potential difference between the diffused layer in the FB-ETCH-1ZN and 3003 ranges from about -70 mv at the surface to -10 mv (measured in 5.3% NaCl + 0.3% H_2O_2 solution) at about 0.25 mm (0.01 in) below the surface.

5. SAMPLE PREPARATION AND HANDLING

Kaiser weighed and prepared the 3004 RFW tubes and did the weight loss determinations on those tubes. Tube samples were 51 cm long, and each had an identification number scribed on it with a Vibrotool. The tubes were degreased with acetone, dried and weighed to the nearest 0.001 g on an analytical balance. A coating of Scotch 1602 Spray Sealer was applied 4.5 cm from both ends to minimize crevice corrosion at the fittings. To protect the tubes from external corrosion from salt spray, the outside surfaces were covered with shrink tubing or a wrap of vinyl electrician's tape (done by UPR personnel).

Trane was responsible for preparation and weight loss

determinations of the 3003 extrusions. Extrusion samples were 46 to 51 cm long. They were cleaned with methyl ethyl ketone and weighed to the nearest 0.01 gram. Sample ends were coated with an enamel sealer to minimize corrosion at the joints. Samples were then covered with heat shrinkable polyolefin tubing to prevent exterior corrosion.

In the flow loops, samples were joined together with molded fittings made from RTV 630 (a silicone rubber compound manufactured by General Electric) and did not come in direct contact with each other. Duplicate samples of the FB-ZN, VB-ZN and bare 3004 were removed after exposure periods of 5, 15, 30, 60, 105, 155 and 185 days. Single samples of the FB-BARE, FB-ETCH-1 ZN, FB-ETCH-1/2 ZN, 5% Alclad and 10% Alclad were removed after exposure periods of 5, 10, 30, 65, 105, 140 and 185 days. In addition, a replicate set of samples of FB-ZN, VB-ZN and single samples of 5% Alclad and 10% Alclad were exposed to chlorinated seawater. Following removal from the flow loops all samples were immediately rinsed in fresh water. The 3004 and Alclad samples were shipped to Kaiser Aluminum and Chemical Corporation and the 3003 extrusion samples were shipped to The Trane Company for weight loss determinations and examination.

When the 3004 tubes were returned from the test, the shrink tubing or tape wrap was removed, and the spray sealant coat was removed from the ends by soaking in warm methyl ethyl ketone, followed by an acetone/MEK wipe. Tubes were cleaned by immersion in 2% CrO_3/5% H_3PO_4 solution at 80°C for 10 minutes, as per ASTM G-1, rinsed in distilled water and acetone, and oven

dried prior to weighing.

At Trane, the polyolefin sleeves were removed from the samples and the enamel coating was stripped from the ends. Samples were cleaned in chromic-phosphoric acid at 80°C for eight minutes in accordance with ASTM G-1, "Preparing, Cleaning, and Evaluating Corrosion Test Specimens." After the extrusions were acid cleaned, they were rinsed and brushed in soapy water by three strokes with a nylon brush and rerinsed. These procedures successfully removed corrosion products from pits. Samples were dried 24 hours at room temperature and weighed to the nearest 0.01 gram. Average corrosion rates in mils per year were calculated by the procedure given in ASTM G-1:

$$\text{Average Corrosion Rate} = \frac{K \times W}{A \times T \times D}$$

where: $K = 3.45 \times 10^6$

W = mass loss in grams

A = exposed area in cm^2

T = exposure time in hours

D = 2.74 gm/cc - density of 3003 or
2.72 gm/cc - density of 3004

Samples were then bisected longitudinally to expose the interior surfaces which were examined visually to assess the type and extent of corrosion. At this point, portions of the

samples were exchanged between the two laboratories for independent evaluation of the type and extent of corrosion.

At the Kaiser laboratory, sections were examined under a low-power microscope, and macrophotos of representative samples were taken with a Polaroid MP-3 industrial camera. Pitted areas, where found, were examined in transverse metallographic cross section under a high-power microscope. General surface condition and the weld area were also examined in cross section. The metallographic samples were etched for 30 seconds in 5% HF/10% H_2SO_4 to disclose the 7072 clad layer. Sections of the Trane 3003 rectangular extrusions received by Kaiser were examined and sectioned in a similar fashion.

At the Trane laboratory, sample surfaces were examined at magnifications of 70X to determine the types and extent of corrosion. Representative areas of samples were studied further with a scanning electron microscope and x-ray spectrometer. Pit depths were measured by an optical microscope by focusing at the top and bottom of the pits and measuring the differential travel of the microscope or by direct measurement from photomicrographs of cross sections. Relationships between the corrosion and microstructure were studied on mounted and polished cross sections.

6. FOULING RESISTANCE

Heat transfer was measured using modified Carnegie-Mellon University (CMU) HTM's (Figure 12) and the STM. The HTM's were acquired from the National Data Buoy Office which had made two minor modifications to them: a) The pipe was moved lower in the housing and the flow meter was attached to the bottom of the housing where it could be easily removed to be cleaned or replaced. b) The signal amplifier card, which had originally been attached to the pipe inside the housing, was mounted in the "T" so that it was more accessible in the event that repairs or adjustments were needed.

The principle of the HTM "is to heat a segment of tube wall slightly above the water temperature and then to observe its cooling rate after the heat input is removed. The cooling curve (versus time) is exponential, according to Newton's law of cooling, with a time constant which is shown to be (apart from small, calculable corrections) inversely proportional to the heat transfer coefficient, h" (12). Cooling of the segment was measured by a thermocouple. The HTM also included a Ramapo Mark V strain gauge flow meter to monitor flow rates and a thermistor to monitor water temperature. Signals from the thermocouple, flow meter, and thermistor were amplified within the HTM. The output from the HTM was carried by shielded cable to a control box located in the data house. The control box, designed at CMU (13), multiplexed the three signals and output them to a computor at two second intervals. Data were stored on a magnetic disk.

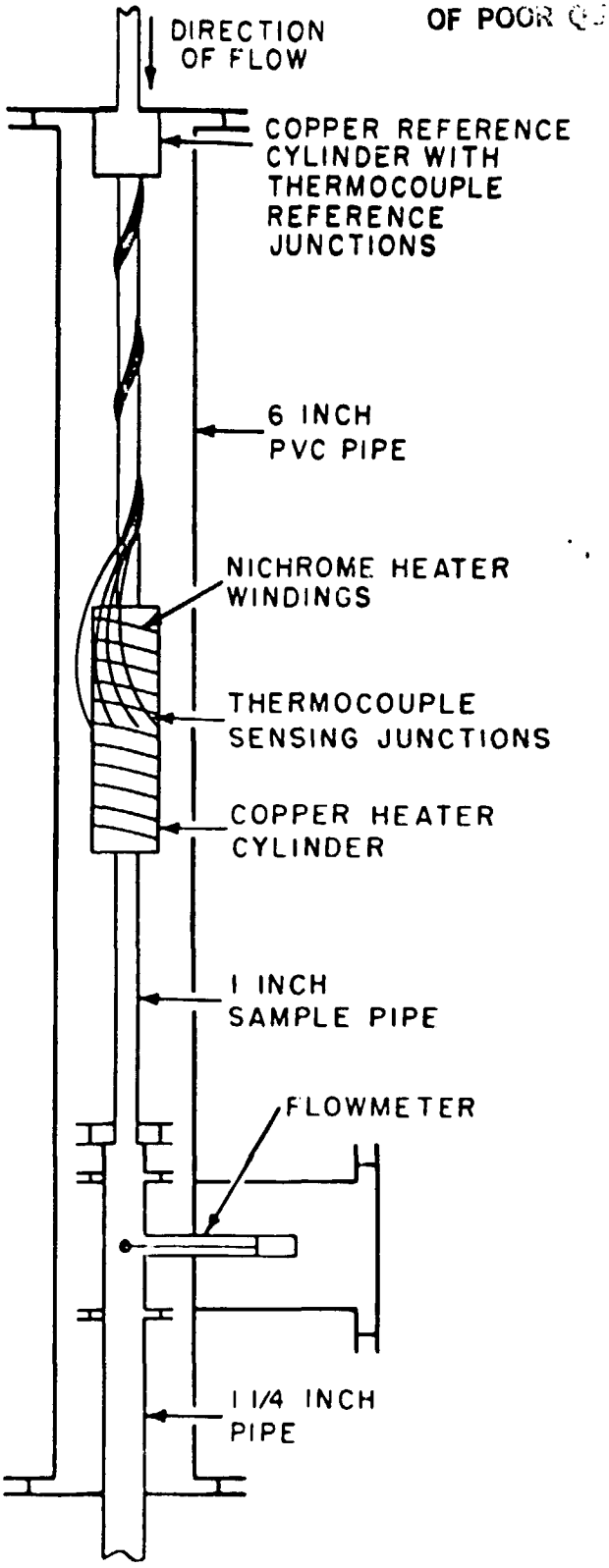

FIGURE 12. Carnegie-Mellon University Heat Transfer Monitor (HTM).

In the data analysis, a time constant was calculated for each cooling curve using a weighted, least-squares-fit program. The time constant along with physical parameters (flow rate, water temperature, tube dimensions, thermal conductivity, etc.) was used to calculate a normalized inverse heat transfer coefficient (1/h). The fouling resistance (R_f) was defined as 1/h minus the 1/h value calculated on the first day ($1/h_o$).

For major runs, made at seven to ten day intervals, one day's data for a unit consisted of at least ten cooling curves, of which eight were analyzed. At least one progress run, consisting of five cooling curves of which four were analyzed, was made between each major run.

Flow-meter and thermistor calibrations were verified whenever a major run was made. Flow meters were calibrated by measuring the fill time of a 38 liter bucket. Zero-flow voltage readings were taken at least twice during each run. Biofouling of the flow meter element was not a problem, but bivalves and serpulid worms did grow in the channel through which the strain gauge passed. This affected the calibration of the flow meters, so periodically it was necessary to disassemble and clean them.

7. CLEANING PROCEDURES.

When the fouling resistance exceeded 8.8×10^{-5} m^2-$^oK/W$ (5×10^{-4} ft^2-hr-^oF/Btu) the units and corrosion samples were cleaned manually with nylon bristle brushes . (The HTM's were used to estimate fouling resistance in the RFW tubes and the STM

was used to estimate fouling resistance in the extrusion samples.) To minimize abrasion of the sample surfaces, only four brush passes were used in cleaning. This resulted in about a 75% reduction in fouling resistance in the HTM's and, because a larger brush was used to clean the STM, about a 95% reduction in fouling resistance in the STM. After the first 60 days of the experiment, cleanings were performed at 10 to 20 day intervals on the RFW tubes and at approximatly 20 day intervals on the Trane extrusions.

Module 4 was chlorinated once a day for 28 minutes at a level of 0.5 ppm. The fouling resistance in this module remained essentially at zero for the entire six months of the experiment, therefore chlorinated samples were never brush cleaned.

8. MACROFOULING.

At the end of the experiment, the flow systems of units one (unchlorinated) and four (chlorinated) along with one intake strainer were dismantled. All macrofouling organisms encountered were preserved in formaldehyde for later analysis. In the laboratory, speciments were sorted and identified, and their wet weights (blot dried) were determined.

9. CORROSION RESULTS AND CONCLUSIONS

Corrosion results and conclusions from the Kaiser and Trane Laboratories are presented here independently.

9.1 KAISER

9.1.1 WEIGHT LOSS RESULTS. Table 3 summarizes the weight loss results for the RFW tubing. Most of the tubes showed varying degrees of salt spray attack on the outside surface at the ends and under the tape/shrink tube cover. Therefore, the true weight loss and hence, corrosion rate values, will be somewhat lower than reported, though probably not by more than a few percent.

Figure 13 displays the data graphically, plotting average corrosion rate (average of duplicate samples) as a function of time. Initial corrosion rates (after five days) ranged from 0.305 mm/yr (12 mils/yr) for the bare 3004 tubing to 0.432 mm/yr (17 mils/yr) for the 10% Alclad tubing. The corrosion rates dropped rapidly, converged after 30 days to 0.076 mm/yr (3 mils/yr) and decreased steadily thereafter. All three types of 3004 RFW tubing reached an average corrosion rate of about 0.015 mm/yr (0.6 mil/yr) when the test was terminated after 185 days.

The results demonstrate no effect of intermittent chlorination on corrosion rate (no bare Alclad types were tested in the chlorinated loops), nor was there any consistent increase in weight loss due to intermittent brushing.

The mode of corrosion was uniform surface attack, with pitting observed in only two of the 42 tubes tested (see below). The maximum weight loss observed on any of these tubes, about 1.0 g, converts to a loss of about 0.010 mm (0.4 mil) of tube thickness (i.e., less than 1 % of total wall thickness) for this six-month exposure, assuming uniform attack.

Table 3. Weight Loss and Corrosion Rate of RFV Tubing Exposed to Flowing Seawater

Exposure Days	Bare 3004			5% Alclad 3004			10% Alclad 3004		
	Wt. Loss** g.	Corr. Rate mdd	Corr. Rate mils/yr.	Wt. Loss** g.	Corr. Rate mdd	Corr. Rate mils/yr.	Wt. Loss** g.	Corr. Rate mdd	Corr. Rate mils/yr.
5	.389	21.9	11.7	.517	29.1	15.5	.635	35.8	19.0
	.400	22.5	12.0	.437*	24.6	13.1	.478*	26.9	14.4
5 Av.			11.9			14.3			16.7
10	-	-	-	.581	16.4	8.71	.846	23.8	12.7
	-	-	-	.557*	15.7	8.36	.892*	25.1	13.4
10 Av.						8.54			13.1
15	.445	8.4	4.47	-	-	-	-	-	-
	.454	8.5	4.52	-	-	-	-	-	-
15 Av.			4.50						
30	.497	4.7	2.50	.571	5.4	2.87	.636	6.0	3.19
	.490	4.6	2.45	.515*	4.8	2.55	.494*	4.6	2.45
30 Av.			2.48			2.71			2.82
60	.549 (8)	2.6	1.38	-	-	-	-	-	-
	.538 (8)	2.5	1.33	-	-	-	-	-	-
60 Av.			1.36						
65	-	-	-	.698 (8)	3.0	1.60	.905 (8)	3.9	2.08
	-	-	-	.693*	3.0	1.60	.921*+	4.0	2.13
65 Av.						1.60			2.11
90	.612 (24)	1.9	1.02	.649 (24)	2.0	1.08	.942 (24)	3.0	1.57
	N.D.(24)	-	-	.679*+	2.1	1.13	.907*	2.8	1.51
90 Av.			1.02			1.11			1.54
140	-	-	-	.729 (32)	1.5	0.78	1.003 (32)	2.0	1.08
	-	-	-	.728*	1.5	0.78	.992*	1.9	1.06
140 Av.						0.78			1.07
155	.707 (32)	1.3	0.68	-	-	-	-	-	-
	.709 (32)	1.3	0.68	-	-	-	-	-	-
155 Av.			0.68						
185	.763 (32)	1.1	0.62	.796 (32)	1.2	0.65	.764 (32)	1.1	0.62
	N.D.(32)	-	-	.758*	1.1	0.61	.737*	1.1	0.60
185 Av.			0.62			0.63			0.61

* = Chlorinated Seawater
** = Number of brush passes in parentheses
\+ = Some pits
N.D. - Not Determined; samples cut prior to cleaning for examination of surface deposit.

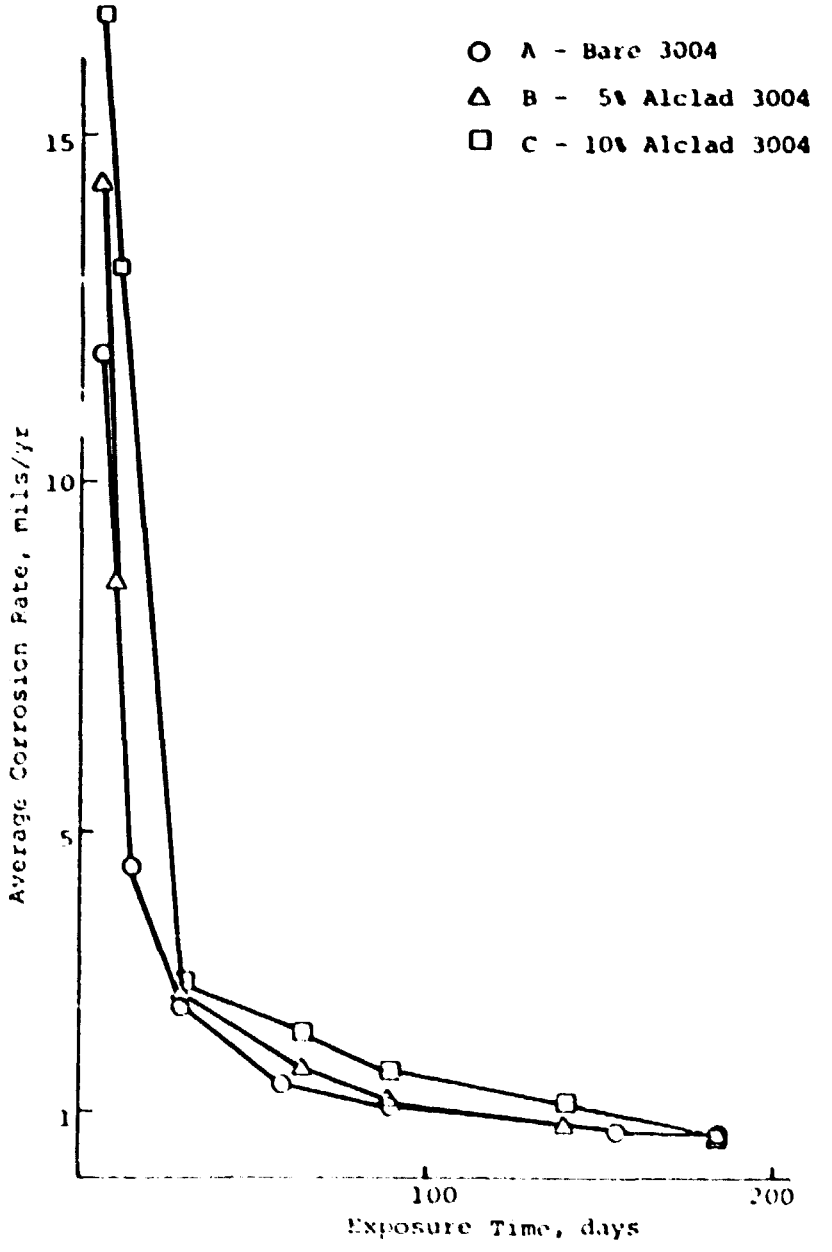

FIGURE 13. Corrosion rate vs time, RFW tubes in seawater flowing at 1.8 m/sec.

Table 4 displays the average corrosion rates in mils/yr for the six varieties of Trane extrusion as reported by their laboratory. The values are averages of replicates, grouping together both chloriated and unchlorinated exposure. These data are combined with the RFW results from Table 3 and displayed in Figure 14, which summarizes the corrosion rate vs. time behavior for all samples studied.

The RFW tubing (both bare and Alclad) values are displayed as points, and the values for the various Trane 3003 extrusions (with and without Zn-diffused surface treatment) are displayed as triangles. The graph shows a wide spread of initial corrosion rates after five days, from 0.076 mm/yr (3 mils/yr) for the Trane FB-Etch-1 Zn to 0.508 mm/yr (20 mils/yr) for the Trane FB-ZN-FE. With the exception of the Trane FB-ZN-FE tubing, the corrosion rates converge rapidly thereafter to a narrow spread of 0.013 to 0.018 mm/yr (0.5 to 0.7 mil/yr) after 185 days exposure. Thus, for the six-month period of exposure, the data show that bare and Alclad RFW tubing and the zinc protected tubing were all comparable in corrosion resistance. The Trane zinc-diffused plus iron material (FB-ZN-FE, open triangles on the graph) was susceptible to intergranular corrosion and appeared to corrode at a rate roughly twice the others.

Figure 15 is a comparison of the corrosion rate vs. time results for the bare 3004 RFW (as reported by Kaiser) and the bare 3003 rectangular extrusions (reported by Trane). The very close superimposition of the curves validates the cleaning,

Table 4. Corrosion Rate vs. Time, Trane 3003 Extrusions, mils/yr, Average of Replicates (Refs 4-6)

Exposure Time Days	VB-Zn	FB-Zn	FB-Etch-1 Zn	FB-Etch-4 Zn	FB-Zn-Fe	FB-Bare 3003
5	19.3	10.5	3.2	4.2	20.7	11.7
15	5.1	4.7	2.2	1.9	11.2	4.4
30	4.6	2.7	1.7	1.6	5.3	3.4
60	2.2	2.4	-	-	-	-
65	-	-	1.4	1.3	3.8	1.2
105	1.1	.84	.78	.80	1.6	.96
140	-	-	.74	.68	2.1	.83
185	1.4	.51	.65	.47	1.2	.57

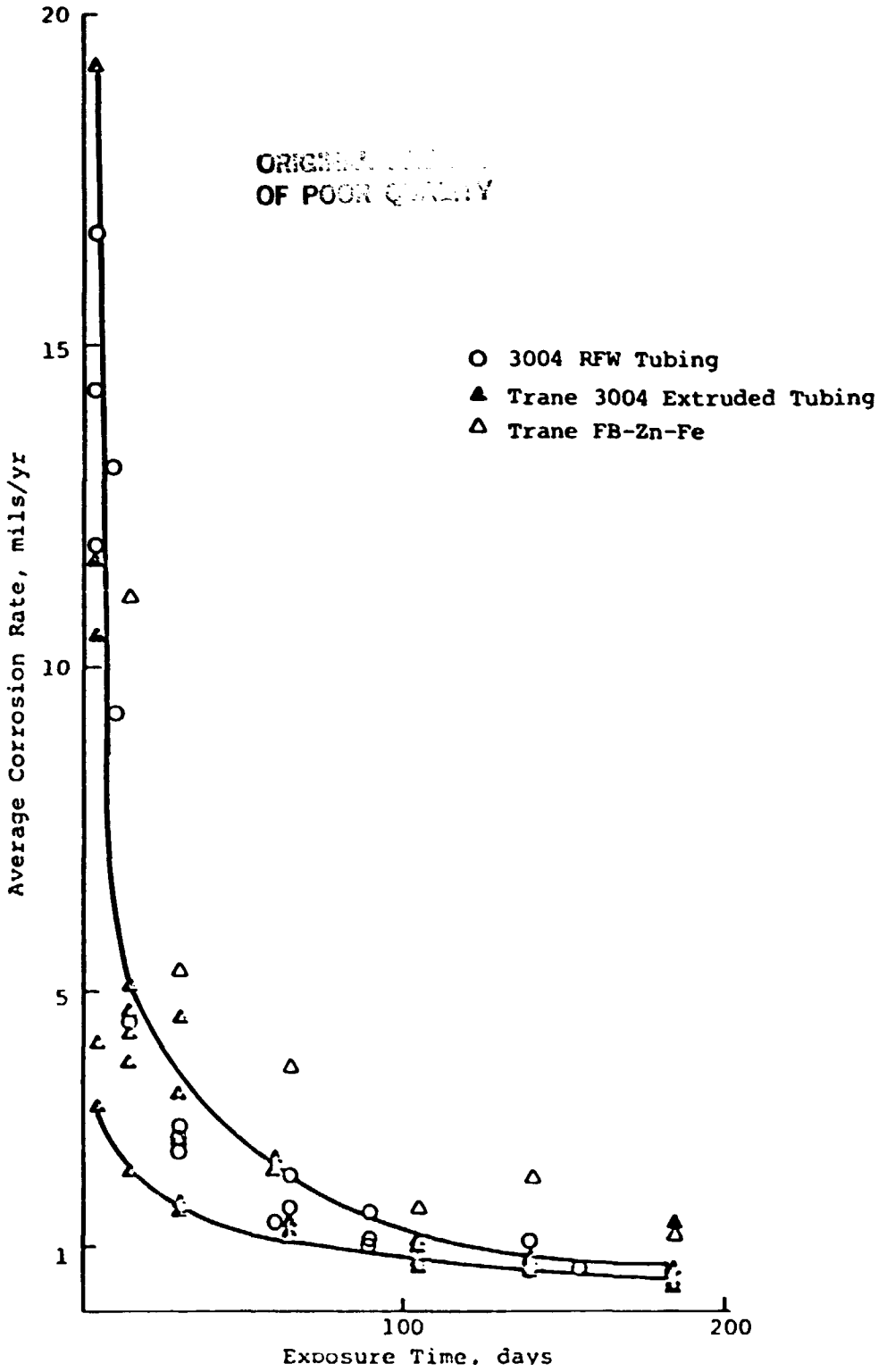

FIGURE 14. Corrosion rate vs. time, all aluminum samples.

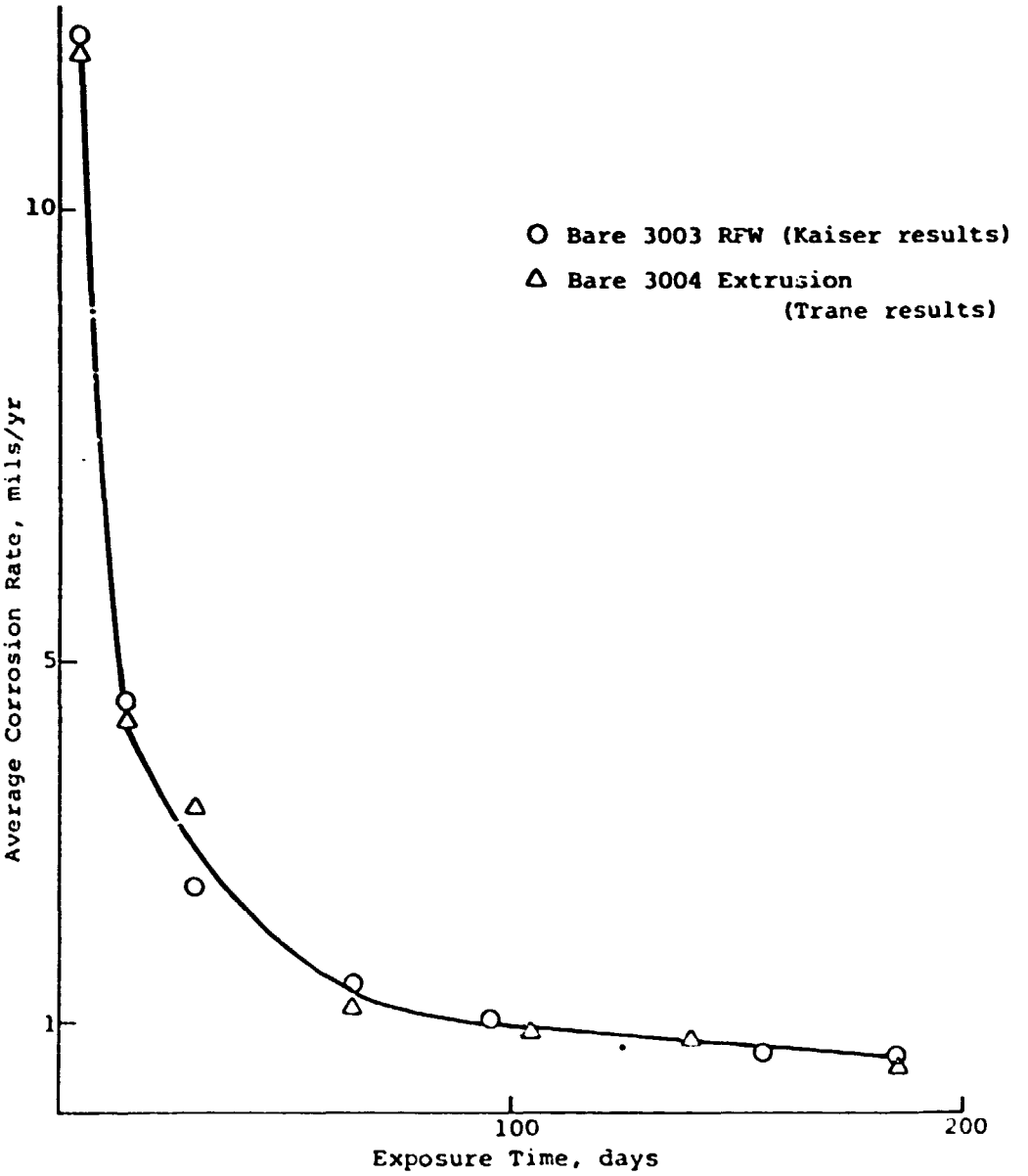

FIGURE 15. Comparison of corrosion rates of bare 3003 and bare 3004 tubing in seawater flowing at 1.8 m/sec.

weighing and calculation procedures between the two different laboratories, as one would expect these two bare alloys to corrode at essentially identical rates. It also suggests that the tube geometry (circular vs. rectangular cross section) had no effect on corrosion rate in this test.

9.1.2 SURFACE EXAMINATION

9.1.2.1 RFW TUBING. Figure 16a-c displays macro-photos of the inner surfaces of the three types of RFW tubing exposed for 185 days. Figure 17a-c displays 2X photos of the same tubes in the weld area. These samples typify the surface condition of all RFW tubes tested. Corrosion was uniform, with pitting observed in only two of the 42 tubes. There was no selective attack of the weld or heat-affected zone, and no evidence of cavitation or erosion-corrosion. Figure 18 displays 100X metallographic cross sections of the three types of RFW tubes after 185 days exposure, showing smoothly corroded surfaces and the absence of pitting.

Pitting was observed in two instances, both Alclad tubes. Tube C-6 (10% Alclad), exposed for 65 days to chlorinated seawater, had three pits near one end. A cross section of the deepest pit is shown in Figure 19a. The pit is 0.119 mm (4.7 mils) deep and confined to the 7072 clad layer. Figure 19b shows a cluster of pits observed near one end of tube B-30, exposed for 90 days to chlorinated seawater. The deepest pit is shown in cross section in Figure 19c. Depth was 0.061 mm (2.4 mils), and again the pitting was confined to the clad layer.

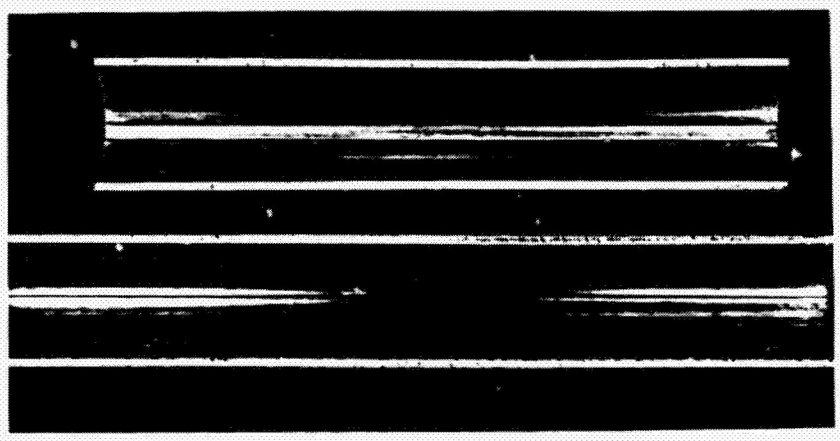

a. Bare 3004 (A-23) 32 brush passes

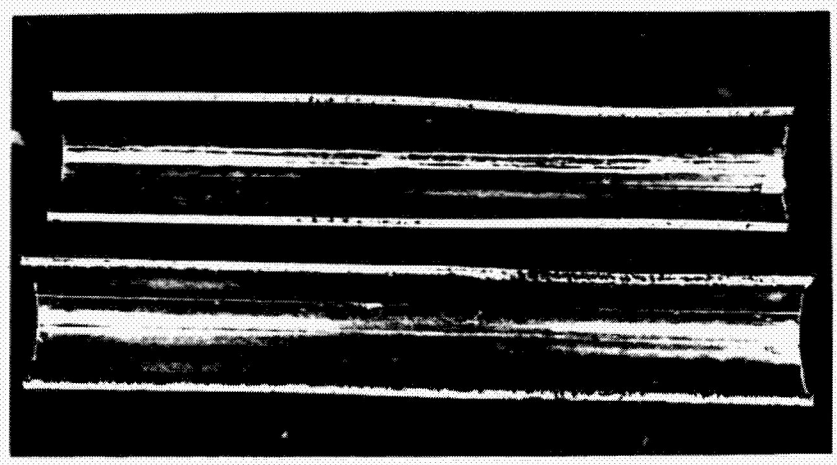

b. 5% Alclad 3004 (B-29) Chlorinated

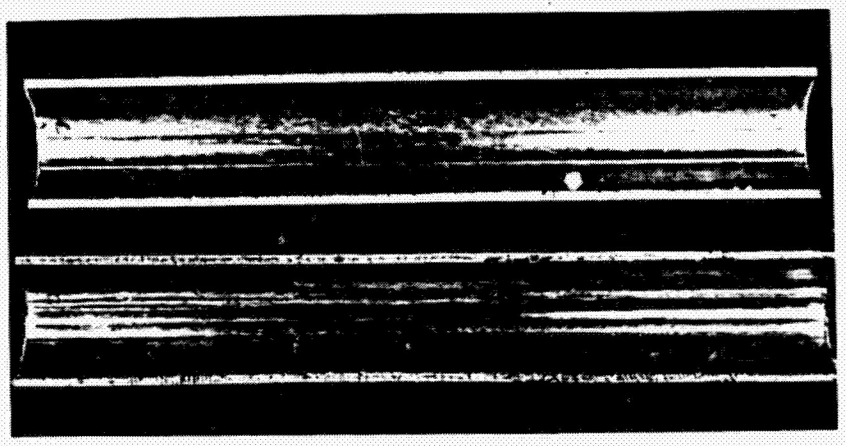

c. 10% Alclad 3004 (C-111) 32 brush passes

FIGURE 16. Surface appearance, RFW tubing, 185 days exposure. Magnification 0.6X.

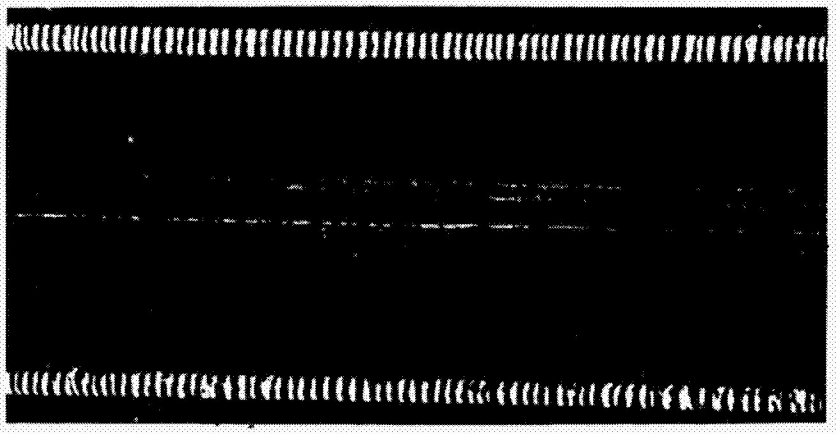

a. Bare 3004 (A-23) 32 brush passes

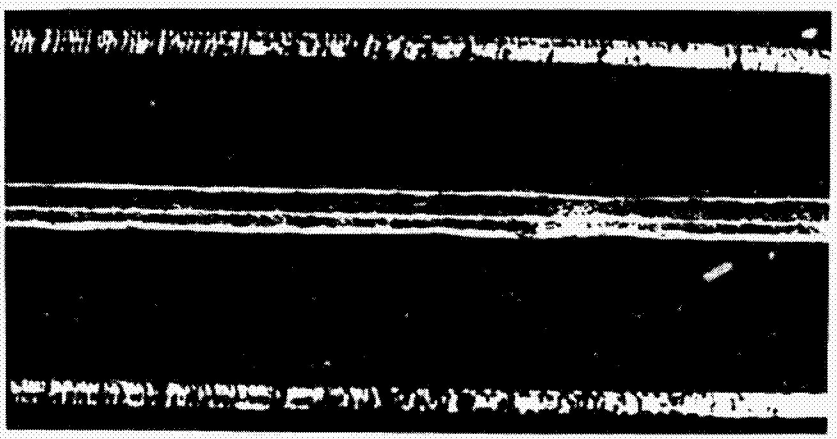

b. 5% Alclad 3004 (B-29) Chlorinated

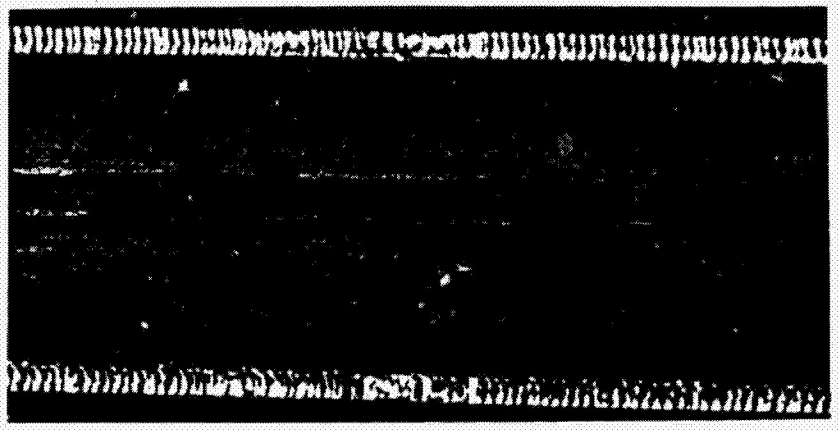

c. 10% Alclad 3004 (C-11) 32 brush passes

FIGURE 17. Surface appearance, RFW tubing, 185 days exposure, weld line, flow direction: left to right. Magnification 2X.

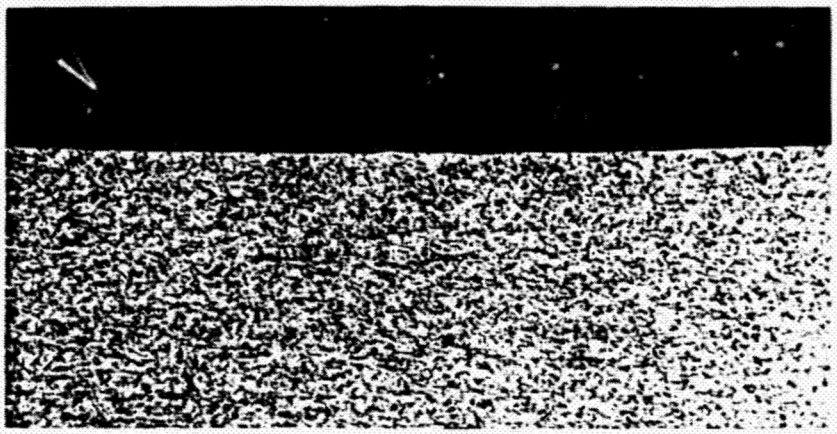

a. Bare 3004 (A-27) 32 brush passes

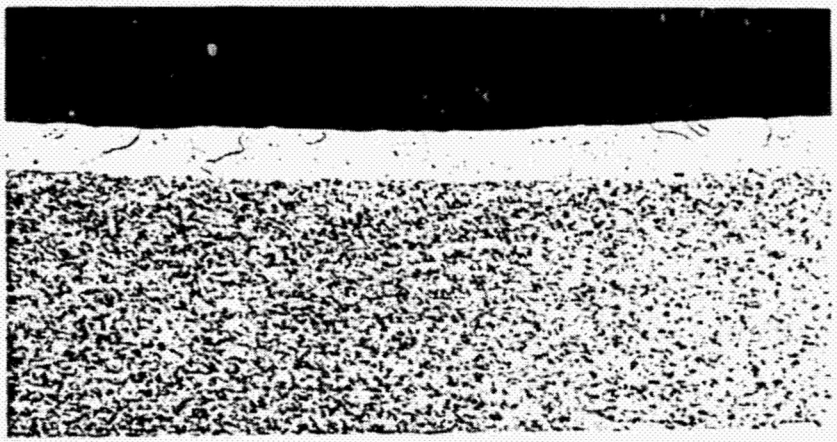

b. 5% Alclad 3004 (B-29) Chlorinated

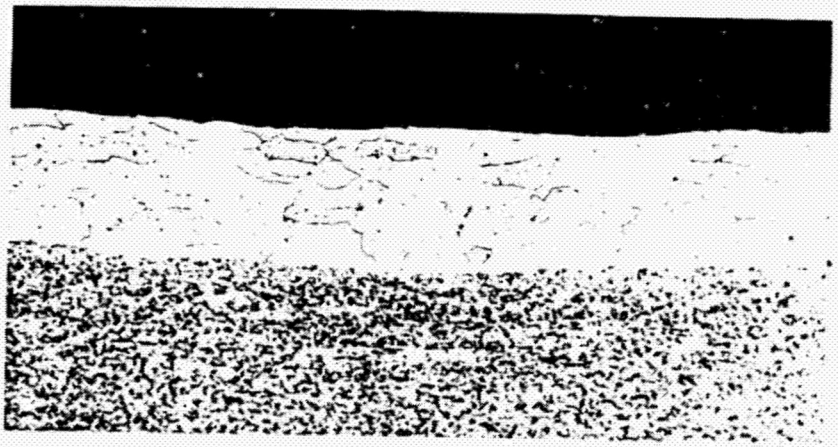

c. 10% Alclad 3004 (C-30) Chlorinated

FIGURE 18. RFW tubing, 185 days exposure, typical cross sections. Magnification 100X.

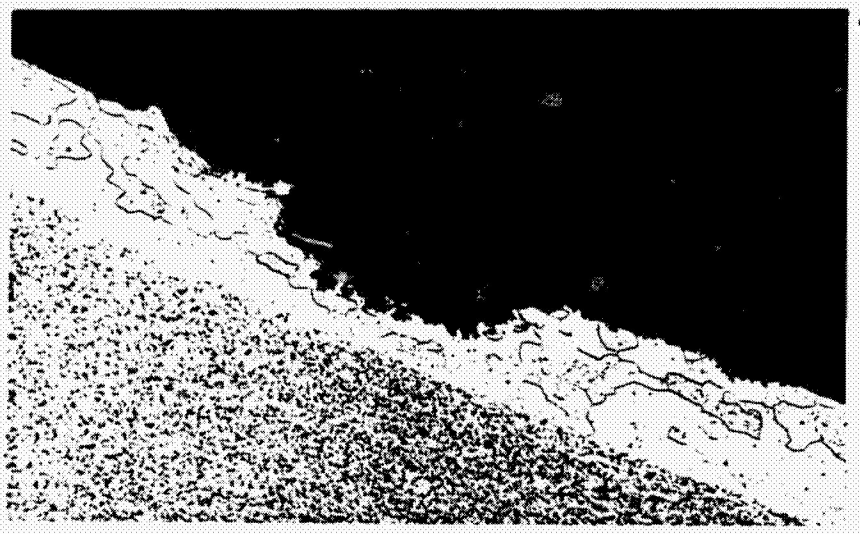

a. 10% Alclad 3004 (C-6) Transverse cross section 65 d. chlorinated

Deepest pit of three pits observed

Pit depth - 4.7 mils. Pitting is confined to 7072 clad layer.

b. 5% Alclad 3004 (B-30)

90 d., chlorinated

Cluster of pits near one end of tube.

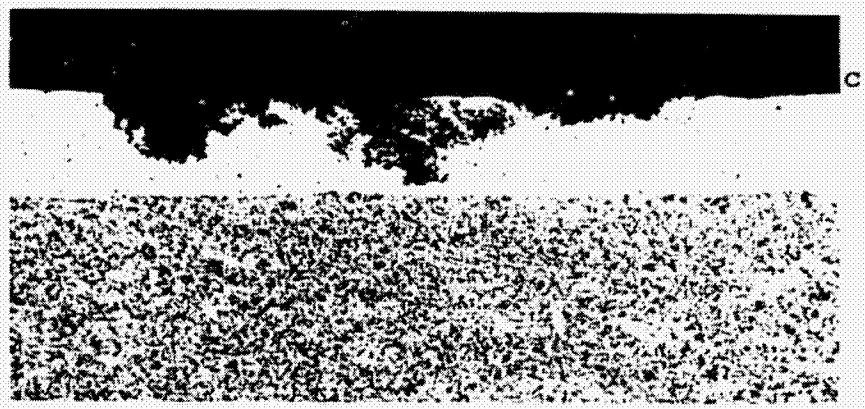

c. Transverse cross section deepest pit in (b) above

Pit depth - 2.4 mils. Pitting is confined to 7072 clad layer.

FIGURE 19. Pitting in RFW tubing. Magnification 200X.

The 2.54 cm (1 in) o.d. RFW tubes tested in this program were produced on prototype tooling using a heliarc welder. This method of fabrication produced crack fissures at the weld metal-tubing (or cladding) interface, typically 0.127 to 0.254 mm (5-10 mils) in length as shown in Figure 20a. Although these cracks might be expected to act as crevices, no selective attack was observed along the fissures in any of the tubes tested, as exemplified by Figure 20a. It should be noted, however, that on a production basis, tubes of this type would be fabricated using a high frequency AC induction welding method. This method produces a much narrower weld zone, and cracking at the weld edges does not occur. Figure 20b is a cross section of an induction weld produced on a 7.6 cm (3 in) o.d. Alclad 3004 tube, in which weld line cracks are absent.

9.1.2.2 TRANE EXTRUSIONS. Although Figure 14 demonstrates that all Trane materials except the FB-ZN-FE type exhibited comparable corrosion rates after six months exposure, there were marked differences in the mode of surface attack. The flux-brazed bare 3003 samples corroded uniformly, without pitting. The two low-zinc etched types (FB-ETCH-1/2 ZN, FB-ETCH-1 ZN) showed occasional shallow, scattered pitting, but the surface appearance overall was similar to that of the bare 3003. The FB-ZN type (2% ZN at the surface) showed more frequent shallow pitting, the pits strung out longitudinally. The VB-ZN type was more susceptible to pitting, with longitudinal grooving of the tube, often more severe along the bends and at the tube

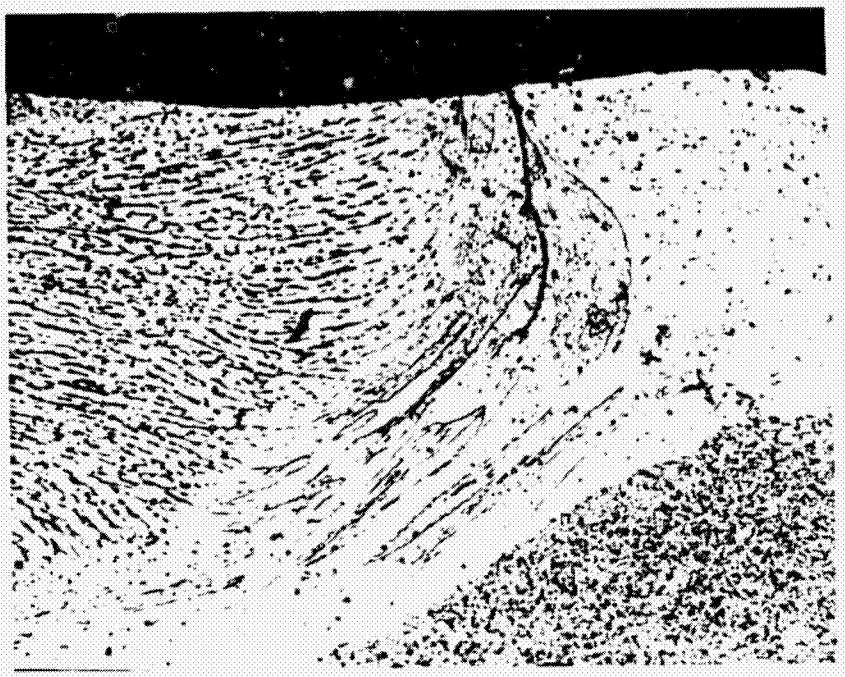

a. 10% Alclad 3004 (C-30) Weld crack in 1-inch heliarc welded RFW tubing.

185 d., chlorinated

Note absence of selective attack of weld, HAZ or crack crevice.

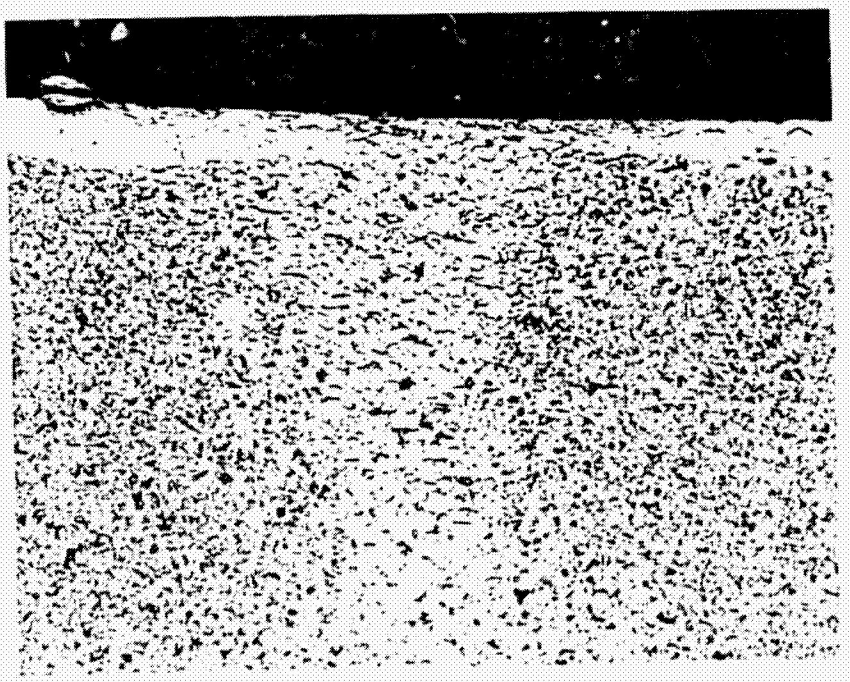

b. High-frequence AC induction weld in 3-inch Alclad RFW tubing.

Note narrow weld zone snd absence of cracks.

FIGURE 20. Weld cross sections, heliarc and induction welded RFW tubing. Magnification 200X.

ends. The FB-ZN-FE type, which exhibited the highest corrosion rates throughout, had the roughest surfaces, as this variety was slightly susceptible to intergranular attack.

Figure 21a-d displays macrophotos of four varieties of the Trane extrusions after 185 days exposure, and Figure 22a-c displays 2X photos of typical surface condition for the three zinc protected types most susceptible to pitting attack. Figure 23a-d displays transverse metallographic cross sections of four of the Trane extrusions. Note particularly the broad, deep (0.198 mm or 7.8 mils) pitting in the VB-ZN sample, and the intergranular attack in the FB-ZN-FE variety.

9.1.3 CONCLUSIONS

1) Average corrosion rates of various types of bare, Alclad and diffused zinc protected aluminum tubing converged to a low value of about 0.015 mm/yr (0.6 mil/yr) after six months exposure to seawater flowing at 1.8 m/sec (6 fps).

2) No pitting was observed in either bare 3003 or bare 3004 aluminum after six months exposure to 1.8 m/sec seawater.

3) Pitting which did occur in the Alclad or zinc-protected tubing did not penetrate to the base metal after six months exposure; hence the efficacy of the corrosion protection afforded by these anodic layers could not be determined in this test.

4) There was no selective attack of the weld metal or heat affected zone in the RFW tubing.

5) The diffused zinc material which contained [illegible] in the

a. FB-Bare 3003 (11)

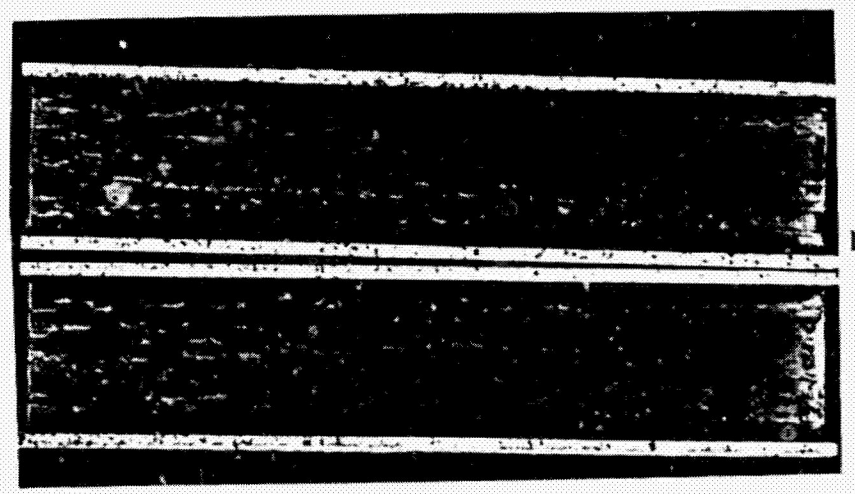

b. FB-Zn 3003 (FG-2) Chlorinated

FIGURE 21. Surface appearance, Trane 3003 extrusions, 185 days exposure. Magnification 0.7X.

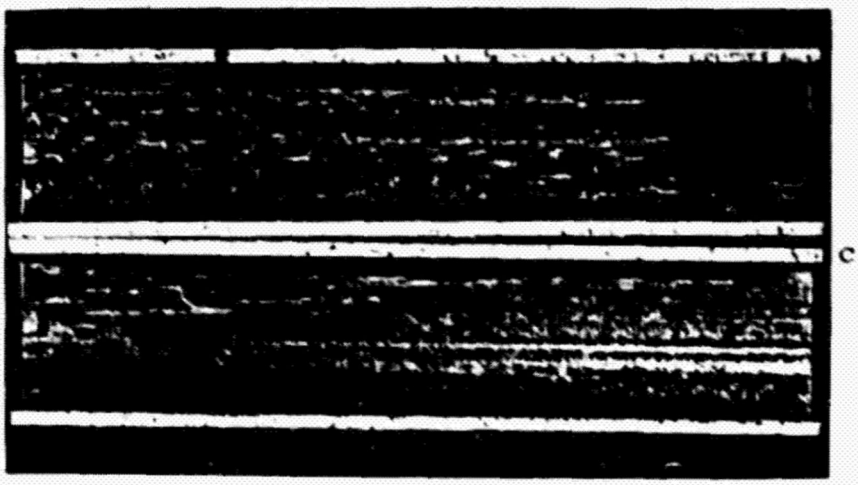

c. VB-Zn 3003 (ZV-10 chlorinated

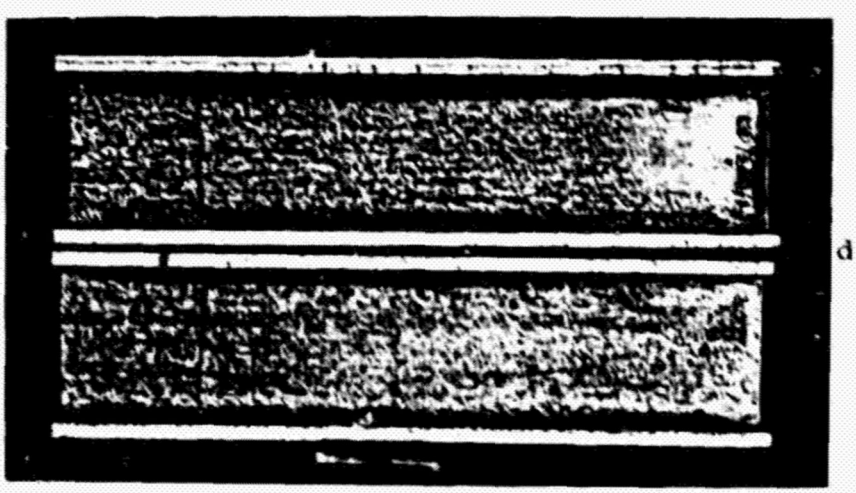

d. FB-Zn-Fe (F-10-2 Chlorinated

FIGURE 21. Surface appearance, Trane 3003 extrusions, 185 days exposure. Magnification 0.7X. (Continued)

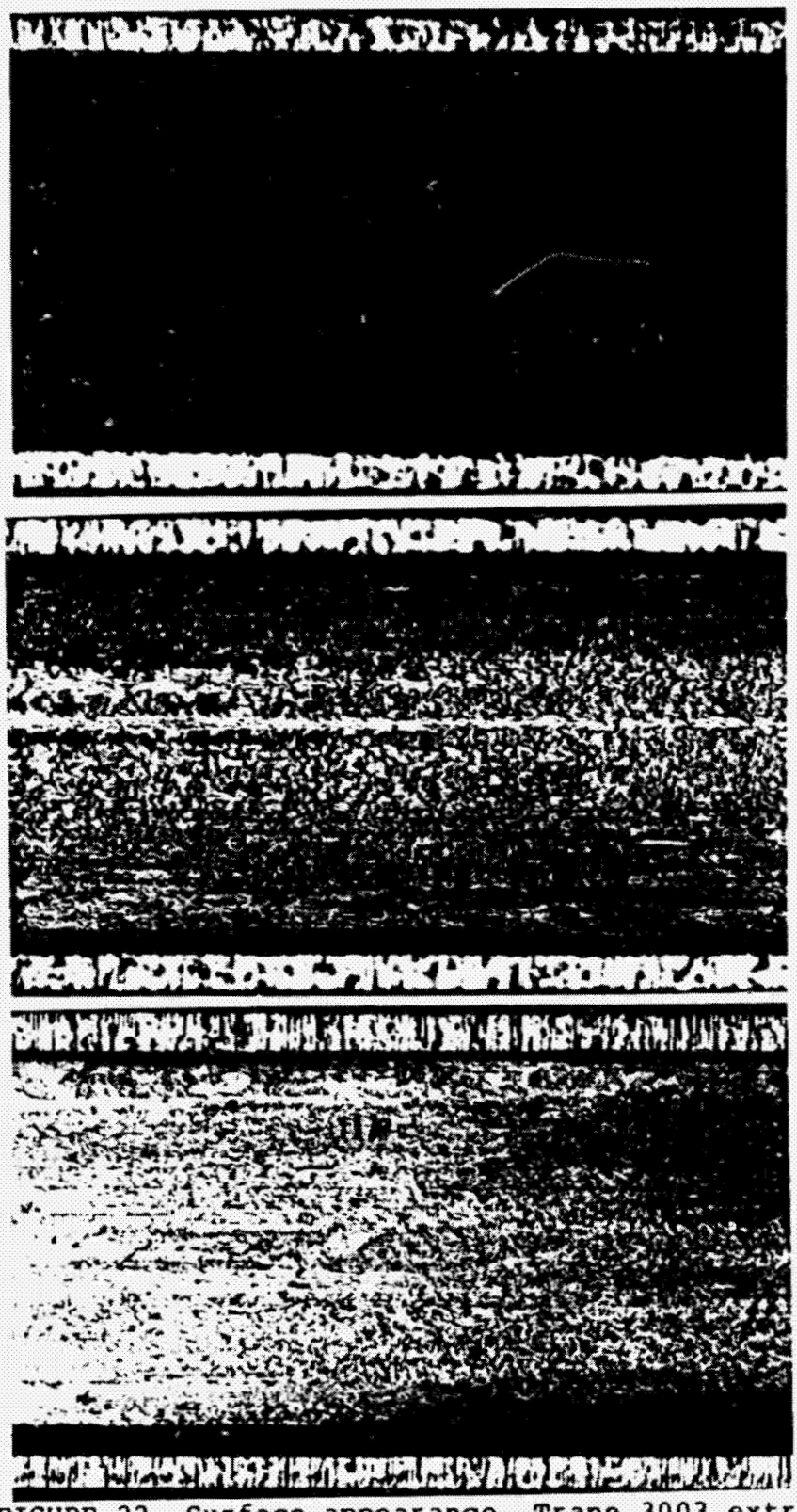

a. FB-Zn (GF20-2) Chlorinated

b. VB-Zn (AV16-2) Chlorinated

c. FB-Zn-Fe (F14-2)

FIGURE 22. Surface appearance, Trane 3003 extrusions, 185 days exposure. Flow direction left to right. Magnification 2X.

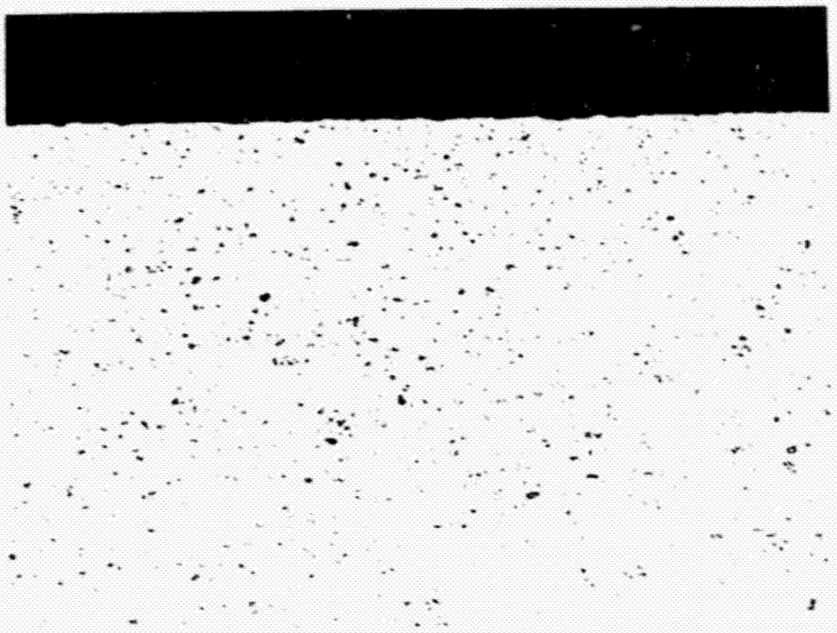

a. FB-Bare (7) 65 d.

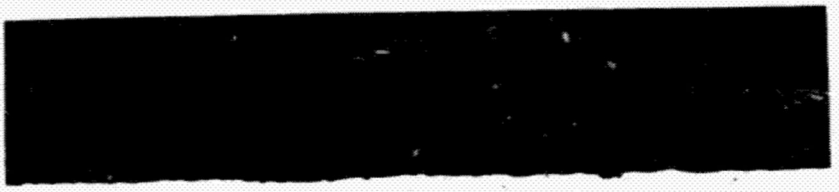

b. FB-Zn (F14-4) 185 d.

FIGURE 23. Trane 3003 extrusions, typical cross sections. Magnification 100X.

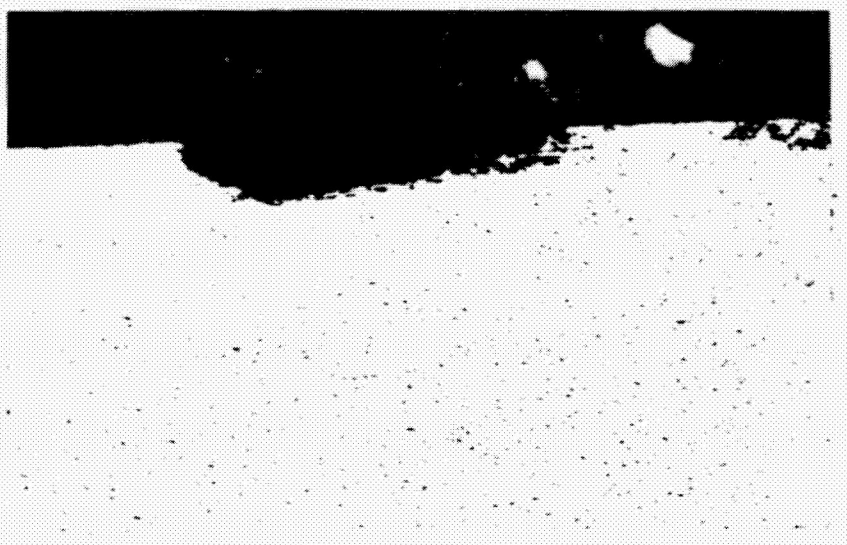

c. VB-Zn (AV-10)

185 d.

Pit depth - 7.8 mils

d. VB-Zn-Fe (F-10-2)

185 d.

Intergranular attack, max. depth - 4.7 mils

FIGURE 23. Trane 3003 extrusions, typical cross sections. Magnification 50X. (Continued)

zinc-rich layer (Trane FB-Zn-Fe) was susceptible to intergranular corrosion and corroded at a higher rate than the other materials.

6) Biofouling countermeasures (intermittent chlorination or brushing) did not affect the corrosion rate or type of attack on the materials studied.

9.2 TRANE

9.2.1 ALL MATERIALS. Corrosion rates of samples exposed to unchlorinated sea water are shown in Figure 24 and are given in Table 5. As shown in Figure 24 corrosion rates of all the aluminum materials varied widely after 5 days but converged rapidly to a narrow range after about 30 days. Corrosion rates of all the materials declined to 0.013 to 0.025 mm/yr (0.5 to 1.0 mil/yr) after 185 days exposure. This marked decrease in corrosion rates with increasing exposure time is in good agreement with previous tests on sea water corrosion of aluminum alloys. Corrosion data for FB-ZN-FE material were not included in Figure 24 because average corrosion rates do not properly represent this material that had significant intergranular corrosion.

The data in Figure 24 for Bare 3003 and Bare 3004 determined by Trane and by Kaiser, respectively, are in excellent agreement. This agreement shows that procedures used by the two laboratories produced comparable results.

Figure 24 also shows that corrosion rates of all the materials were not affected by periodic brushing to remove

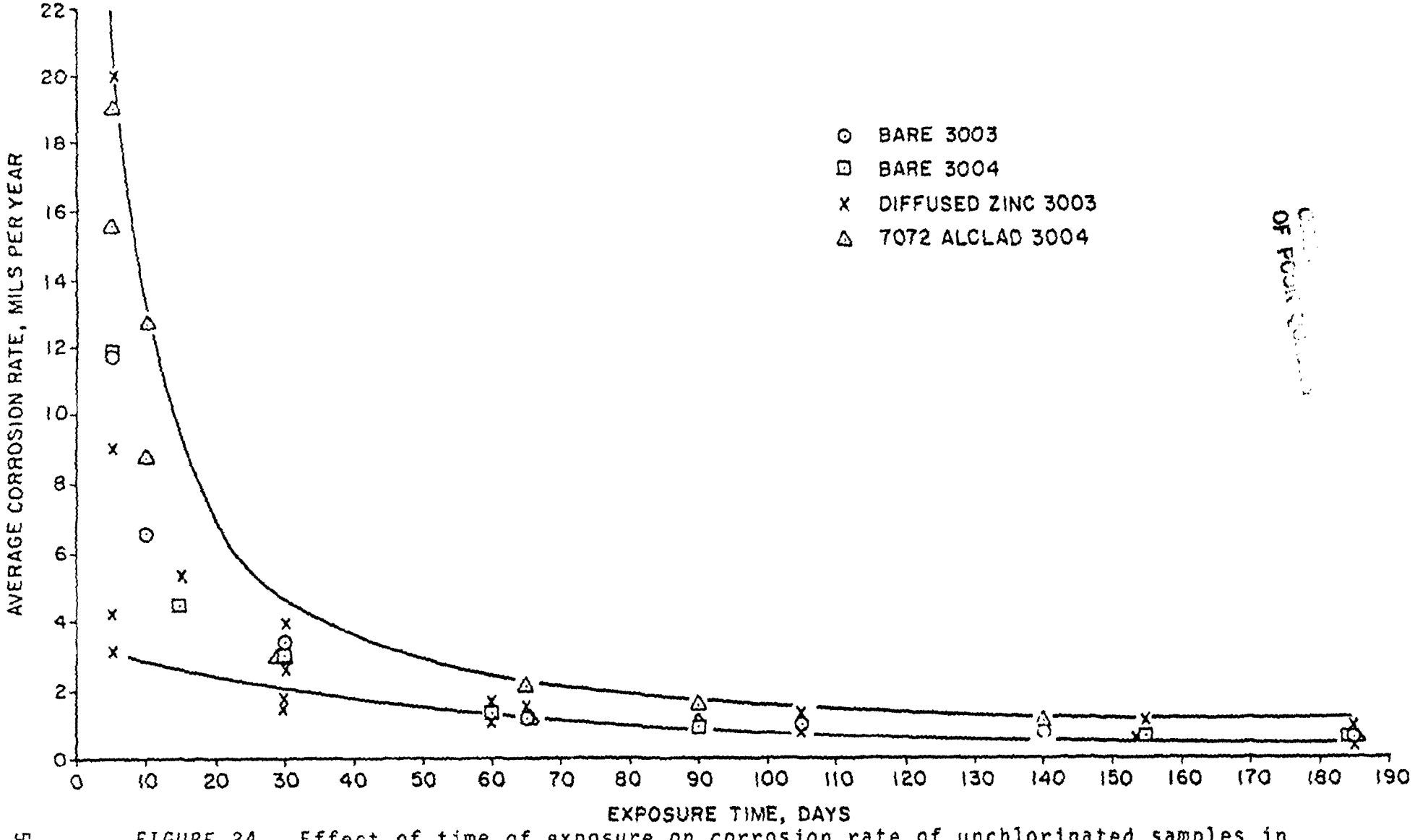

FIGURE 24. Effect of time of exposure on corrosion rate of unchlorinated samples in seawater flowing at 1.8 m/sec.

TABLE 5.

WEIGHT LOSS AND CORROSION RATES MEASURED ON SPECIMENS AFTER EXPOSURE IN SEA WATER FLOWING AT SIX FEET PER SECOND

SAMPLE IDENTIFICATION	EXPOSURE, DAYS	WEIGHT LOSS, GMS	AVERAGE CORROSION RATE, MPY
		FB-BARE 3003	
GF-18-1	5	0.47	11.7
8	10	0.53	6.6
GF-14	30	0.82	3.4
7	65	0.61	1.2
GF10-1	105	0.81	1.0
GF10-2	140	0.93	0.8
11	185	0.85	0.6
		FB-ZN	
F12-3	5	0.46	8.3
GF8-3	5	0.39	9.7
GF20-4	5 cl[a]	0.42	10.5
GF12-3	5 cl[a]	0.41	10.2
GF16-2	15	0.79	6.6
GF16-1	15	0.52	4.3
GF4	15 cl[a]	0.57	4.7
CF14	15 cl[a]	0.40	3.3
B16-2	30	0.45	1.9
GF2-2	30	0.80	3.3
F10-4	30 cl[a]	0.80	3.3
F4-2	30 cl[a]	0.50	2.1
AF20-1	60	0.72	1.5
GF18-3	60	0.55	1.1
AF18	60 cl[a]	2.04	4.2
GF16	60 cl[a]	1.25	2.6
CF14-1	105	0.70	0.8
GF20-3	105	0.80	0.9
GF8	105 cl[a]	0.63	0.8
CF20	105 cl[a]	-	-
GF10-3	155	1.01	0.8
CF20-3	155	0.8	0.6
GF12	155 cl[a]	-	-
GF2-1	155 cl[a]	0.84	0.7
F14-4	185	0.61	0.4
GF6	185	0.63	0.4
GF20-2	185 cl[a]	1.02	0.7
GF2	185 cl[a]	0.72	0.5

SAMPLE IDENTIFICATION	EXPOSURE, DAYS	WEIGHT LOSS, GMS	AVERAGE CORROSION RATE, MPY
		VB-ZN	
AV2	5	0.74	18.5
AV20-1	5	0.85	21.2
AV14-1	5 cl(a)	0.52	13.0
AV2-1	5 cl(a)	0.98	24.4
V8-1	15	0.31	2.3
V14-2	15	1.15	8.6
DV12-2	15 cl(a)	0.72	5.4
V18	15 cl(a)	0.57	4.3
AV16	30	1.14	4.7
AV20	30	0.79	3.3
AV14	30 cl(a)	0.93	3.9
AV12	30 cl(a)	1.52	6.3
DV12	60	0.86	1.6
DV20-3	60	0.79	1.5
DV4-2	60 cl(a)	2.39	4.5
V14-1	60 cl(a)	0.70	1.3
DV2-2	105	1.26	1.3
V10-2	105	1.13	1.2
V18-2	105 cl(a)	0.71	0.8
DV20-2	105 cl(a)	-	-
AV6	155	2.24	1.8
V18-1	155	0.75	0.6
V10-1	155 cl(a)	-	-
DV2	155 cl(a)	-	-
AV10	185	1.68	1.1
AV16-1	185	1.37	0.9
AV16-2	185 cl(a)	2.87	Sample Not Clean
AV8	185 cl(a)	1.2	0.8
		FB-ETCH-1ZN	
CF14-2	5	0.13	3.2
BF2-3	10	0.26	3.2
AF8-3	30	0.41	1.7
GF4-3	65	0.6	1.3
F12-2	105	0.66	0.8
GF6-3	140	0.83	0.7
CF20-1	185	0.96	0.7
		FB-ETCH-1/2ZN	
AF8-R	5	0.17	4.2
BF8-R	10	0.48	6.0
BF6-R	30	0.38	1.6
F16-R	65	0.62	1.2
BF2-R	105	0.67	0.8
BF8-R	140	0.76	0.7
F4-R	185	0.70	0.5

SAMPLE IDENTIFICATION	EXPOSURE, DAYS	WEIGHT LOSS, GMS	AVERAGE CORROSION RATE, MPY
		FB-ZN-FE	
F16-3	5	0.83	20.7
AF6-1	10	1.35	16.8
GF18-2	30	1.28	5.3
BF4-1	65	1.83	3.5
F14-3	105	1.37	1.6
F14-2	140	2.38	2.1
F10-2	185	1.81	1.2
		Bare 3004	
A16	5	0.389	11.7
A7	5	0.400	12.0
A4	15	0.445	4.5
A21	15	0.454	4.5
A8	30	0.497	2.5
A6	30	0.490	2.5
A9	60	0.549	1.4
A17	60	0.538	1.3
A12	90	0.612	1.0
A11	90	-	-
A2	155	0.707	0.7
A28	155	0.709	0.7
A27	185	0.763	0.6
A23	185	-	-
		5% Alclad 3004	
B11	5	0.517	15.5
B24	5 cl[a]	0.437	13.1
B5	10	0.581	8.7
B4	10 cl[a]	0.557	8.4
B1	30	0.571	2.9
B23	30 cl[a]	0.515	2.6
B3	65	0.698	1.6
B26	65 cl[a]	0.693	1.6
B25	90	0.649	1.1
B30	90 cl[a]	0.679	1.1
B28	140	0.729	0.8
B8	140 cl[a]	0.728	0.8
B7	185	0.796	0.6
B29	185 cl[a]	0.758	0.6
		10% Alclad 3004	
C19	5	0.635	19.0
C7	5 cl[a]	0.478	14.4
C3	10	0.846	12.7
C25	10 cl[a]	0.892	13.4

SAMPLE IDENTIFICATION	EXPOSURE, DAYS	WEIGHT LOSS, GMS	AVERAGE CORROSION RATE, MPY
C10	30	0.636	3.19
C13	30 cl[a]	0.494	2.45
C14	65	0.905	2.08
C6	65 cl[a]	0.921	2.3
C8	90	0.942	1.6
C27	90 cl[a]	0.907	1.5
C12	140	1.003	1.1
C5	140 cl[a]	0.992	1.1
C11	185	0.764	0.6
C30	185 cl[a]	0.737	0.6

(a) Sample was exposed to sea water chlorinated to 1/2 ppm for 28 minutes per day.

biofouling. Samples were brushed at about 20 day intervals after 60 days of exposure. Apparently, protective oxides on the samples were not removed by the brushing treatment which was used to maintain thermal resistance within the limits of 1.7 x 10^{-5} to 8.8 x 10^{-5} m^2-$^oK/W$ (1 x 10^{-4} to 5 x 10^{-4} ft^2-hr-^oF/Btu.

Similarly, corrosion rates of the 3003 with diffused zinc and of 7072 alclad 3004 materials were not affected by chlorination at 0.5 ppm for 28 minutes per day to prevent biofouling as shown in Figure 25.

9.2.2 3003 WITH DIFFUSED ZINC. Corrosion rates for samples with diffused zinc are shown on an expanded corrosion rate scale in Figure 26. As shown in Figure 26, initial corrosion rates for the FB-ZN material were significantly higher than corrosion rates for the FB-ETCH-1/2 ZN and FB-ETCH-1ZN materials. However, corrosion rates for all three materials declined to similar low values after about 40 days exposure. The higher corrosion rate for the FB-ZN material probably resulted from increased corrosion of the surface layer with about 45% zinc and from slightly more pitting attack compared with the etched samples. That the samples with diffused zinc contents ranging from less than 0.5% to about 2% near the surface corroded at similar rates after extended exposure time shows the rate is insensitive to zinc content in the range studied. (However, after pits penetrate the diffused zinc layer subsequent corrosion rates of the layer by galvanic action will probably depend on the zinc concentration).

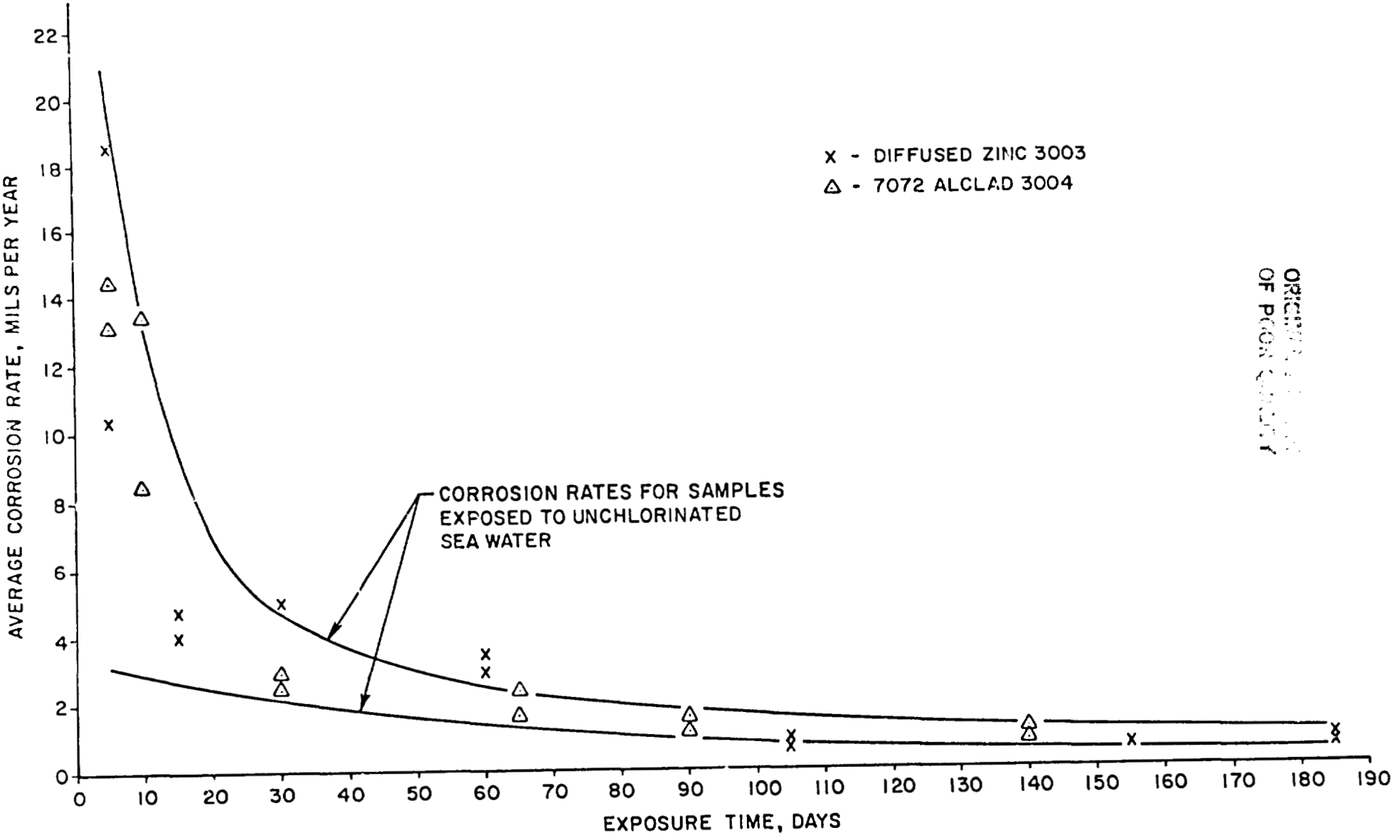

FIGURE 25. Effect of chlorination on corrosion rate of 3003 with diffused zinc and of 7072 Alclad 3004.

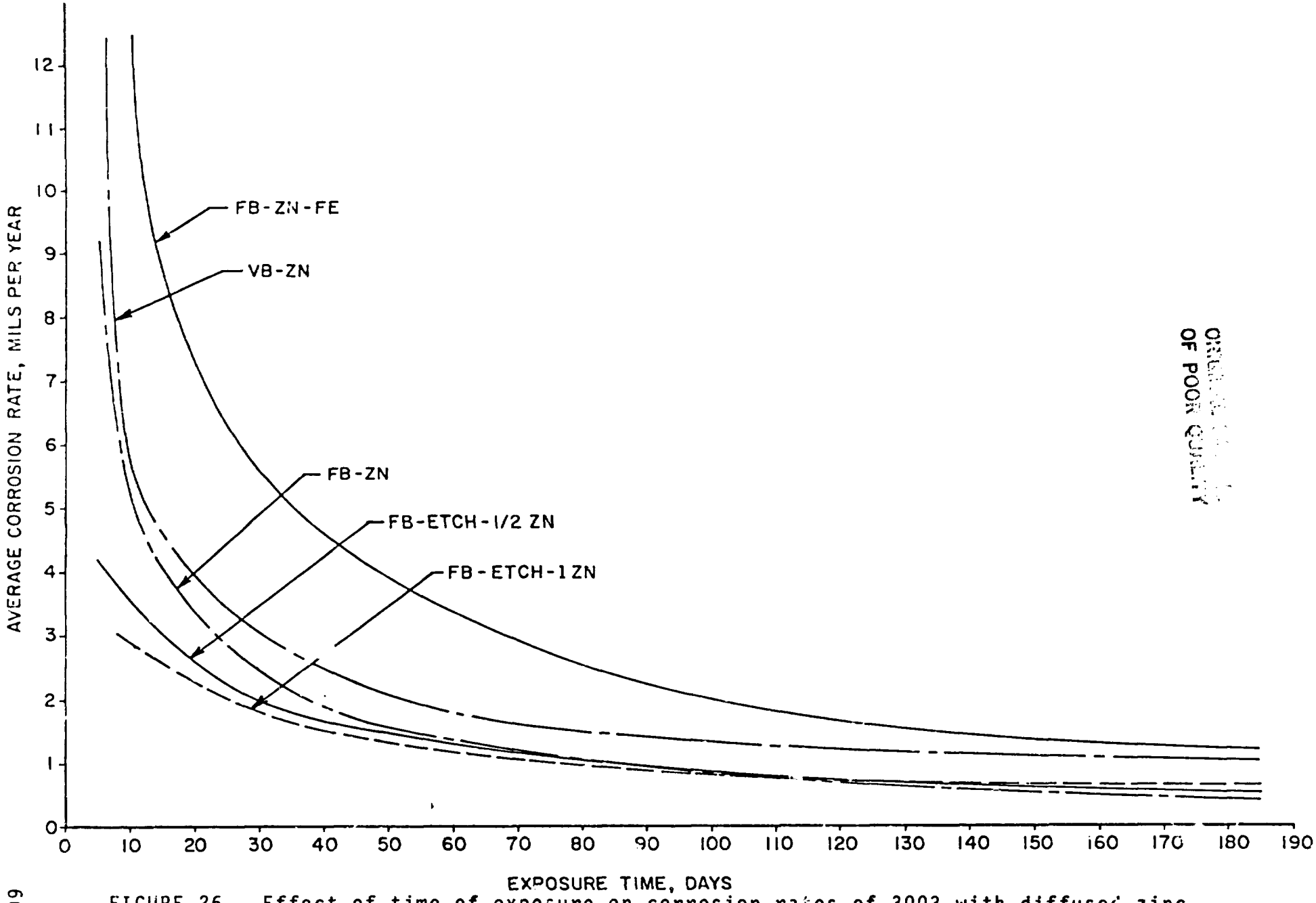

FIGURE 26. Effect of time of exposure on corrosion rates of 3003 with diffused zinc.

Corrosion rates for the VB-ZN material were slightly above rates for the FB-ZN materials for all exposure times. However, the difference in corrosion rates is not considered sufficiently great to preclude use of the vacuum brazing process for fabricating heat exchangers. Cause of the slightly higher corrosion rate for the vacuum brazed material was not determined.

The apparent corrosion rate curve for the FB-ZN-FE material is included in Figure 26 to illustrate that apparent corrosion rates for the zinc diffused layer with low iron content were significantly above rates for the FB-ZN material with a similar zinc concentration but without addition of iron. Low iron content in the diffused zinc layer in aluminum did not retard sea water corrosion as residual iron in zinc anodes does.

Types of corrosion present on the 3003 extrusion samples are summarized in Table 6. Corrosion on samples after 185 days exposure are shown in Figures 27-44. The 3003 alloy samples without diffused zinc corroded by uniform attack. While some areas exhibited slightly localized attack after 185 days exposure, no pits were present. Some pitting attack was present on most samples of 3003 alloy with diffused zinc after all exposure times. The pits were generally shallow and showed some preferential alignment in the flow direction. None of the pits propagated more than about half way through the diffused zinc layer. The depth of pits, 0.051 to 0.178 mm (0.002 to 0.007 in), was about the same after 8 days and after 185 days of exposure. The number of pits and width of pits increased with

TABLE 6.

TYPES OF CORROSION AND MAXIMUM PIT DEPTHS ON SPECIMENS AFTER EXPOSURE TO SEA WATER FLOWING AT SIX FEET PER SECOND

SAMPLE IDENTIFICATION	EXPOSURE, DAYS	TYPES OF CORROSION	MAX. PIT DEPTH, IN.
FB-BARE			
GF18-1	5	General	0.0007
8	10	General	--
GF14	30	Slight local	0.0005
7	65	Slight local	--
GF10-1	105	Slight local	--
GF10-2	140	Slight local	0.0009
11	185	Slight local	--
FB-ZN			
F12-3	5	Pitting	0.006
GF8-3	5	Slight pitting	--
GF20-4	5 cl	Slight pitting	--
GF12-3	5 cl	Pitting	0.004
GF16-2	15	Pitting	0.005
GF16-1	15	Slight pitting	—
GF4	15 cl	Slight pitting	—
CF14	15 cl	General	--
B16-2	30	Slight pitting	0.006
GF2-2	30	Pitting	0.006
F10-4	30 cl	Slight pitting	--
F4-2	30 cl	Slight pitting	0.003
GF18-3	60	Pitting	0.005
AF20-1	60	Pitting	0.005
A18	60 cl	Pitting	0.004
GF16	60 cl	Pitting	0.006
CF14-1	105	Slight pitting	0.006
GF20-3	105	Pitting	0.006
GF8	105 cl	Slight pitting	0.003
CF20	105 cl	General	--
GF10-3(a)	155	—	--
CF20-3(a)	155	--	--
GF12(a)	155 cl	—	--
GF2-1(a)	155 cl	--	--
F14-4	185	Pitting	0.005
GF6	185	Pitting	0.004
GF20-2	185 cl	Pitting	0.004
GF2	185 cl	Pitting	0.004

SAMPLE IDENTIFICATION	EXPOSURE, DAYS	TYPES OF CORROSION	MAX. PIT DEPTH, IN.
VB-ZN			
AV-2	5	Pitting	0.005
AV20-1	5	Slight pitting	0.004
AV14-1	5 cl	Slight pitting	—
AV2-1	5 cl	Slight pitting	--
V8-1	15	General	0.0004
V14-2	15	Slight pitting	0.003
DV12-2	15 cl	Slight pitting	0.003
V-18	15 cl	General	--
AV-16	30	Pitting	0.006
AV-20	30	Slight pitting	--
AV-14	30 cl	Slight pitting	0.0002
AV-12	30 cl	Pitting	0.007
DV-12	60	General	--
DV20-3	60	Pitting	0.006
V14-1	60 cl	Pitting	0.002
DV4-2	60 cl	Pitting	0.003
DV2-2	105	Pitting	0.002
V10-2	105	Pitting	0.003
V18-2	105 cl	General	--
DV20-2	105 cl	General	--
V18-1[a]	155	--	--
AV6[a]	155	--	--
V10-1[a]	155 cl	--	--
DV-2[a]	155 cl	--	--
AV10	185	Pitting	--
AV16-1	185	Pitting	0.004
AV16-2	185 cl	Pitting	--
AV8	185 cl	Pitting	0.002
FB-ETCH-1/2ZN			
AF8-R	5	Slight pitting	0.002
BF8-R	10	General	0.0008
BF6-R	30	General	0.0006
F16-R	65	Slight pitting	0.003
BF2-R	105	Slight pitting	0.003
BF8-R1	140	Slight pitting	--
F4-R	185	Slight pitting	--
FB-ETCH-1ZN			
CF14-2	5	Slight pitting	0.003
BF2-3	10	Slight pitting	0.003
AF8-3	30	Slight pitting	0.003
GF4-3	65	Slight pitting	0.002
F12-2	105	Slight pitting	0.002
GF6-3	140	Slight pitting	0.002
CF20-1	185	Slight pitting	0.003

SAMPLE IDENTIFICATION	EXPOSURE, DAYS	TYPES OF CORROSION	MAX. PIT DEPTH, IN.
FE-ZN-FE			
F16-3	5	Intergranular attack	0.003
AF6-1	10	Intergranular attack	--
GF18-2	30	Intergranular attack, pitting	0.005
BF4-1	65	Intergranular attack, pitting	0.005
F14-3	105	Intergranular attack	0.001
F14-2	140	Intergranular attack	0.004
F10-2	185	Intergranular attack	0.005

(a) Samples were not analyzed but were retained for additional corrosion tests.

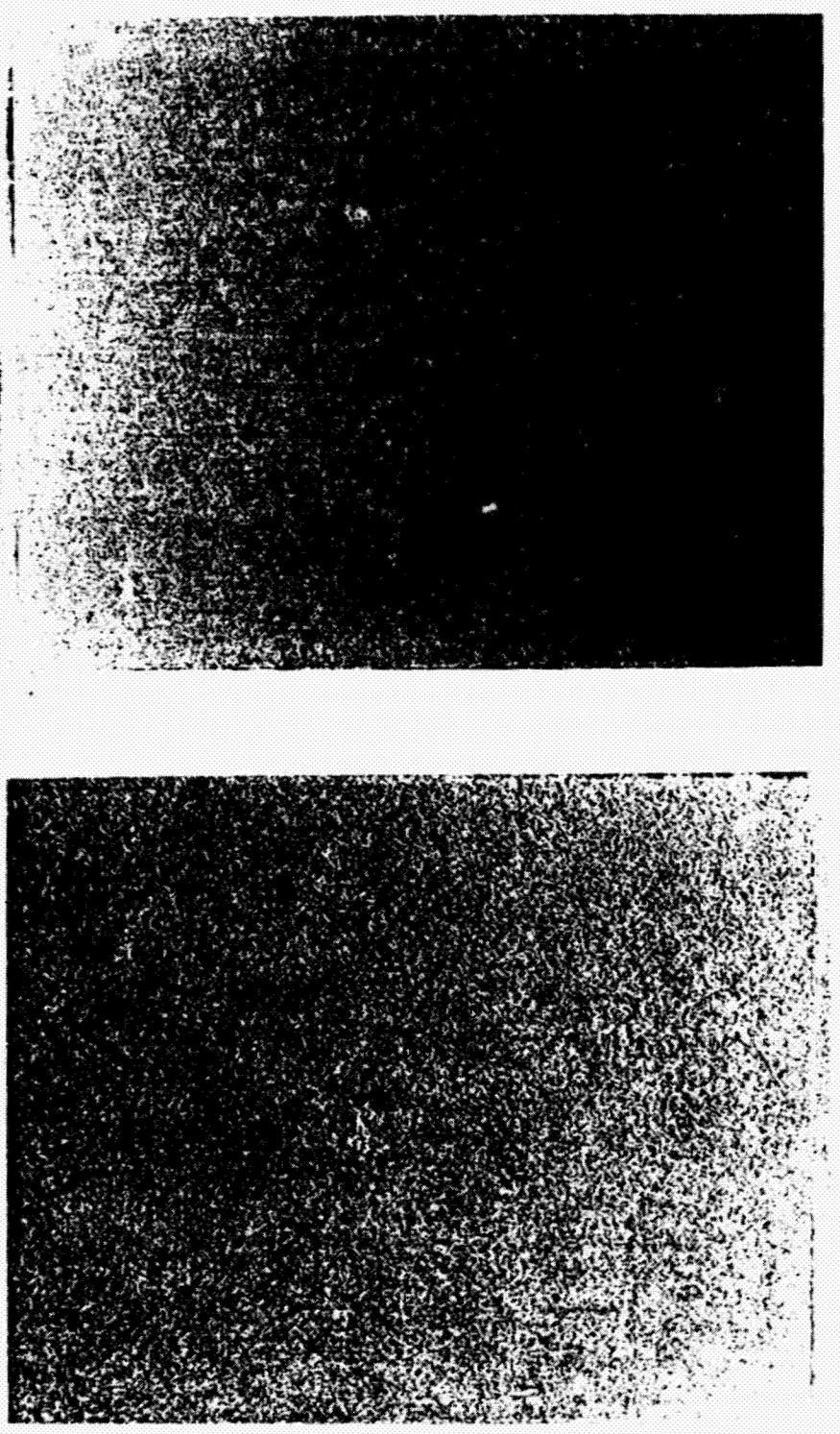

FIGURE 2,. Typical appearance of corrosion on FB-BARE 3003 after 185 days. Magnification 3X above and 10X bottom.

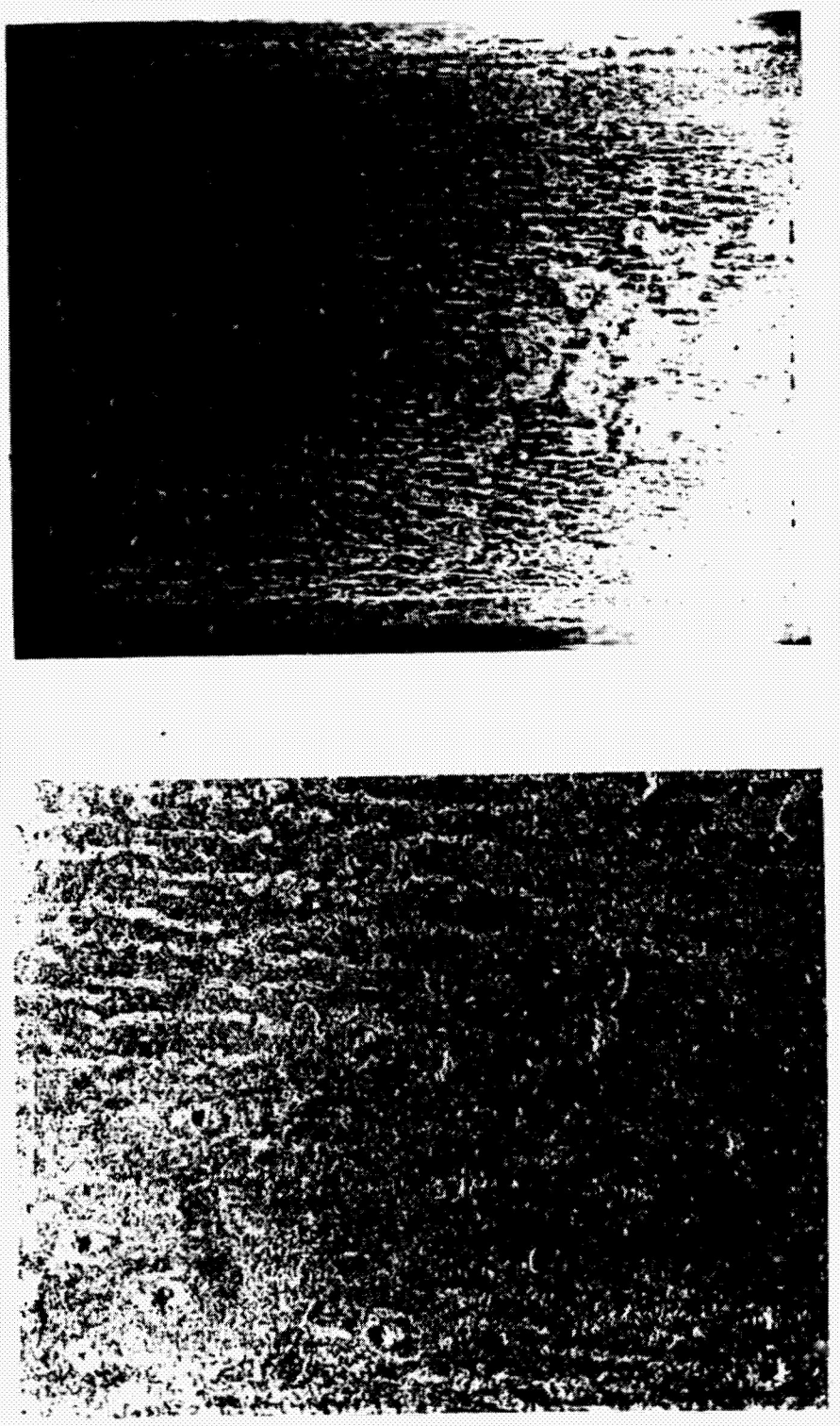

FIGURE 28. Typical appearance of corrosion on FB-ZN after 185 days. Magnification 3X above and 10X bottom.

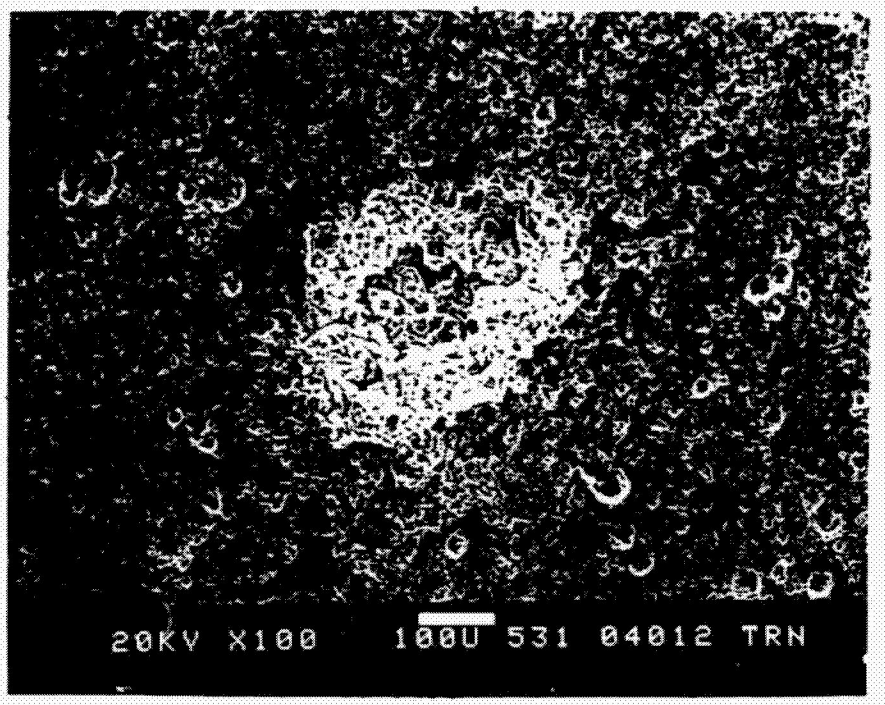

FIGURE 29. Typical corrosion pit on FB-ZN after 185 days. Magnification 100X.

FIGURE 30. Corrosion pits in FB-ZN. They were generally broad and shallow. Pit shown is 0.005 in. deep, partially through the diffused zinc layer. Etch - Poultons Etch, Magnification 100X.

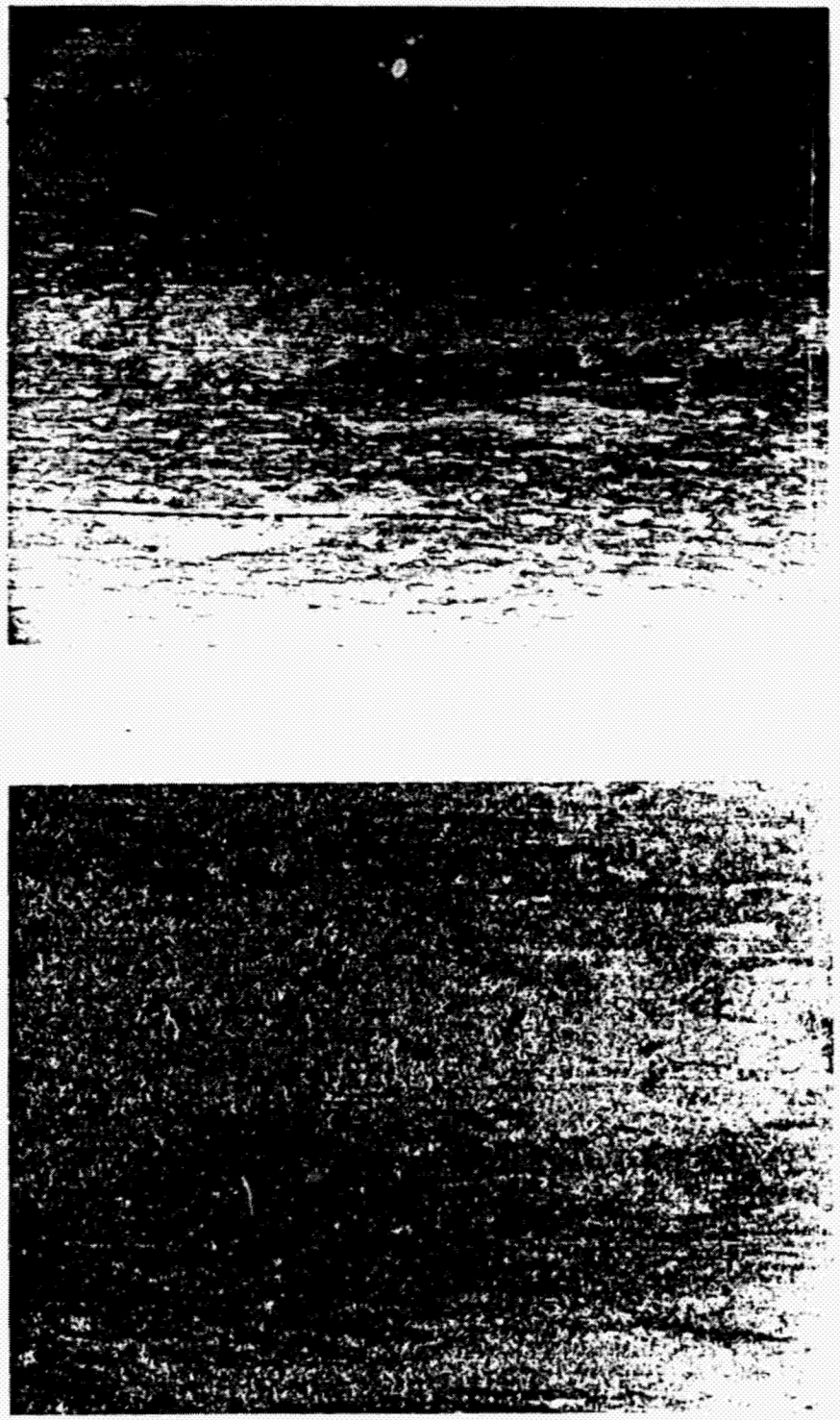

FIGURE 31. Typical appearance of corrosion on VB-ZN after 185 days. Magnification 3X above and 10X bottom.

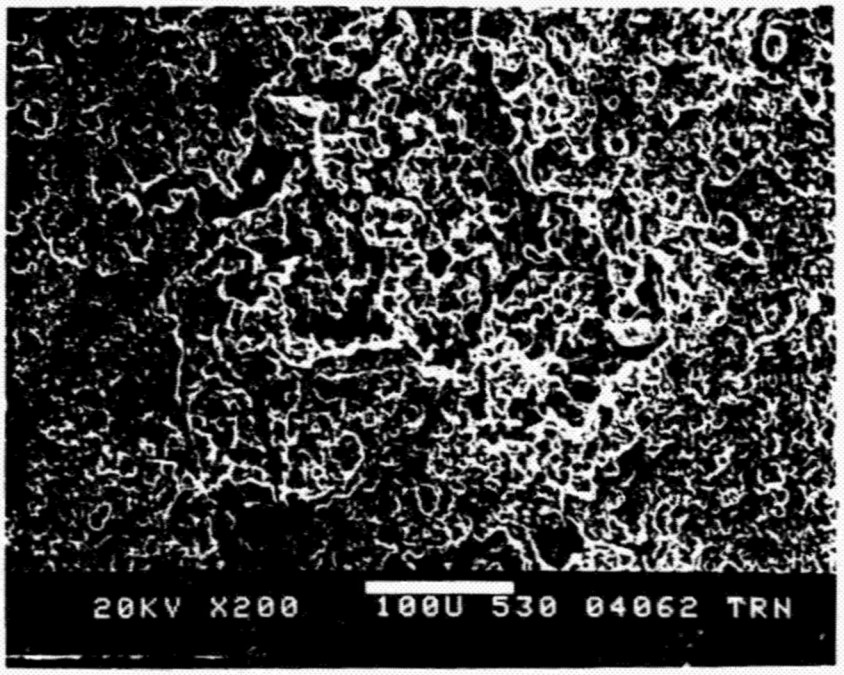

FIGURE 32. Typical corrosion pit in VB-ZN sample after 185 days. Magnification 200X.

FIGURE 33. Corrosion pits in VB-ZN samples. They were generally broad and shallow. Pit shown is 0.003 in. deep. Etch - Poultons Etch. Magnification 100X.

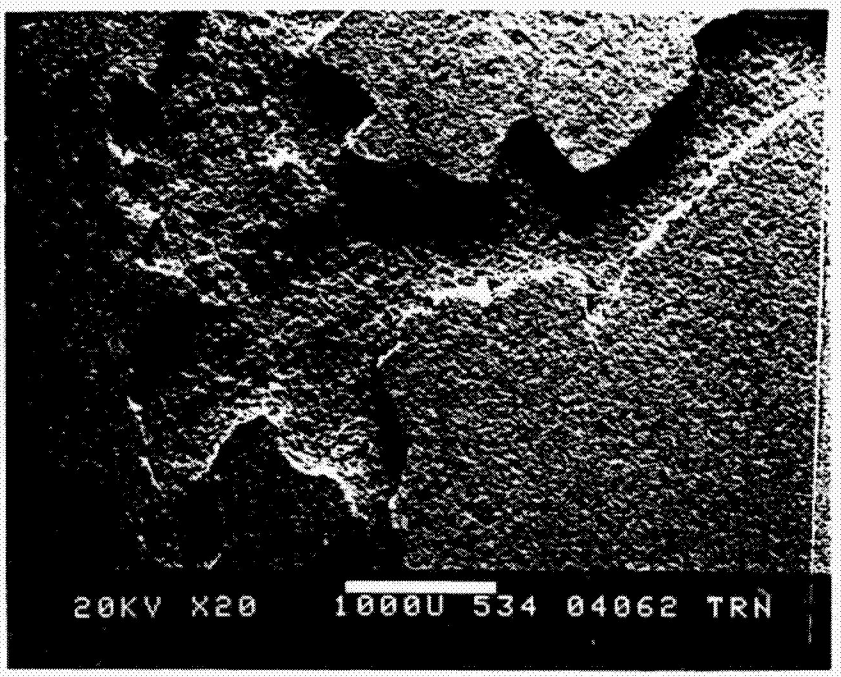

FIGURE 34. Corrosion channel in VB-ZN sample. Sample AV10 was corroded in flow direction. Corrosion occured by galvanic action in diffused zinc areas adjacent to low zinc areas. Magnification 20X

FIGURE 35. Close-up view of corrosion channel in VB-ZN sample. the channel was 0.007 in. deep. The adjacent area to the left with low zinc content was not corroded. Magnification 100X.

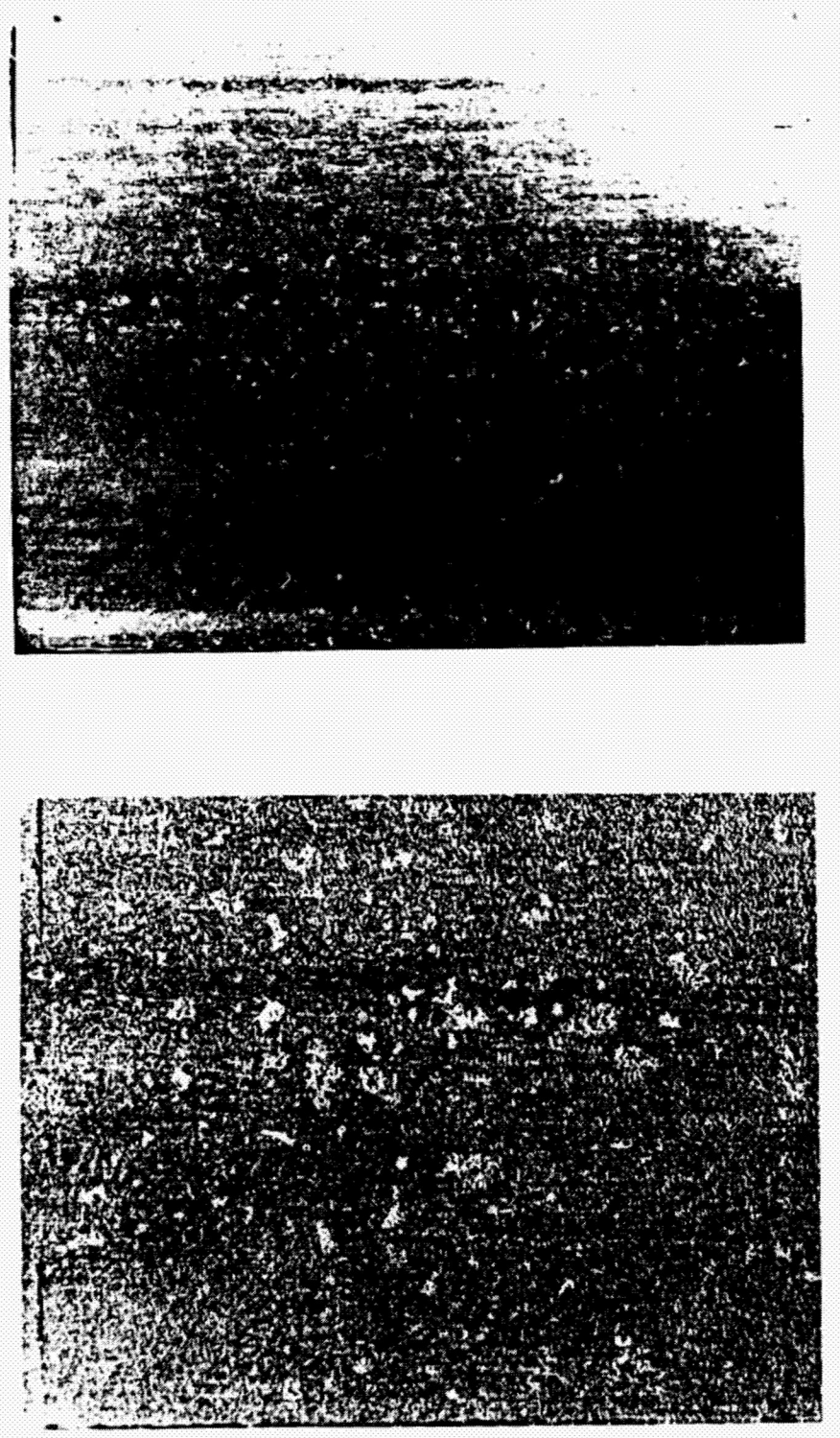

FIGURE 36. Typical appearance of corrosion on FB-ETCH-1 ZN after 185 days. Magnification 3X above and 10X bottom.

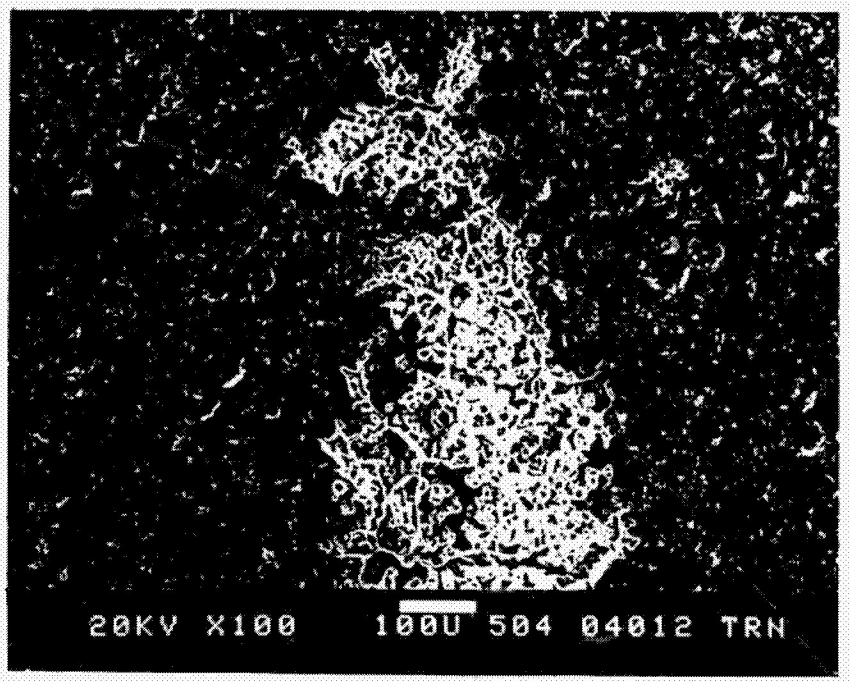

FIGURE 37. Typical corrosion pit in FB-ETCH-1 ZN sample after 185 days.

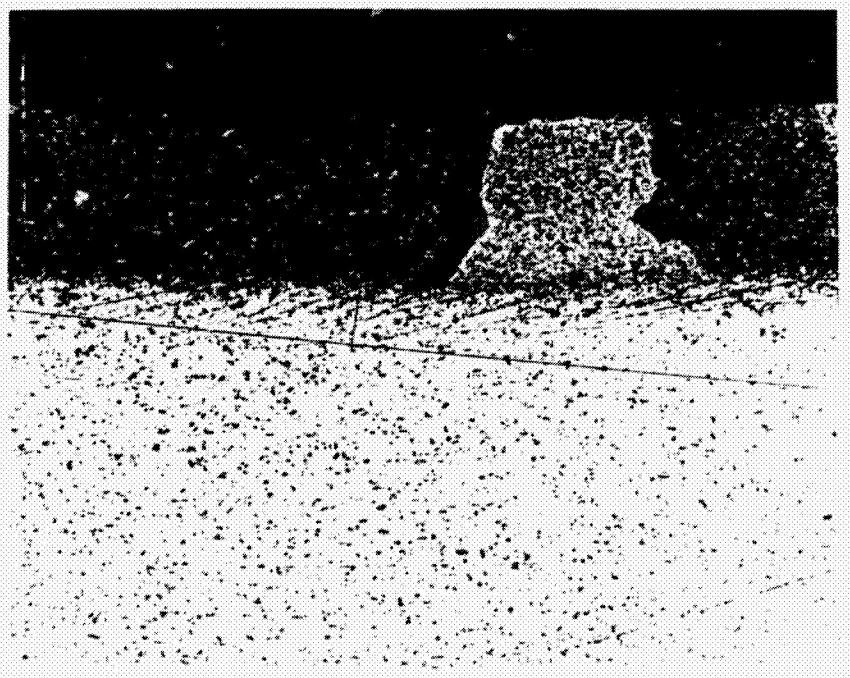

FIGURE 38. Corrosion pit in FB-ETCH-1 ZN samples. They were generally shallow. Pit shown is 0.001 in. deep. Etch - Poultons etch. Magnification 100X.

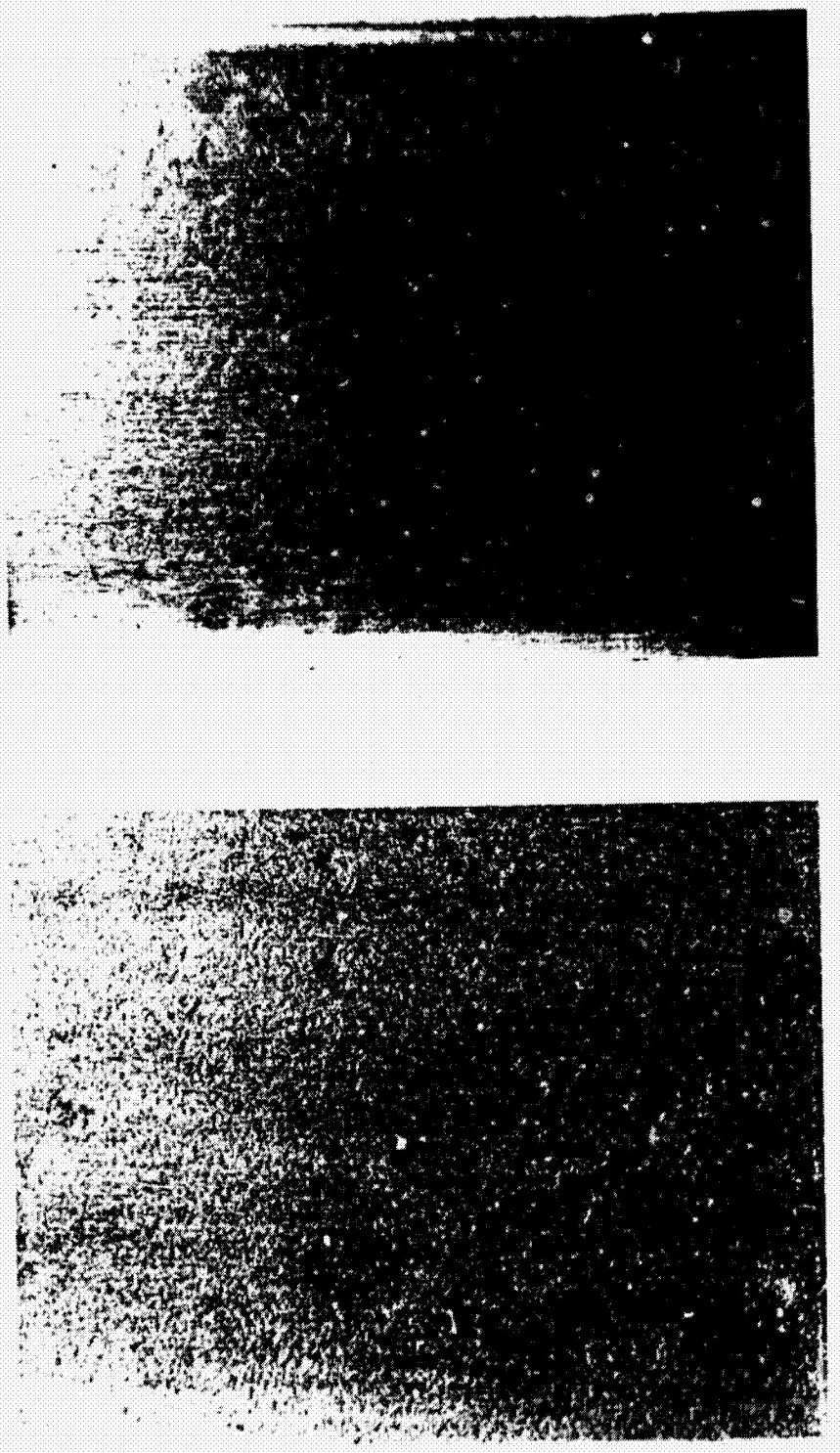

FIGURE 39. Typical appearance of corrosion on FB-ETCH-1/2 ZN after 185 days. Magnification 3X above and 10X bottom.

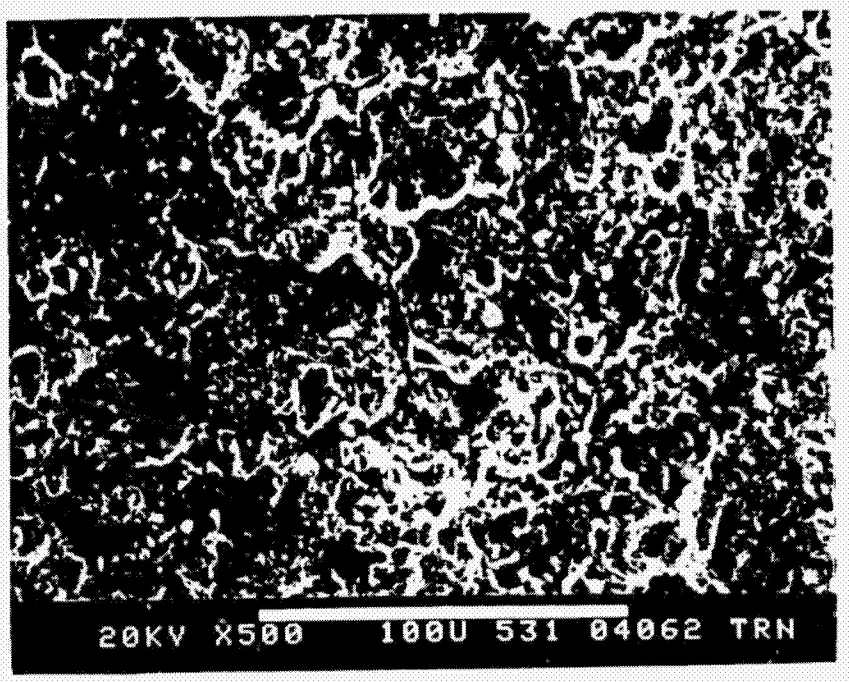

FIGURE 40. Pitting attack on the FB-ETCH-1/2 ZN sample. On these samples as well as on other samples with diffused zinc, pitting attack started at grain boundaries and broadened. Magnification 100X.

FIGURE 41. Corrosion pits in FB-ETCH-1/2 ZN samples. Pits were generally shallow and broad. Pit shown is 0.003 in. deep. Etch - Poultons Etch. Magnification 100X.

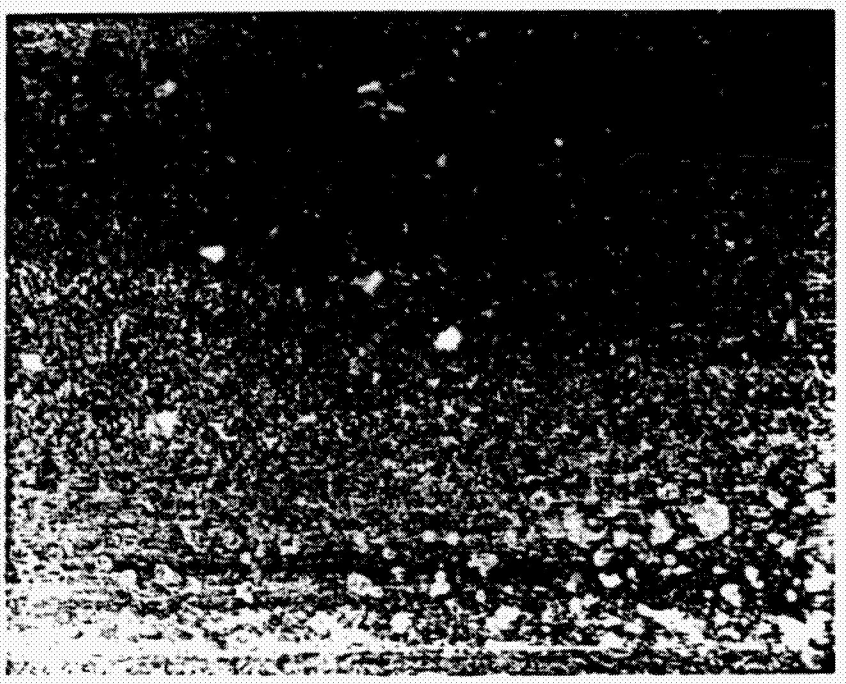

FIGURE 42. Corrosion of [illegible]N-FE samples. These samples were corroded by intergranular attack over much of the area exposed to seawater. Magnification 3X.

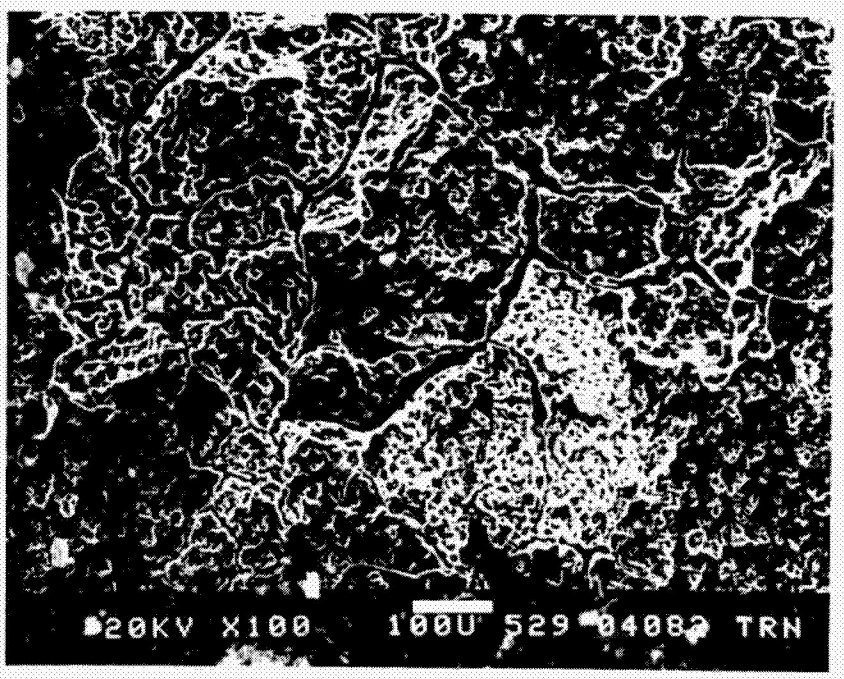

FIGURE 43. Corrosion of FE-2N-[illegible] sample. Corrosion was highly localized in grain boundaries. Magnification 100X.

Attack is 0.003 deep in the grain boundaries. Etch - Poultons Etch. Magnification 100X.

Attack is 0.005 in. deep in the grain boundaries.

FIGURE 44. Intergranular attack on the FB-ZN-FE samples. Depth ranged from 0.003-0.005 in. after 185 days. Etch - Poultons Etch. Magnification 100X.

exposure time but the maximum pit depth was essentially unchanged. Possibly, pits propagated to a depth at which galvanic protection was provided by material of higher zinc concentration near the surface. Rate of pitting attack was apparently very low after pits reached a depth of approx. 0.127 mm (0.005 in).

The VB-ZN and FB-ZN materials contained more and deeper pits than the FB-ETCH-1ZN and FB-ETCH-1/2ZN materials. These results show that removal of the surface layer containing about 45% zinc combined with lower zinc contents in the diffused layer reduced the susceptibility of the diffused layer to pitting attack.

Some VB-ZN samples were corroded to form channels about 0.178 mm (0.007 in) deep. This corrosion resulted from galvanic action in areas with normal zinc concentration adjacent to areas with low zinc content (determined by energy dispersive x-ray analysis). This result is consistent with corrosion potential meausrements that show the diffused layer is significantly anodic to 3003 aluminum.

Only the FB-ZN-FE materials with residual iron in the diffused layer were significantly corroded by intergranular attack. While the intergranular attack produced wide-spread loss of material from the surface, the depth of attack was shallow at 0.0176 to 0.127 mm (0.003 to 0.005 in) after 185 days exposure. The diffused zinc layer with residual iron is less desirable compared with the diffused zinc layers without iron because the intergranular attack would likely strip the diffused

zinc layer more quickly.

Scanning electron microscopy (SEM) studies showed that the pitting attack on the samples with diffused zinc without iron generally started at grain boundries in isolated locations. Corrosion proceeded slightly into the grain boundary then broadened to form pits.

The SEM studies showed that chlorination did not significantly affect the type of corrosion or the microscopic appearance of the corrosion attack. Similarly, studies of samples brushed to remove biofouling showed the surface was not abraded by as many as 56 strokes. The wear resistance of the diffused zinc layer was likely increased by the aluminum manganese particles present in the 3003 alloy.

9.2.3 BARE 3004 AND 7072 ALCLAD 3004. Corrosion present on the roll formed and welded 3004 and 7072 alclad 3004 tubes was studied on 15.2 cm (6 in) sections provided by Kaiser.

All the samples were corroded by uniform surface attack. Only on sample, B30-5% alclad - exposed 90 days to chlorinated sea water was corroded by pitting attack in several isolated locations. The pits propagated to a depth of 0.076 mm (3.0 mils) partially through the 0.096 mm (3.8 mil) thick 7072 alclad layer as shown in Figures 45-47.

The SEM studies showed that no localized corrosion occurred at the weld seams or at cracks in the welds on the roll formed and welded tubes as shown in Figures 48-49.

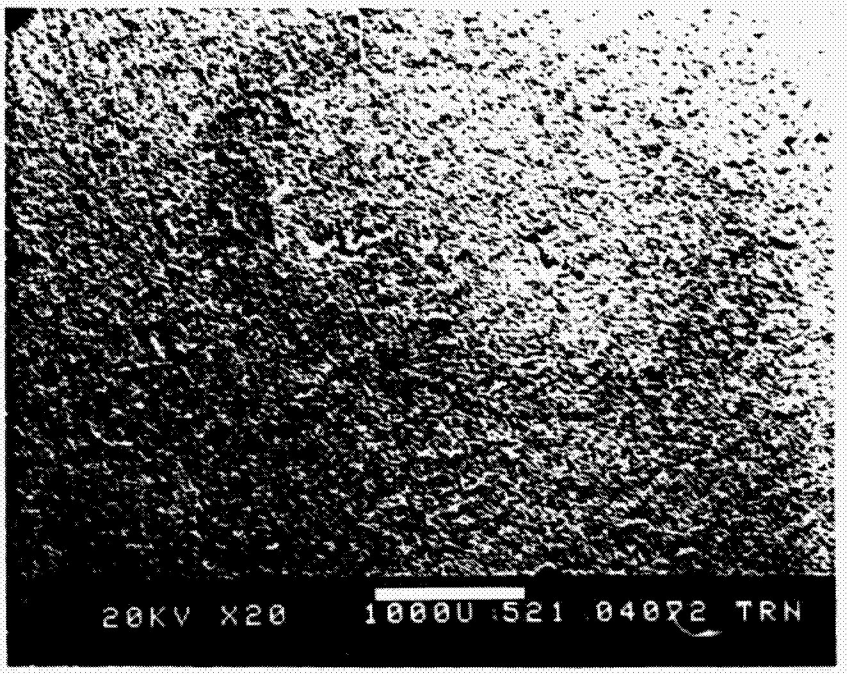

FIGURE 45. Corrosion pits in surface of 5% Alclad 3004 sample B30 after 90 days exposure. Magnification 20X.

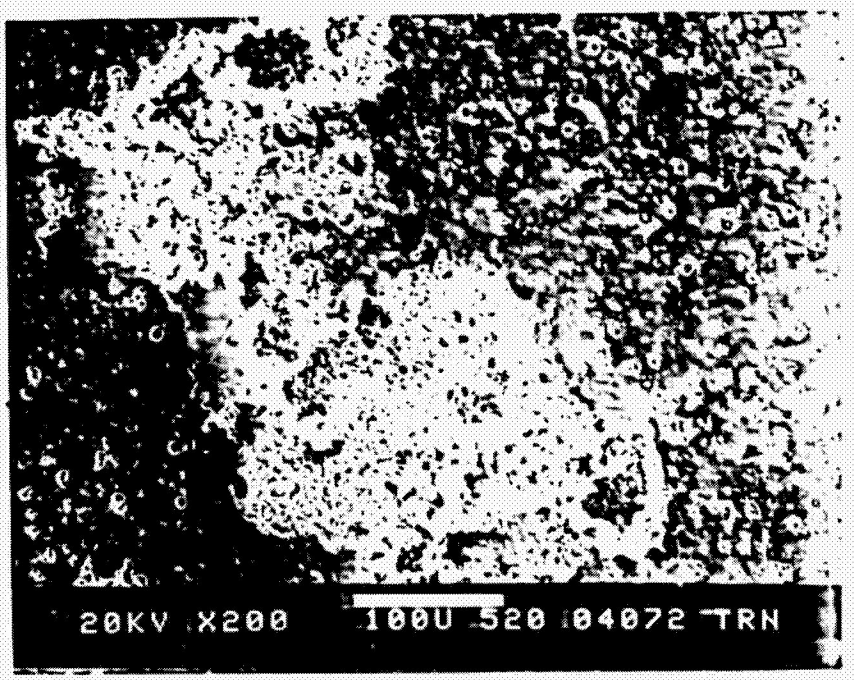

FIGURE 46. Typical appearance of corrosion pits in sample B30. Magnification 200X.

FIGURE 47. Corrosion pits in sample B30 of 5% Alclad 3004. They were 0.003 in. deep in the 0.0038 in. thick cladding. Etch - Poultons Etch. Magnification 100X.

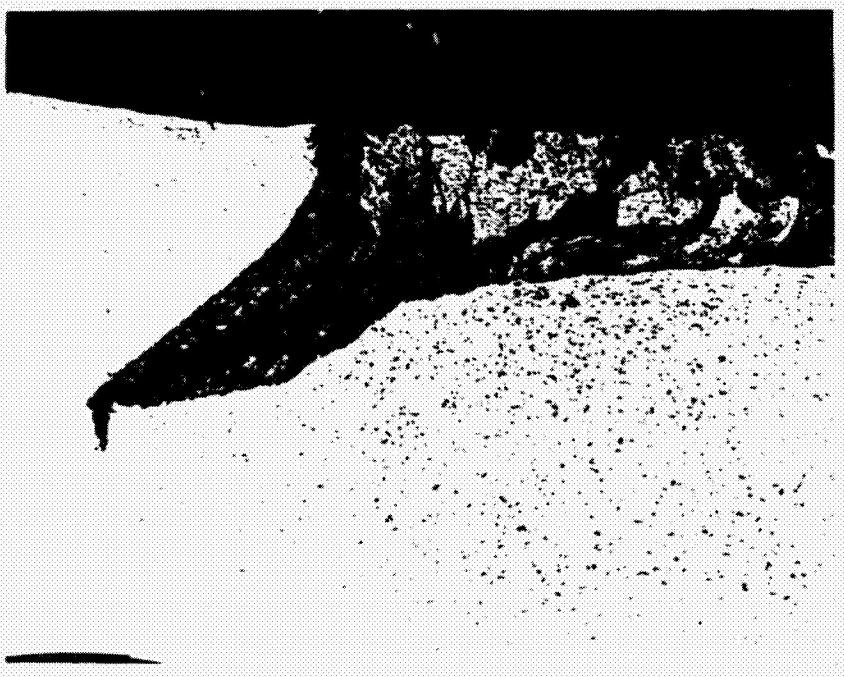

FIGURE 48. No localized corrosion occurred at the weld seam in the RFW Alclad tubes. Etch - Poultons Etch. Magnification 100X.

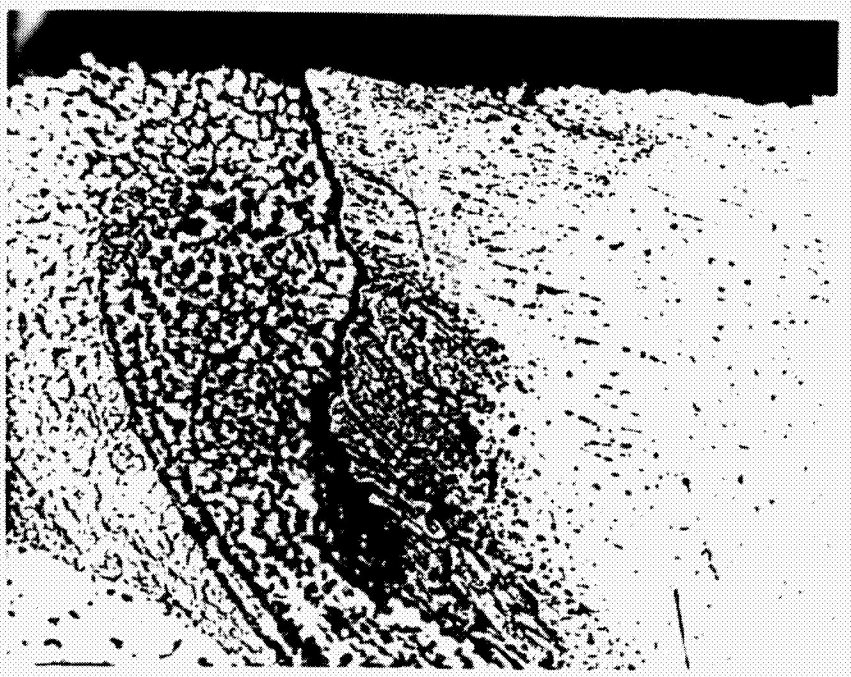

Fig. 49 No localized corrosion occurred in the weld cracks on the RFW Alclad tubes. Etch - Poulton's Etch. Magnification 500X.

9.2.4 CONCLUSIONS

1) Corrosion rates of the aluminum materials tested except the diffused zinc with low iron, were similarly low (about 0.015 mm/yr or 0.6 mpy) after 6 months exposure to sea water flowing at 1.8 m/sec.

2) Diffused zinc and 7072 alclad layers were not pitted to the base material during the 6 month test. Consequently, the anodic protection capability of the layers could not be determined.

3) Biofouling countermeasures used (brushing or chlorination) did not affect the corrosion rate or type of corrosion on the aluminum materials.

4) Corrosion rates of 3003 extrusions with diffused zinc were not significantly affected by the zinc concentrations in the range studied. Consequently, the process is practical for production of commercial heat exchangers with some expected variation in zinc concentration.

5) All conditions with diffused zinc, except the condition with low iron content, provided similar resistance to overall corrosion.

6) The diffused zinc treated 3003 and 7072 alclad 3004 aluminum materials should be evaluated as prototype heat exchangers in sea water service.

10. HEAT TRANSFER RESULTS AND CONCLUSIONS

10.1 RESULTS. Figure 50 shows the results of the fouling resistance (R_f) measurements for the unchlorinated units. These data appear in Appendix 1. At the onset of the experiment, there was an initial induction period during which R_f values remained near zero or were even slightly negative. All units had an induction period of about two weeks, with that of the titanium unit being slightly shorter than those of the aluminum units. It is believed that this induction period is the result of patchiness in microbial growth during the early colonization stages (14).

Following the induction period and following each cleaning, R_f increased almost linearly with time (Figure 50). The fouling rates, dR_f/dt, obtained from the slopes of the fouling resistance curves of Figure 50 are shown in Figure 51 (see also Appendix 2). This Figure shows the near zero and sometimes negative fouling rate for the induction period, the slow increase in fouling rate during the transition period , and the steady state fouling rate of 0.046 +/- .004 m^2-^oK/W-day (0.26 ft^2-hr-^oF/Btu-day) after 80 days. No significant difference in the fouling rate was observed between the titanium HTM, the two aluminum HTM's, and the STM.

There appeared to be sloughing of the biofilm in unit two in early August, in unit three in early September, and in unit five in mid-September. Sloughing of the biofilm also occurred during the first deployment (9). For the first 76 days of this experiment flow velocity through unit three was increased by 100

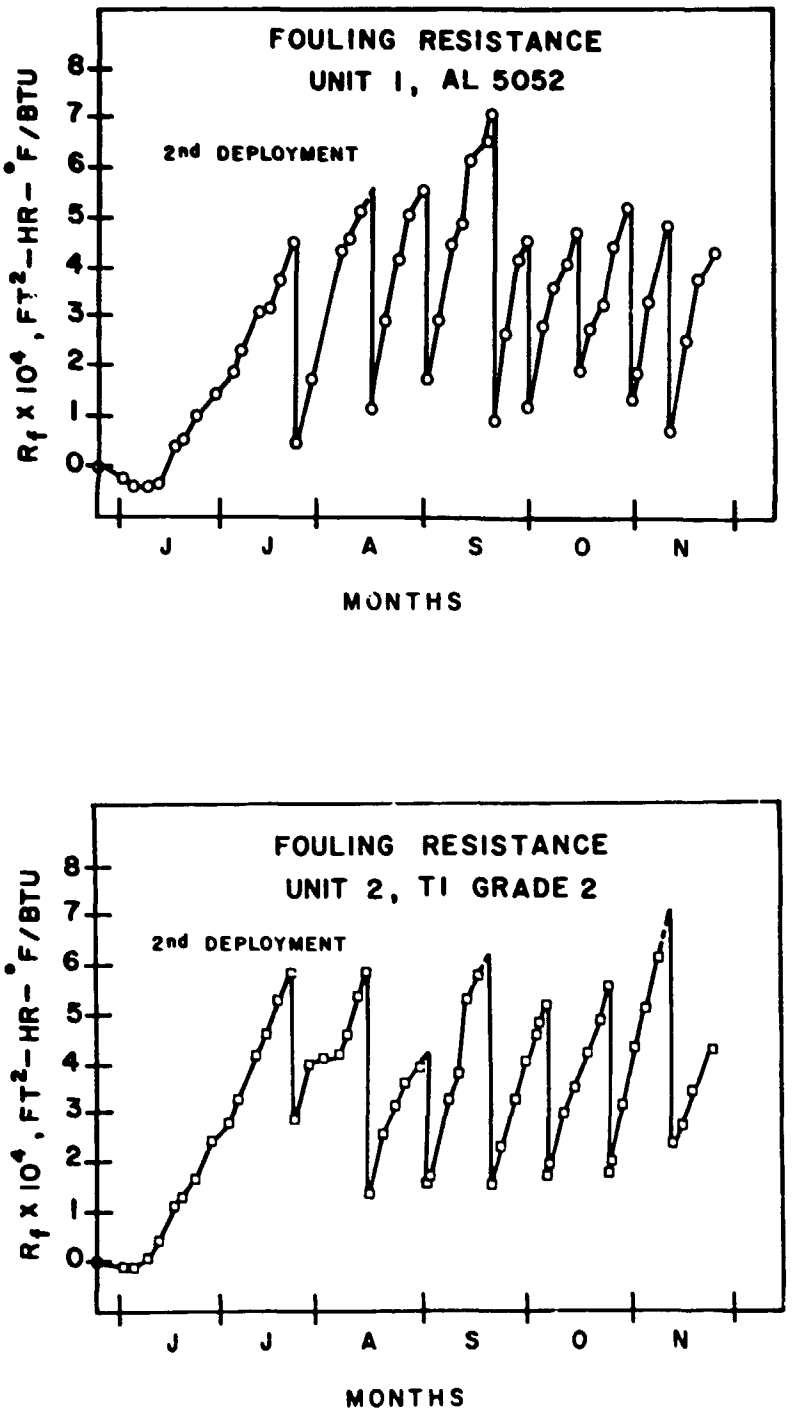

FIGURE 50. Fouling resistance measurements for unchlorinated Heat Transfer Monitoring units showing cycles of growth and cleaning.

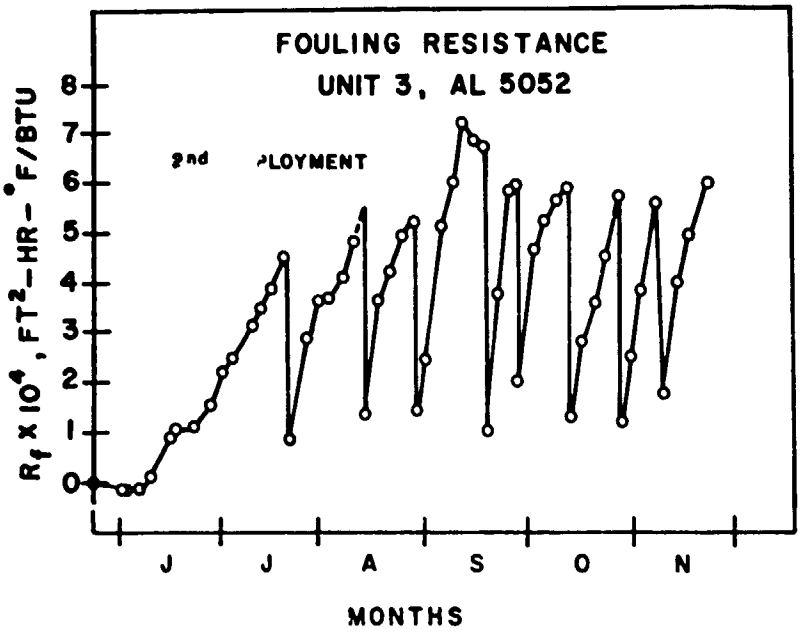

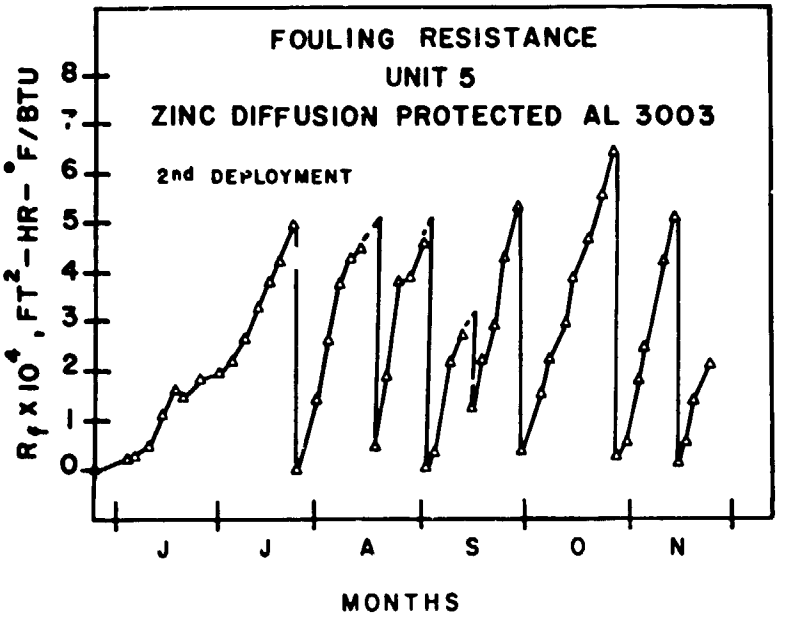

FIGURE 50. Continued.

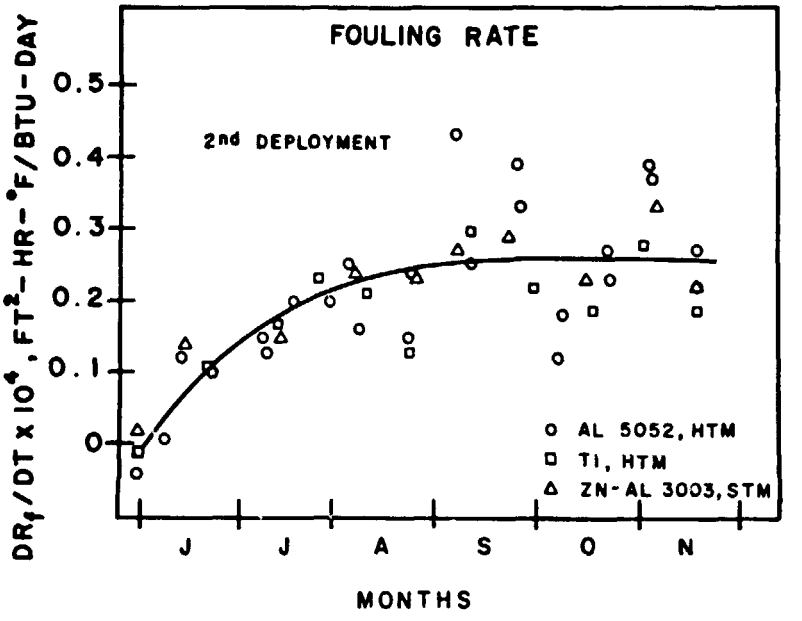

FIGURE 51. Fouling Rates (dRf/dt).

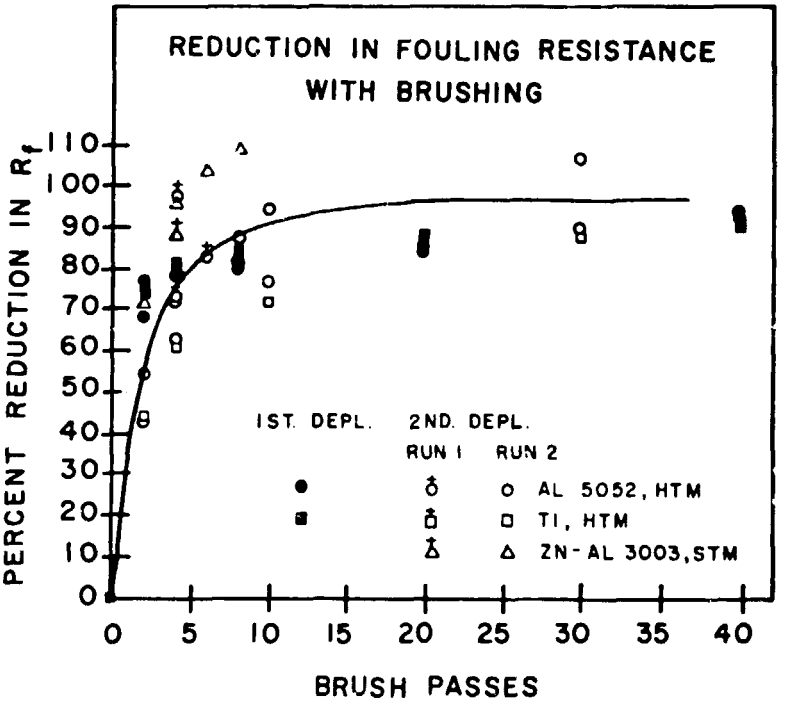

FIGURE 52. Percent reduction in thermal resistance by cleaning with manually operated brushes.

percent for 30 to 60 minutes daily in an attempt to stimulate sloughing of the biofilm, but this had no noticeable affect.

Figure 52 gives a summary of the effectiveness of brush cleaning for both the first and second deployments. Two brush passes were sufficient to reduce R_f by two-thirds, and ten passes reduced R_f by approximately 90 percent. However, only in the early stages of the experiment was in possible to approach an R_f value of zero by brush cleaning. This suggests that the fouling resistance was caused by two distinct biological layers: an upper layer which was removed easily by brushing, and a hard, bottom layer (possibly exuded polysaccharides) which accumulated slowly and could not be removed by brush cleaning.

Intermittent chlorination performed on unit four proved to be an effective method of biofouling control (Figure 53). The R_f value for unit four during the entire six months of the second deployment remained essentially at zero.

Mean surface seawater temperature during the test period was 29 °C. Figure 54 is a plot of surface seawater temperatures during the test.

10.2 CONCLUSIONS. Fouling rates on the rectangular cross sectional water passage from the Crane compact heat exchanger were the same as those on the other units. As a means of controlling biofouling, intermittent increases in flow velocity were not effective. Chlorination for 28 minutes daily at the level of 0.5 ppm effectively controlled biofouling for the duration of six month experiment.

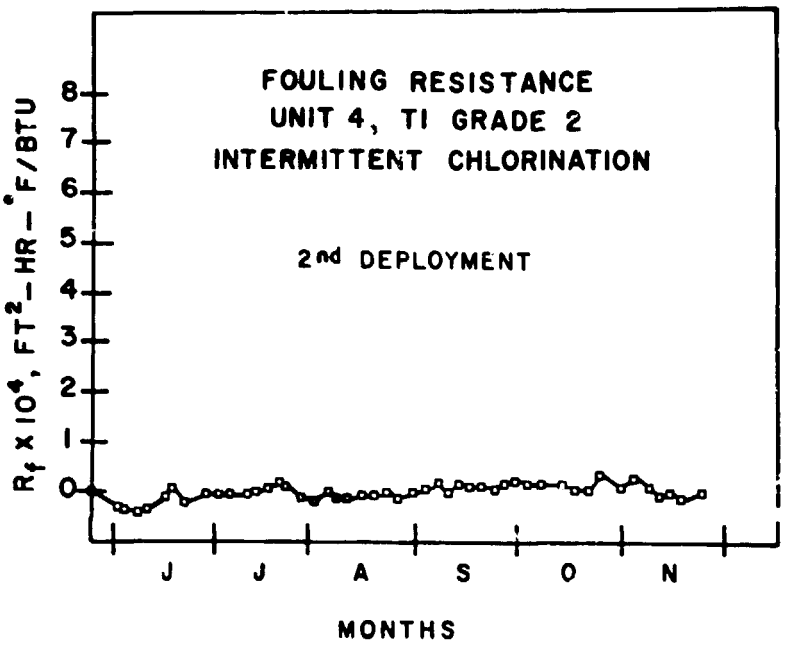

FIGURE 53. Fouling resistance of the chlorinated Heat Transfer Monitoring unit.

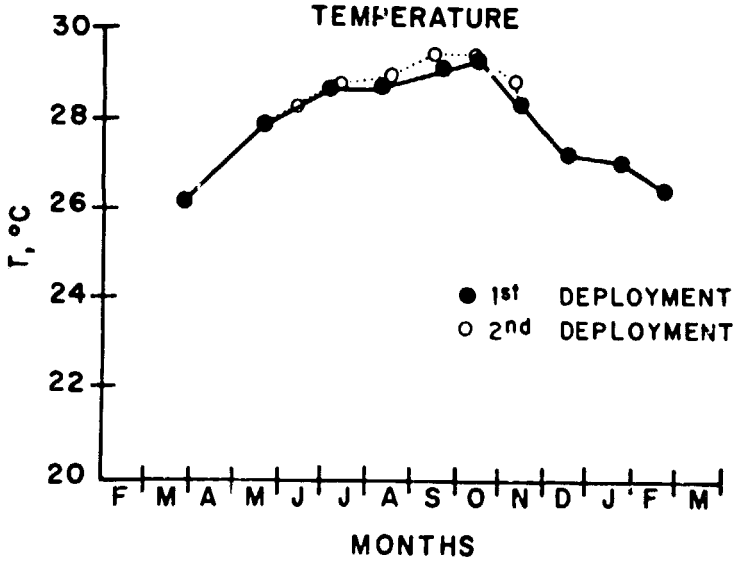

FIGURE 54. Surface seawater temperature during the test period.

11. MACROFOULING RESULTS AND DISCUSSION

11.1 RESULTS. Macrofouling of the flow system was also studied at the end of an earlier deployment which was conducted between January 1980 and March 1981 (15). Table 7 lists the species found in the intake strainers and in the modules of units 1 and ′.

In general, these data are consistent with the results of the first deployment although the macrofouling community in the flow system after the first deployment was slightly more developed. At the end of the first deployment, 54 species with a combined wet weight of 915 g were found in the intake strainer. Following the second deployment, 41 species with a combined wet weight of 459 g were collected from the intake strainers. These differences are due to the fact that the second deployment was of only 6 months duration, while the first deployment lasted 13 months. Major differences between the macrofouling communities from the first and second deployments were in the number and biomass of the bivalve molluscs, ascidians, and of adventitious organisms (in this case errant polychaetes and gastropods) which are the last organisms to appear in fouling communities (16).

In the experimental modules, macrofouling organisms were found in areas of low-flow velocity such as little-used bypass loops and "T"'s where one pathway was entirely plugged. With the exception of the small hydroid Plumularia and an occasional barnacle or oyster, no macrofouling organisms were growing in areas which had a flow rate greater than 3 ft/sec (0.9 m/sec).

C 2

Table 7. Identification, frequency, and wet weight of organisms found in the intake strainers and experimental modules after six months of continuous flow.

SPECIES	NUMBER (WET WEIGHT g)		
	STRAINER	UNIT 1	UNIT 4
Phylum Porifera			
Sycypha sp.	*	•	•
Phylum Cnidaria			
Class Hydrozoa (hydroid)			
Obelia sp.	-	*	*
Plumularia sp.	*	-	*
Class Anthozoa (anemones)			
Order Ceriantharia			
Arachnanthus nocturnus Hartog	1 (0.5)	-	-
Phylum Platyhelminthes (flatworm)			
unidentified sp.	11 (T)	-	-
Phylum Annelida			
Class Polychaeta			
Subclass Errantia			
Eunice sp.	10 (1)	-	8 (1)
Eurythoe complanata (Pallas)	3 (1)	-	-
Hermodice carunculata (Pallas)	9 (5)	-	2 (0.5)
Nereis sp.	1 (T)	-	-
Pisione sp.	3 (T)	-	-
unidentified palmyrid	2 (T)	-	-
unidentified syllid	8 (T)	-	5 (T)
Subclass Sedentaria			
Branchioma sp.	2 (0.5)	-	1 (T)
Phyllochaetopterus sp.	1 (0.5)	1 (0.5)	-
Ficopomatus sp.	•	*	*
Hydroides sp. a	•	•	*
Hydroides sp. b	*	*	*
Vermiliopsis sp.	*	-	•
Phylum Sipuncula			
Golfingia sp.	69 (3)	9 (T)	6 (T)

Phylum Mollusca			
Class Bivalvia (clams)			
Aequipecten muscosus (Wood)	-	1 (1)	-
Anadara notabilis (Roding)	-	-	2 (1)
Anomia simplex Orbigny	2 (T)	2 (T)	-
Chama macerophylla (Gmelin)	3 (T)	14 (0.5)	25 (1)
Isognomon radiatus (Anton)	1 (T)	8 (5)	3 (1)
Leptopecten bavayi (Dautzenberg)	-	-	1 (T)
Lima lima (Linne)	-	1 (T)	-
Lima pellucida Adams	-	2 (T)	-
Lima scabra (Born)	1 (T)	2 (T)	3 (T)
Malleus candeanus (Orbigny)	-	-	1 (1)
Musculus lateralis (Say)	-	20 (T)	67 (T)
Ostrea equestris Say	49 (119)	-	9 (3.5)
Pinctada imbricata Roding	8 (14)	10 (10)	18 (16)
Pinna rudis (Linne)	64 (219)	23 (37)	69 (59)
Phylum Arthropoda			
Class Crustacea			
Subclass Cirripida (barnacles)			
Balanus amphitrite Darwin	-	-	1 (0.5)
Chthamalus stellatus (Poli)	-	10 (0.5)	1 (T)
Lepas sp.	1 (1)	-	-
Tetraclita squamosa (Bruguiere)	-	-	1 (T)
Subclass Malacostraca			
Order Amphipoda (amphipods)			
unidentified caprellid	*	*	*
Elasmopus pocillimanus (Bate)	*	*	*
Stenothoe crenulata (Chevreax)	*	*	*
Order Decapoda			
Suborder Natantia (shrimp)			
Brachycarpus biunguiculatus (Lucas)	1 (1)	-	-
Suborder Reptantia (crabs)			
Pilumnus dasypodus Kingsley	1 (0.5)	-	1 (0.5)
unidentified gonoplacid	-	1 (0.5)	-
Phylum Bryozoa			
Bugula sp.	*	*	*
Phylum Echinodermata			
Class Echinoidea (sea urchins)			
Diadema antillarum (Phillipi)	6 (3.5)	-	-
Eucidaris tribuloides (Lamark)	2 (T)	1 (T)	-

Class Ophiuroidea (brittle stars)			
Ophiocoma echinata (Lamark)	17 (8)	6 (3)	-
Ophiocoma riisei Lufken	71 (43)	1 (1.5)	-
Class Holothuroidea (sea cucumbers)			
Holothuria glaberrima Selenka	-	1 (1)	-
Holothuria sp.	5 (1)	1 (T)	-
Phylum Chordata			
Subphylum Urochordata			
Class Ascideacea (sea squirt)			
Ascidia sydneiensis Stimpson	2 (15)	-	-
Botryllus planus (Van Name)	*	*	-
Herdmania momus (Savigny)	-	-	1 (2)
Pyura vittata (Stimpson)	2 (3)	-	-
Styela plicata (Lesueur)	9 (20)	2 (6)	-

* These are colonial organisms or small organisms too numerous to count
"T" indicates wet weights below 0.5 g

A dense growth of Plumularia covered the inner surface of most of the exhaust manifold in the chlorinated module unit 4. This did not occur in unit 1 or in any of the units during the first deployment.

The level of chlorination administered during this investigation was sufficient to control microfouling of the test surfaces (see figure 53) but did not prevent the development of a macrofouling community in the module of unit 4. This is consistent with the findings of Burton, 1977 (16) who reported that intermittent halogenation is not effective in controlling development and growth of macrofouling communities. There was almost no difference in the number of species found in units 1 and 4 (30 and 31 species, respectively), and unit 4 actually had more biomass than unit 1 (87 g and 66 g, respectively).

Community structure of macrofouling organisms in unit 1 was similar to that found in the two units examined at the end of the first deployment. However, community structure in unit 4 was somewhat different than that encountered in other units. Units 1 and 4 only had 17 species in common. The most notable differences were the absence of echinoderms in the chlorinated unit and the presence of several errant polychaete worms along with the dense growth of Plumularia in this unit. No errant polychaetes or Plumularia were found in unit 1 and at the end of the first deploymert only one errant polychaete along with very little Plumularia was encountered in the experimental modules.

Since most of these organisms were not growing in the main flow path, they were probably exposed to less chlorine than was

introduced into the flow path. The only group which appears to have been adversely affected by the chlorination was the echimoderms. Several echinoderms were encountered in both unit 1 and in the modules examined after the first deployment. The absense of echinoderms - both ophiuroids and echinoids feed on small animals as well as organic detritus (17) - or some other preditor which was also sensitive to chlorination may have allowed the errant polychaetes and the Plumularia to grow in unit 4. An increased number of refuges available to larvae and juveniles in the intake strainers could explain the co-occurrence of these organisms in the strainers.

11.2 CONCLUSIONS.

1) Intermittent chlorination at a level of 0.5 ppm for 28 minutes daily did not prevent the development of a macrofouling community in areas with a low-flow velocity which were not in the main flow path.

2) Macrofouling community structure in the chlorinated unit was different from that found in unchlorinated units.

3) Chlorination appeared to eliminate one or more preditor organisms which resulted in more macrofouling in the chlorinated unit.

12. REFERENCES

1. La Que, F. L. Qualification of Aluminum for OTEC Heat Exchangers, U. S. Department of Energy ANL/OTEC-BCM-003, 1979, 33pp.

2. Faust, H. D. "Constructability of Extended Surface Heat Exchangers for OTEC," Proc. Eighth Ocean Energy Conference, Washington, D. C., June 1981.

3. Faust, H. D. "Brazed Aluminum, Platefin Heat Exchangers for OTEC," Proc. Third Miami International Conference on Alternate Energy Sources, Miami, Florida, December 1980.

4. Bothwell, M. R. "Diffusion Cladding Aluminum Articles with Diffused Zinc Coating," U. S. Patent No. 3,330,970. 1968.

5. Atwood, D. K., P. Duncan. Ocean Thermal Conversion: Resource Assessment and Environment Impact for Proposed Puerto Rico Site, Final Report NSF Grant No. AER 75-00145, 1976.

6. Goldman, G., M. L. Hernandez Avila, J. G. Gonzalez, D. Pesante. Results of Measurements Relatable to an OTEC Installation at Punta Tuna, Puerto Rico, Center for Energy and Environment Research Publication No. CEER-0-57, 1979, 588 pp.

7. Lopez, J. M., P. M. Yoshioka, J. G. Gonzalez, J. E. Capella. "The Structure of the Ocean Off Punta Tuna, Puerto Rico in Relation to OTEC," Proceedings of the Eighth Ocean Energy Conference, Washington, D. C., June 1981.

8. Vargo, S., K. Fanning, T. Hopkins, H. Michele, G. Vargo, E. Hartwig, A. Jones. Physical, Chemical and Biological Measurements off Puerto Rico, U. S. Department of Energy DOE/NBM-1043, 2 vols, 1981.

9. Sasscer D. S., T. R. Tosteson, T. O. Morgan. OTEC Biofouling , Corrosion, and Materials Study from a Moored Platform at Punta Tuna, Puerto Rico, U. S. Department of Energy ANL/OTEC-BCM-023, 1981, 117 pp.

10. Sasscer, D. S., T. Morgan, T. R. Tosteson, G. N. Grannemann. "In Situ Biofouling of Ocean Thermal Energy Conversion (OTEC) Evaporator Tubes," Journal of Solar Energy Engineering, vol. 3, 1981, pp 121-125.

11. Kuzay, T. M., C. B. Panchal, A. P. Gavin. A Special Heat Transfer Monitor (HTM) for the Trane Company OTEC Heat Exchanger, U. S. Department of Energy ANL/OTEC-BCM-016, 1981, 69 pp.

12. Fetkovich, J. G. A System for Measuring the Effect of Fouling and Corrosion on Heat Transfer under Simulated OTEC Conditions, U. S. Department of Energy COO-4041-10, 1976, 294 pp.

13. Findley, R. W., D. L. Meier. Design Report for PS-105 Data Acquisition System for Biofouling Studies of Heat Exchangers in Sea Water, U. S. Department of Energy COO-4041-6, 1977, 36pp.

14. Tosteson, T. R., ". R. Zaidi, R. Revuelta, S. H. Iman, R. W. Axtmayer, D. DeVore, D. L. Ballantine. "OTEC Biofouling, Corrosion, and Materials Study from a Moored

Platform at Punta Tuna, Puerto Rico: Part II - 'Microbiofouling,'" Ocean Science and Engineering, vol. 7(1), 1982, pp 21-73.

15. Sasscer, D. S., T. O. Morgan, C. Rivera. "OTEC Biofouling, Corrosion, and Materials Study from a Moored Platform at Punta Tuna, Puerto Rico: Part III - 'Macrofouling,'" Ocean Science and Engineering, vol. 7(2), 1982, pp 175-186.

16. Burton, D. T. "An Assessment of Intermittent and Continuous Chlorination and Bromochlorination Schemes for Control of Estuarine Fouling Organisms in Once-Through Cooling Systems," Proceedings of the American Power Conference, vol. 39, 1977.

17. Barnes, R. D. Invertebrate Zoology, second edition. W. B. Saunders and Company, 1968, 743 pp.

13. PUBLICATIONS AND PRESENTATIONS GENERATED BY THIS PROJECT

Sasscer, D. S., T. O. Morgan, T. R. Tosteson, B. R. Zaidi, R. Revuelta, S. H. Iman. "Ocean Thermal Energy Conversion (OTEC) Heat Exchanger Bioflouling at Punta Tuna, Puerto Rico." Presented at the Second National Conference on Renewable Energy Technologies (UPADI) in San Juan, PR, 1-7 August 1982.

Sasscer, D. S., T. J. Summerson, R. Ernst. "In Situ Seawater Corrosion of Bare, Diffusion Zinc Treated and Alclad Aluminum Heat Exchanger Materials." Presented at the Oceans '82 Conference (MTS-IEEE) in Washington, D. C., 20-22 September 1982.

Sasscer, D. S., T. R. Tosteson, T. J. Summerson, T. O. Morgan. "In Situ Biofouling, Biofouling Control and Corrosion of Titanium and Aluminum Heat Exchanger Elements at Punta Tuna. Puerto Rico." To be presented at the ASME-JSME Thermal Engineering Joint Conference in Honolulu, Hawaii, 20-24 March 1983.

Sasscer, D. S., R. Ernst, T. J. Summerson, A. C. Scott. "Open Ocean Corrosion Test of Candidate Aluminum Materials for Seawater Heat Exchangers." To be presented at the Corrosion '83 Conference (NACE) in Anaheim, California, 18-22 April 1983.

14. ACKNOWLEDGMENTS

The authors would like to express their appreciation to Messrs. A. P. Gavin, A. Thomas, L. Jennings and T. Kuzay of Argonne National Laboratory for their willing technical support and to Mr. T. J. Sadler, Mr. S. B. Pedersen, Mrs. V. B. Seda and Mrs. E. Cardona of CEER for their invaluable contribution to this project.

X = 0	Y = 0
X = 8	Y = -.27
X = 11	Y = -.44
X = 15	Y = -.45
X = 18	Y = -.35
X = 23	Y = .42
X = 25	Y = .53
X = 29	Y = .98
X = 35	Y = 1.39
X = 39	Y = 1.84
X = 42	Y = 2.28
X = 47	Y = 3.06
X = 50	Y = 3.12
X = 53	Y = 3.71
X = 57	Y = 4.52
X = 58	Y = .46
X = 63	Y = 1.7
X = 71	Y = 4.31
X = 74	Y = 4.6
X = 77	Y = 5.08
X = 80	Y = 1.1
X = 84	Y = 2.89
X = 88	Y = 4.18
X = 91	Y = 5.04
X = 95	Y = 5.54
X = 96	Y = 1.69
X = 99	Y = 2.91
X = 103	Y = 4.45
X = 106	Y = 4.89
X = 109	Y = 6.15
X = 113	Y = 6.56
X = 115	Y = 7.05
X = 116	Y = .88
X = 119	Y = 2.61
X = 123	Y = 4.13
X = 125	Y = 4.52
X = 125	Y = 1.2
X = 130	Y = 2.78
X = 133	Y = 3.55
X = 137	Y = 4.04
X = 140	Y = 4.72
X = 141	Y = 1.89
X = 144	Y = 2.73
X = 148	Y = 3.2
X = 151	Y = 4.39
X = 155	Y = 5.16
X = 156	Y = 1.28
X = 158	Y = 1.81
X = 161	Y = 3.24
X = 166	Y = 4.79
X = 167	Y = .69
X = 172	Y = 2.49
X = 176	Y = 3.75
X = 180	Y = 4.3

Appendix 1a.

R_f data for unit 1

X = days; Y = R_f

X = 0	Y = 0
X = 8	Y = -.11
X = 11	Y = -.12
X = 15	Y = .05
X = 18	Y = .42
X = 23	Y = 1.14
X = 25	Y = 1.28
X = 29	Y = 1.66
X = 35	Y = 2.41
X = 39	Y = 2.76
X = 42	Y = 3.24
X = 47	Y = 4.16
X = 50	Y = 4.55
X = 53	Y = 5.26
X = 57	Y = 5.81
X = 58	Y = 2.83
X = 63	Y = 3.97
X = 67	Y = 4.09
X = 71	Y = 4.16
X = 74	Y = 4.6
X = 77	Y = 5.34
X = 79	Y = 5.81
X = 80	Y = 1.37
X = 84	Y = 2.56
X = 88	Y = 3.15
X = 91	Y = 3.61
X = 95	Y = 3.94
X = 97	Y = 1.59
X = 98	Y = 1.73
X = 103	Y = 3.25
X = 106	Y = 3.82
X = 109	Y = 5.27
X = 112	Y = 5.74
X = 116	Y = 1.52
X = 119	Y = 2.29
X = 123	Y = 3.28
X = 126	Y = 4.05
X = 129	Y = 4.56
X = 130	Y = 4.8
X = 132	Y = 5.19
X = 132	Y = 1.72
X = 133	Y = 1.95
X = 137	Y = 2.94
X = 140	Y = 3.49
X = 144	Y = 4.22
X = 148	Y = 4.9
X = 150	Y = 5.51
X = 150	Y = 1.75
X = 151	Y = 2.01
X = 154	Y = 3.12
X = 158	Y = 4.31
X = 161	Y = 5.12
X = 165	Y = 6.13
X = 169	Y = 2.34
X = 172	Y = 2.7
X = 175	Y = 3.44
X = 180	Y = 4.27

Appendix 1b.

R_f data for unit 2

X = days; Y = R_f

X = 0	Y = 0
X = 8	Y = -.12
X = 10	Y = -.13
X = 14	Y = -.12
X = 17	Y = .13
X = 22	Y = .89
X = 24	Y = 1.04
X = 29	Y = 1.1
X = 34	Y = 1.52
X = 38	Y = 2.16
X = 41	Y = 2.48
X = 46	Y = 3.15
X = 49	Y = 3.52
X = 52	Y = 3.85
X = 56	Y = 4.53
X = 57	Y = .88
X = 62	Y = 2.83
X = 66	Y = 3.64
X = 69	Y = 3.66
X = 73	Y = 4.12
X = 76	Y = 4.79
X = 79	Y = 1.38
X = 83	Y = 3.61
X = 87	Y = 4.23
X = 90	Y = 4.96
X = 94	Y = 5.14
X = 95	Y = 1.39
X = 97	Y = 2.43
X = 102	Y = 5.08
X = 105	Y = 5.98
X = 108	Y = 7.2
X = 111	Y = 6.81
X = 114	Y = 6.72
X = 115	Y = .97
X = 118	Y = 3.73
X = 122	Y = 5.84
X = 124	Y = 5.95
X = 124	Y = 2
X = 129	Y = 4.62
X = 132	Y = 5.25
X = 136	Y = 5.64
X = 139	Y = 5.91
X = 140	Y = 1.32
X = 143	Y = 2.81
X = 147	Y = 3.58
X = 150	Y = 4.49
X = 154	Y = 5.71
X = 155	Y = 1.19
X = 157	Y = 2.48
X = 160	Y = 3.81
X = 165	Y = 5.6
X = 167	Y = 1.77
X = 171	Y = 3.95
X = 174	Y = 4.92
X = 180	Y = 6.03

Appendix 1c.

R_f data for unit 3

X = days; Y = R_f

X = 0	Y = 0
X = 8	Y = -.3
X = 10	Y = -.4
X = 14	Y = -.45
X = 17	Y = -.38
X = 22	Y = -.16
X = 24	Y = .04
X = 28	Y = -.27
X = 34	Y = -.09
X = 38	Y = -.1
X = 41	Y = -.05
X = 46	Y = -.05
X = 49	Y = -.03
X = 52	Y = .04
X = 56	Y = .15
X = 57	Y = .11
X = 62	Y = -.11
X = 66	Y = -.18
X = 70	Y = -.01
X = 73	Y = -.16
X = 76	Y = -.11
X = 80	Y = -.08
X = 83	Y = -.09
X = 87	Y = 0
X = 90	Y = -.12
X = 94	Y = -.02
X = 95	Y = .01
X = 98	Y = .07
X = 102	Y = .17
X = 105	Y = -.03
X = 108	Y = .17
X = 111	Y = .13
X = 115	Y = .13
X = 119	Y = .05
X = 122	Y = .16
X = 125	Y = .2
X = 129	Y = .18
X = 133	Y = .15
X = 139	Y = .16
X = 143	Y = .05
X = 147	Y = .06
X = 150	Y = .33
X = 157	Y = .1
X = 160	Y = .31
X = 165	Y = .13
X = 168	Y = -.08
X = 171	Y = -.02
X = 174	Y = -.11
X = 180	Y = -.01

Appendix 1d.

R_f data for unit 4

X = days; Y = R_f

X = 0	Y = 0
X = 10	Y = .24
X = 12	Y = .3
X = 16	Y = .47
X = 20	Y = 1.09
X = 24	Y = 1.59
X = 26	Y = 1.49
X = 31	Y = 1.81
X = 36	Y = 1.94
X = 40	Y = 2.2
X = 44	Y = 2.69
X = 48	Y = 3.28
X = 51	Y = 3.79
X = 54	Y = 4.22
X = 58	Y = 4.93
X = 59	Y = 0
X = 65	Y = 1.39
X = 68	Y = 2.6
X = 71	Y = 3.75
X = 75	Y = 4.3
X = 78	Y = 4.46
X = 82	Y = .46
X = 85	Y = 1.91
X = 89	Y = 3.82
X = 92	Y = 3.83
X = 96	Y = 4.58
X = 97	Y = .02
X = 99	Y = .32
X = 104	Y = 2.16
X = 108	Y = 2.7
X = 110	Y = 1.23
X = 113	Y = 2.21
X = 117	Y = 2.88
X = 120	Y = 4.26
X = 124	Y = 5.27
X = 125	Y = .33
X = 131	Y = 1.55
X = 134	Y = 2.23
X = 138	Y = 2.98
X = 141	Y = 3.84
X = 145	Y = 4.66
X = 149	Y = 5.52
X = 152	Y = 6.45
X = 153	Y = .31
X = 156	Y = .56
X = 160	Y = 1.81
X = 162	Y = 2.49
X = 167	Y = 4.2
X = 170	Y = 5.13
X = 171	Y = .19
X = 173	Y = .55
X = 176	Y = 1.4
X = 180	Y = 2.1

Appendix 1e.

R_f data for unit 5

X = days; Y = R_f

Appendix 2.

Time Rate of Change of Fouling Resistance

Unit #	Days Average	Slopes	Slopes Average
1	70	.25	.27 +/- .06
	89.5	.24	
	107	.25	
	122	.33	
	135	.18	
	149.5	.23	
	162	.37	
	176	.27	
2	75	.21	.22 +/- .06
	89.5	.13	
	107.5	.3	
	125.5	.22	
	143.5	.19	
	159.5	.28	
	176	.19	
3	72.5	.16	.27 +/- .12
	88.5	.15	
	102.5	.43	
	121	.39	
	134	.12	
	148.5	.27	
	161	.39	
	175.5	.22	
5	71.5	.24	.26 +/- .04
	90.5	.23	
	103.5	.27	
	118.5	.29	
	141.5	.23	
	163	.33	
	175	.22	

Slope average for the 4 units = .26 +/- .02

Appendix 3a.

Percent Reduction of R_f vs Brush Strokes
1st Deployment

Unit 1 Aluminum

1.	X = 0	Y = 6.82	0
2.	X = 2	Y = 1.90	73 %
3.	X = 4	Y = 1.32	81 %
4.	X = 8	Y = 0.92	87 %
5.	X = 20	Y = 0.79	89 %
6.	X = 40	Y = 0.63	91 %

Unit 2 Titanium

1.	X = 0	Y = 6.75	0
2.	X = 2	Y = 2.33	74 %
3.	X = 4	Y = 1.78	80 %
4.	X = 8	Y = 1.44	84 %
5.	X = 20	Y = 1.01	89 %
6.	X = 40	Y = 0.83	91 %

Unit 3 Aluminum

1.	X = 0	Y = 5.85	0
2.	X = 2	Y = 2.06	68 %
3.	X = 4	Y = 1.45	78 %
4.	X = 8	Y = 1.18	82 %
5.	X = 20	Y = 0.96	85 %
6.	X = 40	Y = 0.66	90 %

Unit 4 Aluminum

1.	X = 0	Y = 5.91	0
2.	X = 2	Y = 1.96	74 %
3.	X = 4	Y = 1.56	79 %
4.	X = 8	Y = 1.19	84 %
5.	X = 20	Y = 0.95	87 %
6.	X = 40	Y = 0.77	90 %

Appendix 3b.

Percent Reduction of R_f vs Brush Strokes
2nd Deployment First Cleaning

Unit 1 Aluminum

1.	X = 0	Y = 4.70	0
2.	X = 4	Y = 0.19	96%

Unit 3 Aluminum

1.	X = 0	Y = 4.63	0
2.	X = 4	Y = 1.25	73 %
3.	X = 6	Y = .81	83 %

Unit 5 Aluminum

1.	X = 0	Y = 5.10	0
2.	X = 4	Y = 0.63	88 %

Appendix 3c.

Percent Reduction of R_f vs. Brush Strokes
2nd Deployment Last Cleaning

Unit 1 Aluminum

1.	X = 0	Y = 4.30	0
2.	X = 2	Y = 1.99	54 %
3.	X = 4	Y = 1.16	73 %
4.	X = 10	Y = .25	94 %
5.	X = 30	Y = -.30	107 %

Unit 2 Titanium

1.	X = 0	Y = 4.27	0
2.	X = 2	Y = 2.37	44 %
3.	X = 4	Y = 1.68	61 %
4.	X = 10	Y = 1.21	72 %
5.	X = 30	Y = .52	88 %

Unit 3 Aluminum

1.	X = 0	Y = 6.03	0
2.	X = 2	Y = 3.42	43 %
3.	X = 4	Y = 2.29	62 %
4.	X = 10	Y = 1.39	77 %
5.	X = 30	Y = .69	89 %

Unit 5 Aluminum

1.	X = 0	Y = 2.10	0
2.	X = 2	Y = .58	72 %
3.	X = 4	Y = .09	96 %
4.	X = 6	Y = -.08	104 %
5.	X = 8	Y = -.18	109 %